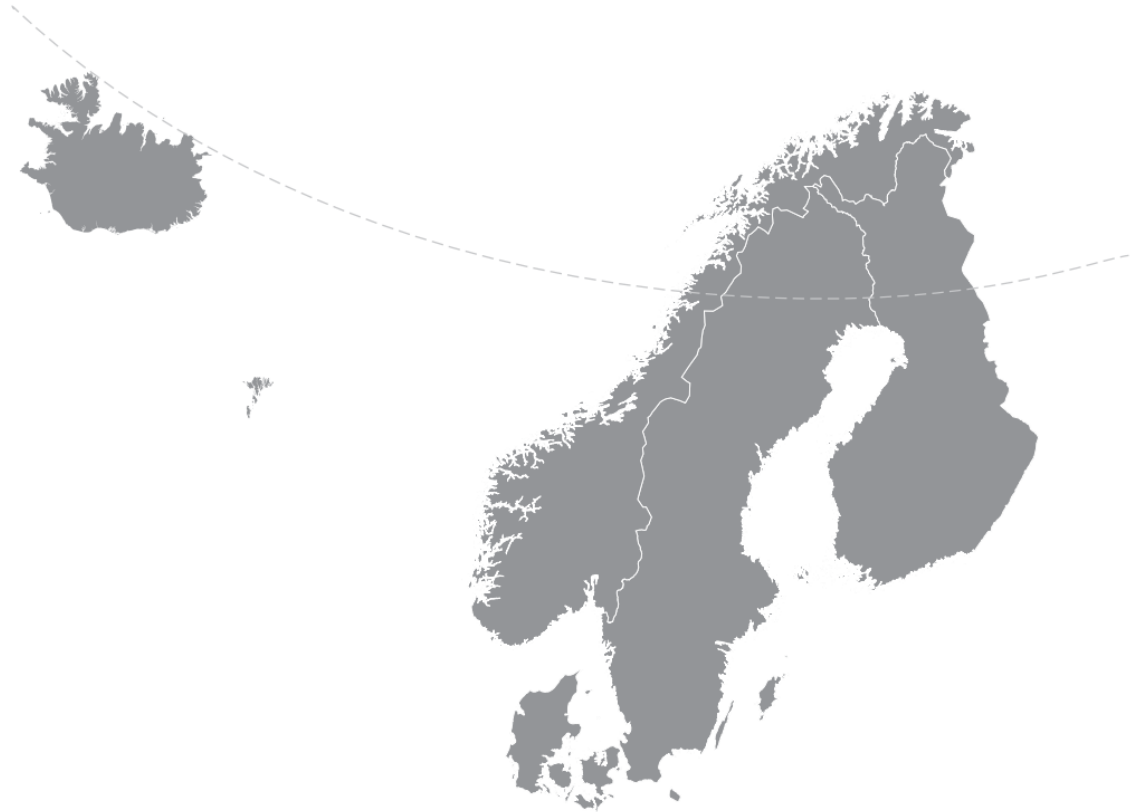


# CRACK WIDTH CALCULATION METHODS FOR LARGE CONCRETE STRUCTURES

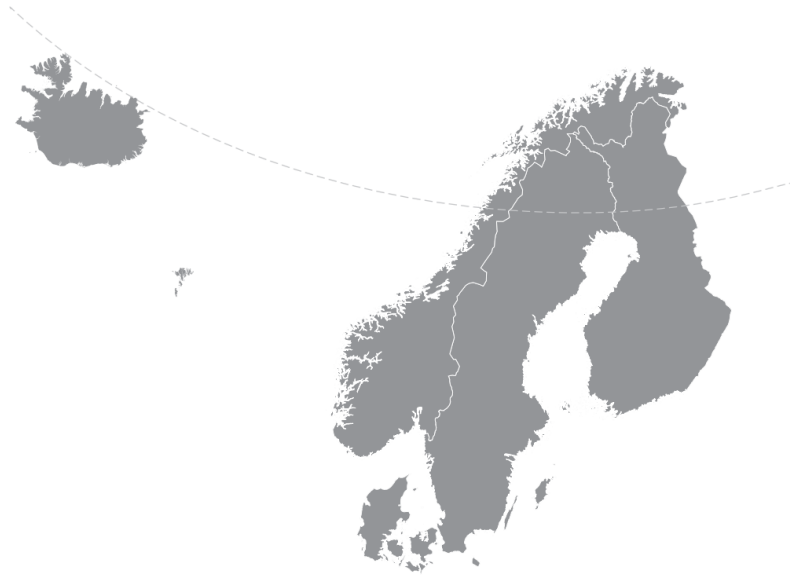
WORKSHOP PROCEEDINGS FROM A NORDIC MINISEMINAR  
OSLO, NORWAY, AUGUST 29.-30., 2017



Nordic  
Concrete  
Federation



# Crack width calculation methods for large concrete structures



**WORKSHOP PROCEEDINGS NO. 12**  
FROM A  
**NORDIC MINISEMINAR**  
Oslo, Norway  
August 29<sup>th</sup>-30<sup>th</sup>, 2017



Nordic  
Concrete  
Federation



## **Preface**

The Nordic mini-seminar: Crack width calculation methods for large concrete structures has been organized under the auspices of the two ongoing Norwegian research projects; The Ferry-free E39 and Durable Advanced Concrete Structures (DaCS). The Ferry-free E39 is a research project carried out under the auspices of the Norwegian Public Roads Administration, which is a development of a ferry free coastal high way route that is set to be 1100 km long along the west coast of Norway. The coastal way route will consist of multiple fjord crossings, which may be up to several kilometres long. Serviceability of these structures are thus of significant importance. The research project DaCS looks to increase the knowledge of sustainable and competitive reinforced concrete structures in harsh environment and is funded by The Research Council of Norway, in addition to several industrial partners. One of the ongoing activities related to the aforementioned research projects is the PhD project entitled “*Evaluation and improvement of crack width calculation methods in large concrete structures*” carried out by Reignard Tan.

The seminar is to be hosted by NTNU and Multiconsult ASA in a joint collaboration. The main goal is to increase the understanding and knowledge of crack width calculations for relatively large concrete structures in the Serviceability Limit State. This booklet documents the collection of extended abstracts of all the given lectures during the seminar. The organizing committee would like to thank all the speakers and contributors at the seminar, and the financial support of the research projects Ferry-free E39 and DaCS.

Oslo, August 2017.

Terje Kanstad, Max A.N. Hendriks, Morten Engen (ed.) and Reignard Tan (ed.)



# TABLE OF CONTENTS

<b>LIST OF PARTICIPANTS .....</b>	<b>5</b>
<b>KEYNOTE LECTURES .....</b>	<b>9</b>
<b>The CEOS.fr research project - Behaviour and assessment of massive structures: cracking and shrinkage</b>	
Philippe Bisch.....	11
<b>Proposal of new crack width formulas in the Eurocode 2, background, experiments, etc.</b>	
Alejandro Pérez Caldentey .....	17
<b>Crack Widths in Structural Concrete Subjected to In-Plane Loading</b>	
Walter Kaufmann.....	21
<b>Deformation-based crack width control in large restrained concrete members</b>	
Dirk Schlicke .....	27
<b>An improvement to Eurocode 2 and <i>fib</i> Model Code 2010 methods for calculating crack width in RC structures: mathematical model and simplified method</b>	
Maurizio Taliano .....	33
<b>SEMINAR LECTURES .....</b>	<b>39</b>
<b>Evaluation of crack width calculation methods used in design of offshore concrete structures</b>	
Dan-Evert Brekke .....	41
<b>Uncertainties of Crack Width Models for Macro and Meso Levels of RC Structural Elements</b>	
Vladimir Cervenka.....	43
<b>The modelling uncertainty of non-linear finite element analyses of concrete structures</b>	
Morten Engen .....	49
<b>Influence of cracking on reinforcement corrosion</b>	
Karla Hornbostel.....	53
<b>Control of cracking due to restrained deformations imposed at early ages or later (Related to a new Annex proposed for Eurocode 2)</b>	
Terje Kanstad.....	61
<b>Consequences of cracking related to tightness</b>	
Anja B. E. Klausen .....	65
<b>Crack Width Verification of Large Disturbed Regions in Practice</b>	
Kenneth C. Kleissl.....	67
<b>Finite element analysis with the Cracked Membrane Model</b>	
Mário Pimentel .....	73
<b>Crack width verification challenges for large RC structurers in practice</b>	
Uffe Graaskov Ravn .....	79
<b>Evaluation of crack width calculation methods according to Eurocode 2 and <i>fib</i> Model Code 2010 and suggestions to improvements</b>	
Reignard Tan .....	83

**Crack predictions using random fields**

Ab van den Bos..... 87

**Strain level and cracking of the lightweight aggregate concrete beams**

Jelena Zivkovic ..... 95

## **LIST OF PARTICIPANTS**



<b>Name</b>	<b>Affiliation</b>
Assis Arano Barenys	NTNU
Mikael Basteskår	Concrete Structures
Philippe Bisch	EGIS Industries
Daniela Bosnjak	Norconsult
Dan-Evert Brekke	Multiconsult
Alejandro Pérez Caldentey	Technical University of Madrid
Vladimir Cervenka	Cervenka Consulting
Susanne Christiansen	COWI
Morten Engen	Multiconsult
Erland Fjeldstad	Rambøll
Kjell Tore Fosså	Kværner
Erik Gottsäter	Lund University
Truls Haave	Aas-Jakobsen
Håvard Hafnor	Norconsult
Jørn Hagen	Norconsult
Max Hendriks	NTNU/TU Delft
Bjørn Magne Hope	Norconsult
Karla Hornbostel	Statens Vegvesen
Geir Horryngmoe	Sweco
Håvard Johansen	Statens Vegvesen
Terje Kanstad	NTNU
Walter Kaufmann	ETH Zürich
Remi André Kjørtaug	Norconsult
Anja Klausen	SINTEF
Kenneth Kleissl	COWI
Per Norum Larsen	Johs Holt AS
Nils Leirud	Mapei AS
Steinar Leivestad	Standard Norge
Liliya Draganova	Statens Vegvesen
Gro Markeset	HiOA
Egil Møen	Multiconsult
Paulius Bagdonas	Statens Vegvesen
Mário Pimentel	University of Porto
Uffe Graaskov Ravn	COWI
Dirk Schlicke	TU Graz
Maurizio Taliano	Politecnico di Torino
Reignard Tan	NTNU/Multiconsult
Henric Thompsson	Johs Holt AS
Ab van den Bos	DIANA FEA
Jelena Zivkovic	NTNU



## **KEYNOTE LECTURES**



## **The CEOS.fr research project - Behaviour and assessment of massive structures: cracking and shrinkage**



Philippe Bisch  
Ingénieur Civil des Ponts & Chaussées  
Professor at Ecole des Ponts ParisTech  
Chairman of CEN/TC250/SC8  
EGIS Industries, Montreuil France  
e-mail: [philippe.bisch@egis.fr](mailto:philippe.bisch@egis.fr)

### **ABSTRACT**

The CEOS.fr project is dedicated to cracking of massive reinforced concrete structural elements. This article presents a brief overview of the outcomes of the project and associated proposals. It focusses mainly on cracking of tie beams, free or restrained beams and shear walls.

**Key words:** Massive concrete structures, crack spacing, crack width, tension stiffening, probabilistic scale effect, tri-dimensional effect, shrinkage, creep, THM effects, optimum design, kinematic compatibility.

## **1. THE CEOS.fr PROJECT**

### **1.1 The background of the project**

The majority of concrete structures have to fulfil a number of structural functions beyond that of simple resistance. These include behavioural requirements for: stability, reinforced concrete cracking, deformability, water and air leak-tightness and sustainability.

Most European concrete structures today are designed for cracking in accordance with Eurocode 2 (EC2), which uses a performance-based approach related to durability and functionality at Serviceability Limit State (SLS).

For massive and more general non-standard structures, the EC2 standard rules do not fully reflect the complete behaviour related to cracking, for which Thermo-Hydro-Mechanical (THM) effects, scale effects and structural effects induce cracks spacing and crack width. For massive slabs and walls, shrinkage and creep are prevalent at an early and long-term age. This approach may lead to structures that are not optimised, especially for reinforcement.

To address these concerns, the French Civil Engineering Community decided in 2008 to launch a joint national research programme project, CEOS.fr, with the aim of making a significant step forward in the engineering capabilities for predicting the expected crack pattern of special structures under anticipated in-service or extreme conditions.

### **1.2 The CEOS.fr programme**

The aims of the CEOS.fr project are to:

- develop numerical non-linear and damage models, to simulate concrete behaviour under loading and imposed deformation;
- provide engineering guidelines to optimise the design of massive concrete structures;
- propose further rules for crack width and crack spacing assessment in massive concrete structures, in addition to EC2 or *fib* Model Code 2010 (MC2010).

Three types of actions have been completed from February 2008 up to 2013, namely:

- modelling: applying existing numerical models and developing specific new models;
- testing: implementing tests on large scale mock-ups (tie beams, full scale beams and 1/3 scale shear walls and beams), with well controlled boundary conditions and accurate measurements of cracking development;
- engineering methods: rules or guidelines developed from test results and computer simulation.

The main topics addressed by the project were:

- monotonic loading;
- thermo-hydric-mechanical behaviour (THM);
- cyclic loading on shear walls.

There is a huge volume of output data, which can be downloaded from the web site CHEOPS [3]. Some interpretations related to cracking are presented here. A more extensive presentation may be found in [5].

## **2 EXPERIMENT**

Specific tests on various full or 1/3 scale test bodies were performed as part of the CEOS.fr project. They included:

- Tests on 9 large tie beams with various reinforcements (1, 4 or 8 bars).
- Tests under monotonic loading on 7 blocks, RL1 to RL7 (6,10 m × 1,60 m × 0,80 m). Before loading, the blocks were matured with free deformations during at least one month then submitted to loading on a 4-points flexural bench. The blocks were made of different concrete mixes and had various reinforcements and concrete cover.
- Tests on 3 blocks subject to restrained shrinkage RG1 to RG3 (6,00 m × 0,50 m × 0,80 m), with different reinforcement and concrete cover.
- Tests on 6 concrete blocks at 1/3 scale under continuous loading (1,90 m × 0,25 m × 0,44 m), similar to RL blocks. The purpose of these tests was to highlight the scale effect in comparison with full-scale test bodies.
- Tests on shear walls at 1/3 scale with different concrete mix and reinforcement (test body dimensions: 4,20 m × 1,05 m × 0,15 m): 1 wall under cyclic non reversing loading and 3 walls under cyclic reversing loading.

All test bodies were comprehensively instrumented in order to locate and follow crack propagation and measure crack spacing and width. Test data, including measurements from Digital Image Correlation (DIC) instrumentation, provides confidence in the reliability of the test results.

## **3 RESULTS CONCERNING ALL TYPES OF ELEMENTS**

### **3.1 Three-dimensional effect**

An important result from the mock-up tests and from simulations is that the mean value of the mean tensile strength is reduced. This effect is mainly due to the combination of the tri-dimensional (3D) effect and of the probabilistic scale effect.

In simulating the effect of the non-uniform strains, resulting from the 3D deformation of the concrete section, the 3D effect may be taken into account. This results in a more refined definition of  $A_{c,eff}$ .

### 3.2 Probabilistic Scale effect

However, the variation and concentration of tensile concrete strains are not the only phenomena that explain the reduced tensile strength observed. The volume of concrete submitted to high tensile stresses is larger compared to that submitted to tensile stresses in a specimen under tensile test and this results in the reduction of tensile strength. This effect (the probabilistic scale effect) can be simulated by using the Weibull theory [6] and a lower value of the tensile strength can be mainly explained by the use of a simplified approach based on this theory.

### 3.3 Effect of shrinkage

Before cracking, shrinkage induces a tensile stress in concrete ( $\sim 0,2$  MPa) and a compressive stress in steel ( $\sim 17$  MPa).

### 3.4 THM effects at early age

These effects induce cracks due to:

- Temperature gradients between the core and the surface of the massive element.
- Internal strains generated by the temperature profile, shrinkage and creep.

## 4 CRACKING OF TIES

The outcomes of the experiment on ties were as follows:

- Early cracking occurred (1 or 2MPa compared to the 3MPa predicted), due to scale effect, restrained shrinkage and 3D effects.
- Cracks spacings are overestimated by both codes (MC2010 and EC2), although MC2010 gives much better results.

A statistical analysis of the results of 131 tests found in the literature has shown that:

- A formula for spacing based on a linear combination of cover and  $\phi/\rho$  gives a satisfactory correlation with the tests results.
- The combination coefficients used in MC2010 and EC2 are too high, and the following combination better fits the experimental results:

$$s_{r,max} = 1,7 \left( 1,37c + 0,117 \left( \frac{\phi}{\rho} \right) \right) \quad (1)$$

where 1,7 is the assumed ratio between the higher characteristic value and the mean value of spacing, which was confirmed by numerical experiments based on a probabilistic approach.

- Tension stiffening is overestimated by codes and the  $\beta$  factor (MC2010) should be taken equal to 0,36 instead of 0,6.

The analysis of the experimental results and a FEM analysis have shown that the value of  $A_{c,eff}$  as given in both codes is not appropriate and a different approach has been proposed, with a  $\gamma_c$  factor representing the ratio  $A_{c,eff}/A_c$  depending on crack spacing and other parameters.

Finally, taking both the three-dimensional stress distribution by the factor  $\gamma_c$  and a better representation of bond stress vs. slip between bar and concrete as proposed in [1] can lead to more refined expressions of cracks spacing and crack width.

#### **4 CRACKING OF BEAMS**

For 1/3 scale beams, the test results demonstrate that the mean crack spacing and widths, at the stabilised cracking stage, are consistent with the crack spacing and width calculated using the MC2010 formula. It is noted that the beam sizes correspond to test results and on site observations used to establish the code formula. The average crack width measured values provide a scattered distribution, partly explained by THM effects.

The most significant finding from the CEOS.fr project is an improved understanding of the THM effects at an early age. During concrete maturation, the massive elements are submitted to non-uniform strains, which induce a first cracking pattern at the surface of the beam. This effect is unavoidable in practice and is generated by:

- Temperature gradients between the core and the surface of the massive element.
- Internal strains generated by the temperature profile, shrinkage and creep.

In addition, assessment and interpretation of the test results for massive elements (scale 1) has improved the understanding of the influence of two phenomena: 3D effects (as the massive elements are always submitted to 3D non-uniform strains) and probabilistic scale effect.

#### **4 CRACKING OF WALLS**

The main results obtained from the experiment on four walls at 1/3 scale are:

- The mean structural tensile resistance  $f_{ctm}$  is 40% less than the theoretical value  $f_{ctm}$  when the first crack occurs.
- $f_{ct}$  demonstrates some impact (approximately 20%) on  $s_r$  value and cannot be neglected, although it is not reflected in codes formulas.
- In test 4, the reinforcement ratio decreases from 1% for the other tests down to 0,8%, while it is observed that  $s_r$  increases up to 22%. However, the application of code formula leads to an opposite variation. This is mainly due to  $A_{c,eff}$ , which appears to be inappropriate.

Engineering aspects have been developed, based on experimental results:

- If the reinforcement layers are in accordance with the good engineering practice, an error in angle  $\theta$  assessment does not result in a significant error in the assessment of crack spacing and crack width.
- The so-called Vecchio & Collins formula [7] is acceptable in the vicinity ( $\pm 20^\circ$ ) of the optimum (see also [4]).
- It is advisable to use, for calculation purposes, either the cover for each rebar layer or the mean value of the two covers in the both directions, the latter being simpler.
- Considering only kinematic compatibility, it may be shown that there exist an approximate (and conservative) relationship between crack width and extension of the rebars:

$$\frac{w}{s_r} \approx \varepsilon_{s,x} \sin \theta + \varepsilon_{s,y} \cos \theta \quad (2)$$

This relation is more accurate in the vicinity of the optimum. The extension of the rebars may be obtained by equilibrium at the crack.

- Another consequence of kinematic compatibility is the link between crack width and distortion of the wall.

Conclusions related to cyclic loadings and guidance for control of cracking in a seismic situation have also been drawn in the frame of the project [2].

## **REFERENCES**

- [1] Balázs G. “Cracking analysis based on slip and bond stresses”, ACI Materials Journal, Title no. 90-M37, 1993.
- [2] Bisch P., Erlicher S., Huguet M., Ruocci G.: “Experimental and theoretical results on cracking of reinforced concrete walls submitted to a cyclic action”, 9ème colloque national de l’AFPS, 2015.
- [3] IREX, National Project CEOS.fr - General Programme: <http://www.ceosfr.org>. Data base: <https://cheops.necs.fr/>, 2008.
- [4] Kaufmann W., Marti P.: “Structural concrete: Cracked membrane model”, Journal of Structural Engineering, 124(12):1467-1475, 1998.
- [5] Research Project CEOS.fr: Control of Cracking in Reinforced Concrete Structures”, ISTE, WILEY, 2016.
- [6] Rossi P., WU X., Le Maou F. Scale effect on concrete in tension Materials and structures, vol. 27, no. 8, pp. 437-444, 1994.
- [7] Vecchio FJ, Collins MP: “The Modified Compression-field Theory for Reinforced Concrete Elements subjected to shear”, ACI Journal, 83(2):219-231, 1986.



## **Proposal of new crack width formulas in the Eurocode 2, background, experiments, etc.**



Alejandro Pérez Caldentey  
PhD, member of SC2.PT1  
Technical University of Madrid.  
FHECOR Ingenieros Consultores, Madrid, Spain  
e-mail: [apc@fhecor.es](mailto:apc@fhecor.es)

### **ABSTRACT**

The Eurocodes are being revised in a significant effort undertaken by the Civil Engineering community with partial funding from the European Union. The new version was initially due to be published in 2020, but a more realistic date is 2023. For this revision, the guidelines call to improve ease-of-use, reduce nationally determined parameters and incorporate new, mature, knowledge. On the other hand, changes are to be kept to a minimum since changes imply significant costs in education and updating of existing software.

Within this context, this paper focuses on the updating of Chapter 7 and more specifically on cracking.

**Key words:** Cracking, stabilized cracking, flexure vs. tension, restraint, Eurocode 2, ease-of-use

### **1. INTRODUCTION**

The responsibility for the review of EN 1992 falls to CEN-TC-250/SC2. In view of the importance of this task, SC2 created, ahead of time, in 2012, before any funding was approved by the European Commission, Working Group1 (WG1) with the task of preparing the new draft of EN 1992-1-1. One of the first decisions of WG1 was to avoid an object-oriented approach and to try to merge part 1-1 with part 1-2 and part 1-3 of EN 1992-1-1. WG1 created several task groups (TGs) do deal with new topics or topics requiring special attention. These topics were: Fibre reinforced concrete, Fibre reinforced Polymers, Existing Structures, Shear and torsion, Fire, Analysis, Time-dependent behaviour of concrete, Fatigue, Bridges and Durability. In 2015, when funding became available, the first project team, (SC2.PT1) was established with the task of writing the first draft of EN 1992-1-1:2020, excluding new topics, and of course fire, which are to be handled by two further project teams. The task of the PT is to take material from the TGs and the existing text from the Eurocode and achieve a new text which should be easier to use and with a significant reduction in nationally determined parameters and with due account for new, mature knowledge.

The current proposal for EN 1992-1-1:2020, which is still evolving, is the result of a gradual process which has involved discussions among the members of Project Team, together with the Convenors of SC2 and WG1, and, also, within WG1 itself. It has also been influenced by the comments received by the National Mirror Groups during the systematic review in 2012 and by comments to subsequent drafts from the PT.

For the topic of cracking the current text is the result of discussions within the PT and WG1 since no TG was tasked with this topic.

## 2 ADOPTING THE MC 2010 MODEL

The initial draft respected the current EN 1992-1-1 model because, even though, there is evidence that the MC2010 model provides better predictions of experimental data [1], it was not initially deemed to be a sufficient reason for change, given the large scatter of experimental data. However, when consideration was given to defining how time effects are to be considered, the fact that MC2010 considered also the effect of shrinkage was enough to justify the change.

Besides calibration and the consideration of the addition of the shrinkage strain to the strain due to loads for stabilized cracking, shifting to MC2010 involved another big difference: whether crack spacing is different for bending and for pure tensile stresses. EN 1992-1-1:2004 includes factor  $k_2$  which halves the contribution of the bond term to crack spacing when the section is subjected to bending. The argument is that, in bending, due to the triangular distribution of stresses, it is necessary to transmit to concrete half of the tensile force to produce a new crack that it would be necessary for a uniform distribution of stresses (see Figure 1).

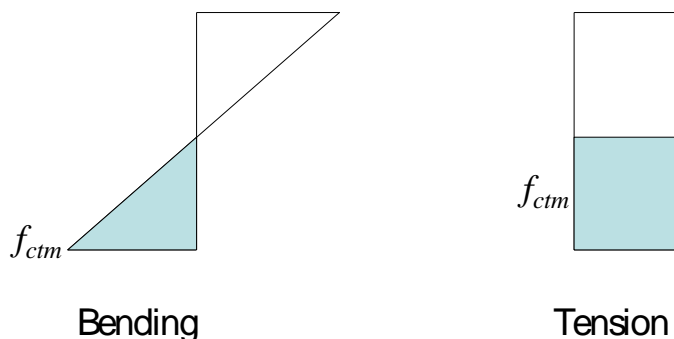


Figure 1 – Tension stress block in bending and tension. According to EN 1992-1-1:2004, the force to be transmitted to concrete through bond in order to produce a new crack would be half for bending than for tension (hence,  $k_{2,bending}=0.5$ ).

MC2010, on the other hand, considers that, in bending, an effective concrete area forms around the bar and that, within this area, the stress variation is minimal (see Figure 2), and therefore there is no  $k_2$  factor. Experimental evidence shows that the situation may be more similar to Figure 1 for small elements [2] and more similar to Figure 2 for larger elements [3] with some type of transition in between.

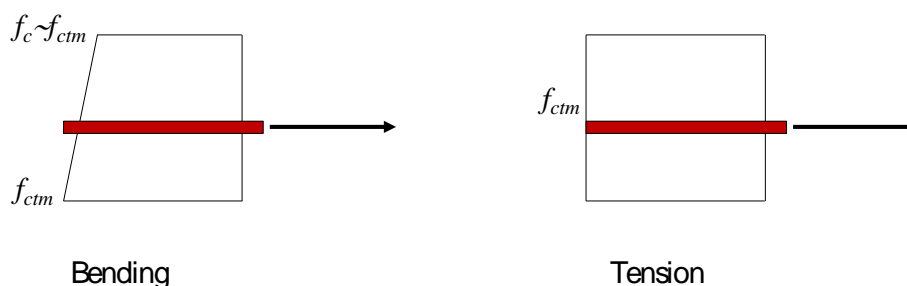


Figure 2 – Tension stress block in bending and tension. According to MC2010, the force to be transmitted to concrete through bond in order to produce a new crack would be more or less the same for bending than for tension (no  $k_2$  factor).

This dual vision of the same problem is further complicated by another effect related to curvature which favours tension over bending and would tend to offset the favourable effect of a smaller

crack spacing for bending. This effect shows that the crack width grows proportionately with the curvature as it is measured farther away from the bar.

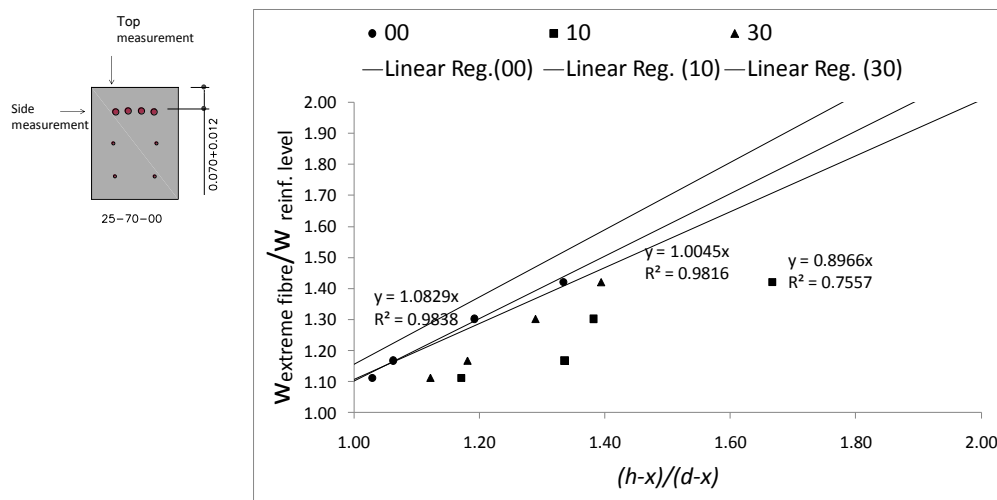


Figure 3 – Experimental evidence showing that the crack width grows proportionally with the curvature as it is measured farther away from the bar [4].

Adopting the MC2010 model was made difficult by the fact that considering the shrinkage strain made the model much more conservative for long term stabilized cracking. This problem was solved thanks to a comment by the French Mirror group, pointing out that adding the shrinkage strain directly implied full restraint. In fact, in most practical cases, the restraint is close to zero since the axial stiffness of a slab is much larger than the flexural stiffness of its supports, so that the slab can move freely. Therefore, the MC2010 equation was modified accordingly, where  $R_{ax}$  is the restraint factor:

$$w_{k,cal} = s_{r,max,cal} (\varepsilon_{sm} - \varepsilon_{cm} - R_{ax} \eta_r \varepsilon_{cs}) \quad (1)$$

### 3 INTEGRATING EN 1992-1-3 INTO EN 1992-1-1:2020

As stated above it was one of the early decisions to avoid an object-oriented approach in EN 1992-1-1:2020 so that the clauses should be applicable to all concrete structures. For cracking, this meant integrating the content of EN 1992-1-3 into the Part 1-1. In particular, EN 1992-1-3 deals with cracking due to imposed deformations and the differences in behaviour when an element is restricted at the ends with respect to an element that is restricted at the edges. In the first case which is the typical example of a tie, cracking affects the distribution of forces along the whole tie, so that the formation of a new crack implies a drop in the axial force. In this way, while cracks are forming (crack formation stage), the axial force is never higher than the cracking force and is independent of the applied imposed strain. In the case of an element restrained at the edges, such as a wall restrained by a previously cast foundation or a slab supported by longitudinal walls on the sides, cracking only affects forces locally and the crack width is a function of the imposed strain. This dichotomy has been integrated into the proposal for the EN 1992-1-1 :2002 text as follows:

For elements subject to direct loads (stabilized cracking) or restrained at the ends and subject to imposed strains (crack formation phase),  $\varepsilon_{sm} - \varepsilon_{cm}$  may be calculated from:

$$\varepsilon_{sm} - \varepsilon_{cm} = \frac{\sigma_s - k_t \frac{f_{ct,ef}}{\rho_{p,ef}} (1 + \alpha_e \rho_{p,ef})}{E_s} \geq 0,6 \frac{\sigma_s}{E_s} \quad (2)$$

For elements subjected predominantly to restrained imposed strains (crack formation phase) and restrained at the edges,  $\varepsilon_{sm} - \varepsilon_{cm} - \eta_r \varepsilon_{cs}$  may be calculated from:

$$\varepsilon_{sm} - \varepsilon_{cm} - R_{ax} \eta_r \varepsilon_{cs} = R_{ax} \varepsilon_{free} - k_t \frac{f_{ct,ef}}{E_{cm}} \quad (3)$$

#### 4 EASE-OF-USE

Among other things, in the PT's vision, ease of use means consistent methods, presenting, easier to use, particular formulations first and afterwards more general equations for more complex problems and using tables to group concepts so that they are easier to grasp, altogether avoiding a list of different but related conditions, lost within the text.

For the case of cracking, the second principle is illustrated by the removal of section 7.3 *Verification of cracking without calculation*, which currently consists of a couple limited tables valid for very particular situations with a series of correction factors to account for other situations by a single formula consistent with the general method which allows the determination of the stress compatible with a given crack width opening, based on the safe-sided assumption that the provided reinforcement is equal to the minimum required reinforcement, according to equation (4):

$$\sigma_s = \frac{3,6 f_{ct,ef}}{\phi} \left[ \sqrt{c^2 + 0,5 w_{k,cal} \phi_s \frac{E_s}{f_{ct,ef}}} - c \right] \quad (4)$$

#### REFERENCES

- [1] Barre, F., Bisch, P., Chauvel, D., Cortade, J., Coste, J.-F., Dubois, J.-P., Erlicher, S., Gallitre, E., Labbé, P., Mazars, J., Rospars, C., Sellier, A., Torrenti, J.-M. and Toutlemonde, F. : "Control of Cracking in Reinforced Concrete Structures. Research Project CEOS.fr", Wiley (2016). CEOS.fr Project Presentation, in Control of Cracking in Reinforced Concrete Structures: Research Project CEOS.fr, John Wiley & Sons, Inc., Hoboken, NJ, USA. DOI: 10.1002/9781119347088.ch1
- [2] Gribniak, V., Rimkus, A. "Experimental investigation of cracking parameters of ties and beams". Test report. Vilnius Gediminas Technical University (2017).
- [3] Pérez Caldentey, A., García R. "Report of tension tests of large ties". Test Report on ties 25-20 and 25-70 (2017)
- [4] Pérez Caldentey, A., Corres Peiretti, H., Peset Iribarren, J. and Giraldo Soto, A.: "Cracking of RC members revisited: influence of cover,  $\phi/\rho_{s,ef}$  and stirrup spacing – an experimental and theoretical study", Structural Concrete, 14: 69–78 (2013).

## **Crack Widths in Structural Concrete Subjected to In-Plane Loading**



Walter Kaufmann  
Dr. sc. techn., Professor, Chair of Concrete Structures  
ETH Zurich, Institute of Structural Engineering (IBK)  
Stefano-Franscini-Platz 5  
CH-8093 Zurich

e-mail: [kaufmann@ibk.baug.ethz.ch](mailto:kaufmann@ibk.baug.ethz.ch)  
<mailto:reignard.tan@multiconsult.no>



Jaime Mata-Falcón  
Dr., Postdoctoral research associate  
ETH Zurich, Institute of Structural Engineering (IBK)  
Stefano-Franscini-Platz 5  
CH-8093 Zurich

e-mail: [mata-falcon@ibk.baug.ethz.ch](mailto:mata-falcon@ibk.baug.ethz.ch)

### **ABSTRACT**

In-plane loading (“plane stress”) is a frequent loading situation in concrete structures. While many studies investigated the ULS behaviour of such elements over the past decades, serviceability aspects have received much less attention. Only few existing models yield information on crack spacings and crack widths, which in addition have hardly ever been systematically recorded in experiments. The present paper outlines how the load-deformation behaviour, including crack spacings and crack widths, can be analysed based on the Cracked Membrane Model [1]. The predicted crack widths correlate well with experimental evidence.

**Keywords:** Cracking, in-plane shear and normal forces, plane stress, tension stiffening, tension chord model, compression field approaches, cracked membrane model.

### **1. INTRODUCTION**

Structural concrete is not an isotropic material, even if “isotropic reinforcement” (equal reinforcement in orthogonal directions) is provided. For example, elements subjected to pure shear with respect to the reinforcement directions are significantly softer, exhibit larger crack openings and a lower load bearing capacity than elements under biaxial tension-compression of the same magnitude (same stress field rotated by 45°). In the present paper, orthogonal reinforcement in the  $x$ - and  $z$ -directions is assumed (Fig. 1a).

### **2 COMPRESSION FIELD APPROACHES**

The load-deformation behaviour of diagonally cracked orthogonally reinforced panels can be analysed using compression-field approaches, which were developed for linear [2] as well as nonlinear constitutive relationships [3] several decades ago. The basic concepts of such models are shown in Fig. 1: equilibrium requires  $\sigma_x = \sigma_{cx} + \rho_x \sigma_{sx}$ ,  $\sigma_z = \sigma_{cz} + \rho_z \sigma_{sz}$ ,  $\tau_{xz} = \tau_{cxz}$  (Fig. 1c), where  $\rho =$  geometric reinforcement ratio and  $\sigma_c, \sigma_s =$  stresses in concrete and reinforcement,

respectively. Noting that the strains are related by  $(\varepsilon_x - \varepsilon_3) \cot\theta = (\varepsilon_z - \varepsilon_3) \tan\theta$  (Fig. 1b), and expressing  $\sigma_{sx}$ ,  $\sigma_{sz}$ ,  $\sigma_{cx}$ ,  $\sigma_{cz}$  and  $\tau_{cxz}$  in terms of  $\varepsilon_x$ ,  $\varepsilon_z$  and  $\varepsilon_3$  (or any 3 non-collinear strains) using the stress-strain relationships of concrete and reinforcement, the states of stress and strain can be determined iteratively (3 equations for 3 unknowns).

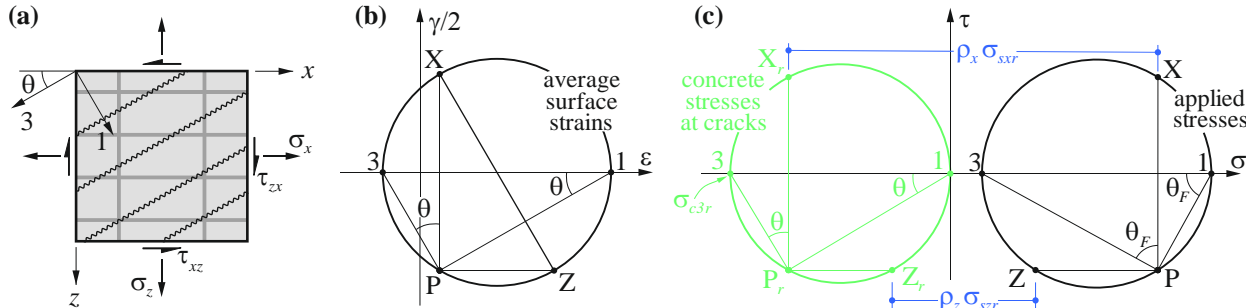


Figure 1 – Compression field approaches: (a) notation; (b) strains; (c) stresses.

Response predictions of compression field approaches typically overestimate the deformations since tension stiffening is neglected and rotating, stress-free rather than fixed, interlocked cracks are considered. To overcome these drawbacks, the modified compression field theory [4] (MCFT) was developed by Vecchio and Collins. In the MCFT, tension stiffening is accounted for as concrete property by expressing equilibrium in terms of average stresses between cracks, including concrete tension. However, the respective empirical constitutive equations disregard the fact that tension stiffening strongly depends on the reinforcement ratio and do not yield information on the maximum stresses at the cracks nor on crack spacings and crack widths.

### 3 CRACKED MEMBRANE MODEL (CMM)

#### 3.1 CMM with fixed, interlocked cracks

In its general formulation, the CMM [1] allows treating cracks as fixed and interlocked rather than as rotating and stress-free while accounting for shear and normal stresses on the crack faces as well as bond stresses transferred between concrete and reinforcement. Equilibrium conditions are expressed in terms of stresses at the cracks, and crack spacings and tensile stresses between the cracks are determined from basic mechanical principles using the Tension Chord Model [5] (TCM).

#### 3.2 CMM with rotating cracks

##### General remarks

An appropriately dimensioned reinforcement will not yield under service loads and consequently, the principal directions will not significantly change. Hence, the response under service load can be accurately predicted using a simplified CMM, considering rotating, stress-free cracks.

##### Tension Chord Model

As in the general formulation of the CMM, tension stiffening is accounted for based on the TCM, as shown in Fig. 2a-b, assuming a stepped, rigid-perfectly plastic bond shear stress-slip relationship with  $\tau_b = \tau_{b0} = 2f_{ctm}$  for  $\sigma_s \leq f_y$  and  $\tau_b = \tau_{b1} = f_{ctm}$  for  $\sigma_s > f_{ys}$ . Hence, at serviceability load levels ( $\sigma_s \leq f_y$ ) constant bond stresses are considered, similar to the simplification adopted by many codes. Treating both reinforcement directions as tension chords, Fig. 2 d-e, the distribution of bond shear, steel and concrete stresses and hence the strain distribution between two cracks can be determined for any given value of the maximum steel stresses (or strains) at the cracks.

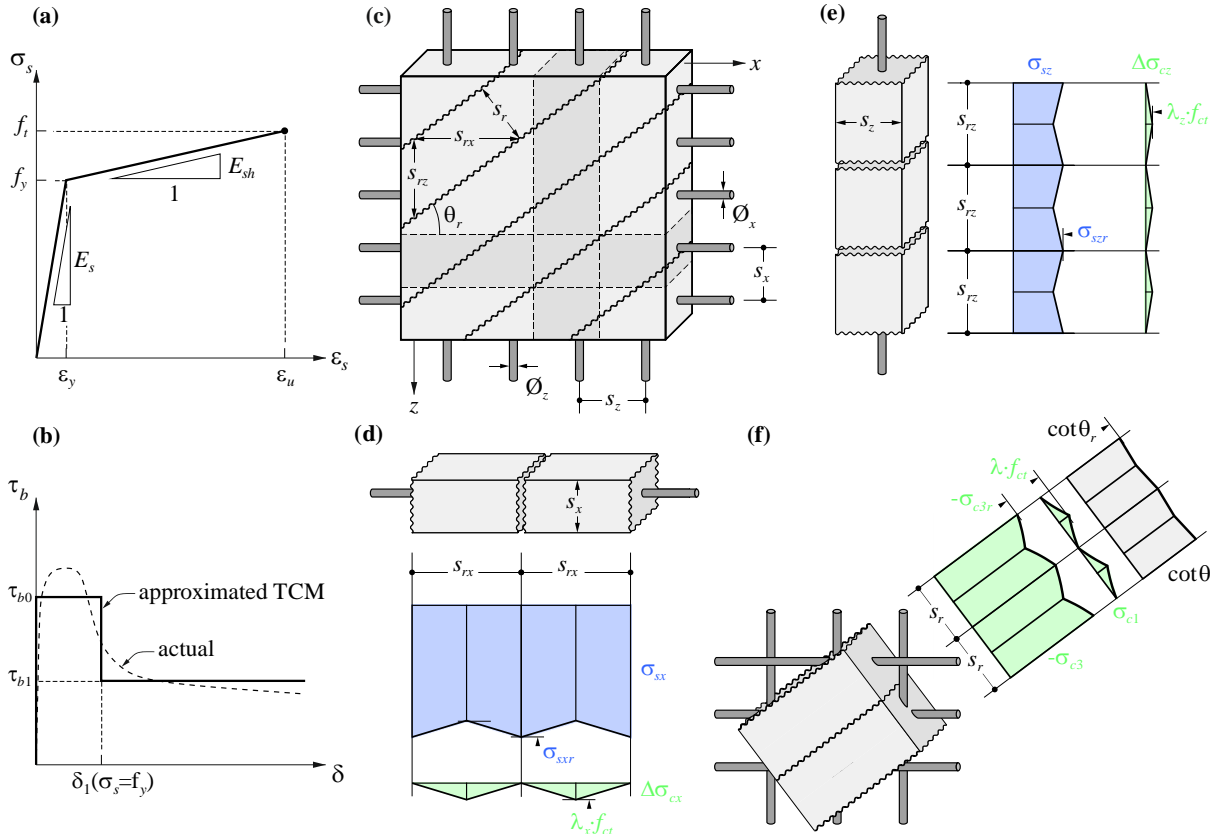


Figure 2 – TCM and CMM: (a), (b) TCM constitutive relationships; (c) notation and tension chords; (d),(e) stresses in  $x$ - and  $z$ -direction; (f) principal stresses in the concrete. Approximate analytical solution

### Crack spacing and crack width

Fig. 2f illustrates the distribution of the principal stresses in the concrete,  $\sigma_{c1}$  and  $\sigma_{c3}$ , and the variation of  $\theta$  (inclination of  $\sigma_{c3}$  to the  $x$ -axis). While  $\sigma_{c1} = 0$  is assumed at the cracks, tensile stresses are transferred to the concrete between the cracks by bond shear stresses. Limiting  $\sigma_{c1}$  to a maximum value of  $f_{ct}$  at the centre between two cracks, the theoretical maximum values of the crack spacings for uniaxial tension in the  $x$ - and  $z$ -directions,  $s_{rx}$  and  $s_{rz}$ , are given by  $s_{rx0} = \phi_x f_{ct} (1 - \rho_x) / (2\tau_{b0} \rho_x)$  and  $s_{rz0} = \phi_z f_{ct} (1 - \rho_z) / (2\tau_{b0} \rho_z)$  [5]. Noting that the crack spacings are related by  $s_r = s_{rx} \sin \theta_r = s_{rz} \cos \theta_r$  (Fig. 2c) the theoretical maximum diagonal crack spacing  $s_{r0}$  can be determined from  $\sigma_{c1} = f_{ct}$  [1]. A good upper bound approximation for  $s_{r0}$  is given by:

$$s_{r0} = \left( \sin \theta_r / s_{rx0} + \cos \theta_r / s_{rz0} \right)^{-1} \quad (1)$$

For  $s_r = s_{r0}$ , a new crack may form or not because at the centre between two cracks  $\sigma_{c1} = f_{ct}$ . Consequently, like in uniaxial tension, the crack spacing may vary by a factor of two, i.e.  $s_r = \lambda s_{r0}$ , with  $\lambda = 0.5 \dots 1.0$ . Assuming a certain value for  $\lambda$ , and expressing equilibrium in terms of the stresses at the cracks – which in turn, knowing the crack spacing, can all be expressed as functions of  $\varepsilon_x$ ,  $\varepsilon_z$  and  $\varepsilon_3$  (or any three non-collinear strains) – the states of stress and strain can be determined for any applied stresses, just as in compression field approaches neglecting tension stiffening.

Neglecting the typically small reduction of the crack widths caused by the tensile strains of the concrete between the cracks, the crack widths are obtained by multiplying the crack spacing with the average principal tensile strain,  $w_r = s_r \varepsilon_1 = \lambda s_{r0} \varepsilon_1$ . Concrete shrinkage  $\varepsilon_{cs} < 0$  can be accounted for by evaluating the reinforcement and concrete stresses for adjusted strains  $\varepsilon_{x,eff} = \varepsilon_x + \varepsilon_{csx}$ ,

$\varepsilon_{z,eff} = \varepsilon_z + \varepsilon_{csz}$  and  $\varepsilon_{3,eff} = \varepsilon_3 + (\varepsilon_{csx} - \varepsilon_{cs}) \cos^2 \theta + (\varepsilon_{csz} - \varepsilon_{cs}) \sin^2 \theta$ , with  $\varepsilon_{csx} = \varepsilon_{cs} (1 - \rho_x) / (1 + n \rho_x - \rho_x)$  and  $\varepsilon_{csz} = \varepsilon_{cs} (1 - \rho_z) / (1 + n \rho_z - \rho_z)$ . Note that to activate the same concrete and reinforcement stresses, larger strains are thus required than without shrinkage, resulting in wider cracks.

Assuming a linear elastic behaviour and supposing that the stresses at the quarter points between two cracks characterise the overall behaviour the following equation for the crack inclination  $\theta_r$  can be derived [1]:

$$\begin{aligned} \tan^2 \theta_r \rho_x (1 + n \rho_z) + \tan \theta_r \rho_x (\sigma_z - 0.5 f_{ct} (\lambda_z + n \rho_z (\lambda_x + \lambda_z - 1))) / \tau_{xz} = \\ \cot^2 \theta_r \rho_z (1 + n \rho_x) + \cot \theta_r \rho_z (\sigma_x - 0.5 f_{ct} (\lambda_x + n \rho_x (\lambda_x + \lambda_z - 1))) / \tau_{xz} \end{aligned} \quad (2)$$

where  $\lambda_x = s_{rmx} / s_{rmx0}$  and  $\lambda_z = s_{rmz} / s_{rmz0}$  are the ratios of the actual crack spacings to the theoretical maximum crack spacings for uniaxial tension in the corresponding directions. Note that for  $f_{ct} = 0$ , Eq. (2) corresponds to the inclination given by Baumann [2] (neglecting tension stiffening).

#### 4 COMPARISON WITH TEST RESULTS

As mentioned in the introduction, crack spacings and crack widths have only been systematically recorded in few experiments on elements loaded in plane stress. While the authors are currently carrying out a series of own tests in a new experimental facility, calculations according to the simplified version of the CMM (assuming rotating cracks) and considering shrinkage are compared in Fig. 3 to selected tests by Proestos et al. [6].

The agreement is seen to be satisfactory for both average and maximum observed crack widths, even beyond serviceability load levels and using the approximate analytical solution given by Eq. (2).

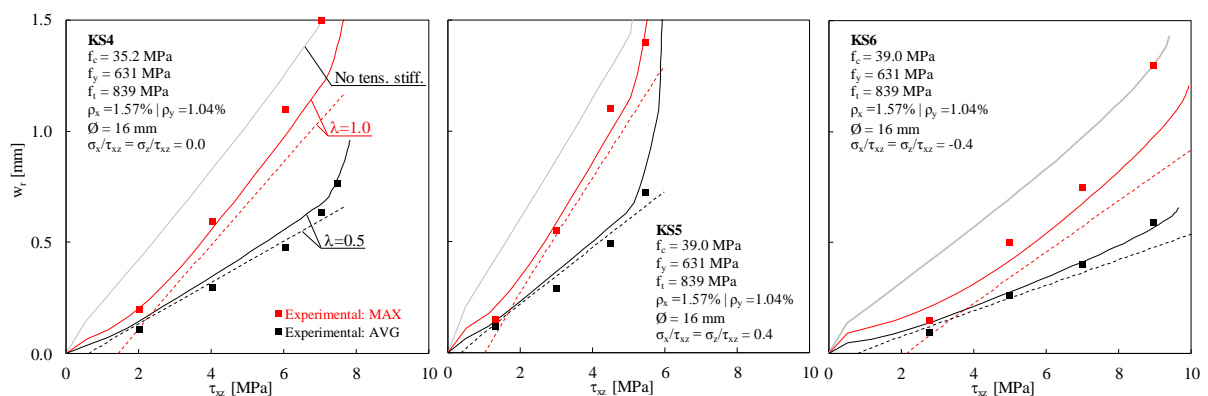


Figure 3 – Crack widths calculated from the CMM compared to tests KS4-KS6 by Proestos [6]. Solid lines: numerical solution, dashed lines: approximate analytical solution.

#### REFERENCES

- [1] Kaufmann, W. and Marti, P.: Structural Concrete: Cracked Membrane Model. Journal of Structural Engineering, ASCE. 124, (1998), 1467–1475.
- [3] Baumann, T.: Zur Frage der Netzbewehrung von Flächentragwerken. Bauingenieur. 47, 10 (Oct. 1972), 367–377.

- [3] Mitchell, D. and Collins, M.P.: Diagonal Compression Field theory - A Rational Model for Structural Concrete in Pure Torsion. *ACI Journal*. 71, 8 (Aug. 1974), 396–408.
- [4] Vecchio, F.J. and Collins, M.P.: The Modified Compression Field Theory for Reinforced Concrete Elements Subjected to Shear. *ACI Journal*. 83, 2 (Apr. 1986), 219–231.
- [5] Marti, P., Alvarez, M., Kaufmann, W. and Sigrist, V.: Tension chord model for structural concrete. *Structural Engineering International*. 8, 4 (1998), 287–298.
- [6] Proestos, G.T.: Influence of High-Strength Reinforcing Bars on the Behaviour of RC Nuclear Containment Structures. Subjected to Shear, University of Toronto, 2014



## **Deformation-based crack width control in large restrained concrete members**



Dirk Schlicke  
Assistant Professor, Dr.  
Graz University of Technology, Institute of Structural Concrete,  
8010 Graz, Austria  
e-mail: [dirk.schlicke@tugraz.at](mailto:dirk.schlicke@tugraz.at)

### **ABSTRACT**

This contribution presents an alternative design approach for the crack width control in large restrained concrete members. Contrarily to current design rules, which are derived from the force equilibrium while taking up the cracking forces, this approach aims at the consideration of the compatibility of deformations along the member before and after cracking. Altogether, this enables a more realistic assessment and effective control of cracking due restraint stressing, especially in case of large concrete members with significant thickness.

**Key words:** Cracking, large concrete structures, crack width control, deformation compatibility.

### **1. INTRODUCTION**

Restraint stressing arises from the deformation behaviour of concrete as soon as it is restrained. The size of restraint stressing depends on a time-dependent interplay of the imposed deformation (usually thermal dilation, shrinkage and viscoelasticity) and the stiffness properties of restrained member and restraining situation. From a structural level perspective the principle of restraint stressing is the compatibility of deformations. In detail, all restrained concrete deformations were realised with stress-dependent strains.

Once critical stresses are reached, crack formation is to be expected. But also after cracking the compatibility of deformations is the decisive principle, whereby crack widths provide an additional contribution to absorb the imposed deformations. This behaviour can be applied in a deformation-based crack width control. Basic aspects of this approach are given in this extended abstract, further details can be found in [1] or [2].

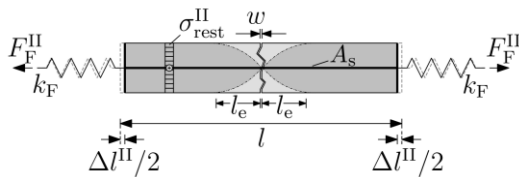
### **2. BASIC IDEA AND GENERAL PROCEDURE OF DESIGN**

The basic idea of the deformation-based crack width control is the specific consideration of the compatibility of deformations within the design. As illustrated in Fig. 1 for a member in the cracked state, this aims at the compatibility of the imposed deformations with the response of the member. In detail, the imposed deformation is exemplified by an equivalent temperature  $\Delta T_{eq}$  and the response of the member consists of the released deformation in the crack ( $w$ ), the real shortening of the member ( $\Delta l^H$ ) according to the restraining condition (here considered in form of springs with the stiffness  $k_F$ ) as well as the elastic strains of the uncracked parts according to the restraint stressing in the equilibrium after cracking ( $\sigma_{rest}^{II}$ ) with respect to the distribution of concrete stresses in the transfer length ( $l_e$ ) according to the shape factor ( $k_t$ ) of [3].

The application of deformation-based crack width control is illustrated in Fig. 2. Firstly, the restraint stressing of a given design task will be determined for the uncracked state. If cracking is to be expected but not acceptable the system is to be optimized (design principle: exclusion of cracking). If cracking can be accepted as long as it is sufficiently controlled the compatibility of deformations will be formulated for the cracked system. In this stage only the cracking due to the restraining situation without the presence of reinforcement is considered (primary cracking)

whereby two situations can occur: (i) crack width criteria is fulfilled already without reinforcement and (ii) crack width criteria is not fulfilled. In the latter case, reinforcement is needed to produce additional cracks in order to distribute the theoretical crack opening of the primary crack among several secondary cracks produced by reinforcement.

Deformation impact:  $\alpha_T \cdot \Delta T < 0$



Compatibility of deformations:

$$-\alpha_T \cdot \Delta T \cdot l = w - \Delta l^{II} + \frac{\sigma_{rest}^{II}}{E_c} \cdot (l - 2 \cdot l_e \cdot (1 - k_t))$$

Force equilibrium:

$$F_F^{II} = F_s = \sigma_{rest}^{II} \cdot A_c \cdot (1 + \alpha_E \cdot \rho_s)$$

Figure 1 – Compatibility of deformations in a cracked RC member.

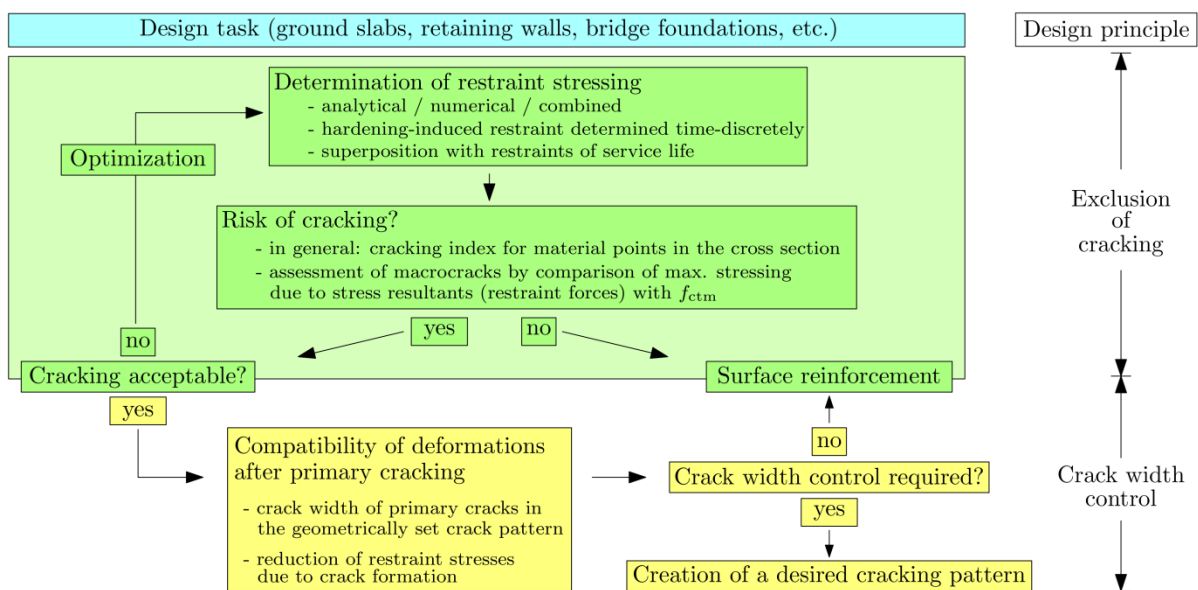


Figure 2 – General procedure of deformation-based crack width control.

A key point of this procedure is the crack risk assessment. Established recommendations usually concentrate on the crack index comparing maxima in the stress field of the cross section with strength criteria, see e.g. [4]. Besides, a detailed analysis of the stress field with respect to stress resultants and Eigenstresses, as exemplified in Fig. 3, provides the opportunity for a targeted crack assessment. The risk of *any cracking at all* is hereby assessed with Eq. (1) according to the crack index (including Eigenstresses). The risk of *macrocracking*, however, is assessed on basis of stresses due to stress resultants (excluding Eigenstresses) and a strength criteria with regard to stress redistribution within the cross section, see also [1], [2] and [5].

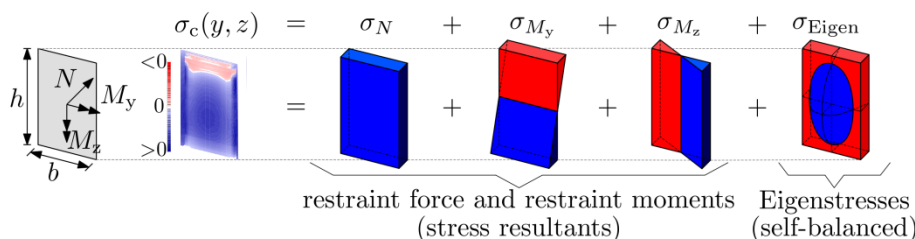


Figure 3 – Detailed analysis of the stress field of a cross section.

risk of any cracking at all:  $\sigma_c(y, z, t) \leq 0.8 \cdot f_{ctk,0.05}(y, z, t)$  (1)

risk of macrocracking:  $\sigma_N(t) + \sigma_{M_y}(t) + \sigma_{M_z}(t) \leq f_{ctm}(t)$  (2)

### 3. COMPATIBILITY OF DEFORMATIONS ON STRUCTURAL LEVEL

On structural level the formulation of the compatibility of deformations depends significantly on the assumed length in longitudinal direction. An appropriate assumption for this length is the distance between primary cracks ( $l_{cr}$ ), whereby this distance is geometrically set according to the type of imposed deformations and the restraining condition. The primary cracks can be assumed to be independent from each other, so that the compatibility of deformations between the decisive primary cracks is representative for the whole member.

In case of thicker ground slabs significant temperature gradients occur due to the insulating effect of the ground, whereas the activation of self weight restrains the associated curvature. As a result, bending cracks occur in a defined distance from each other.

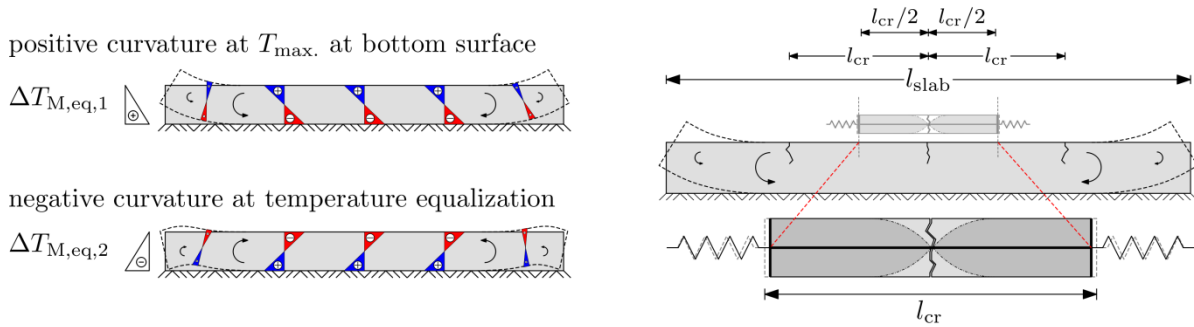


Figure 4 – Compatibility of deformations for design case of 'ground slabs'.

In case of wall on foundations the imposed deformation is mainly uniformly distributed over the cross section, whereas the foundation eccentrically restrains the associated length change. As a result, separating cracks occur in a defined distance from each other.

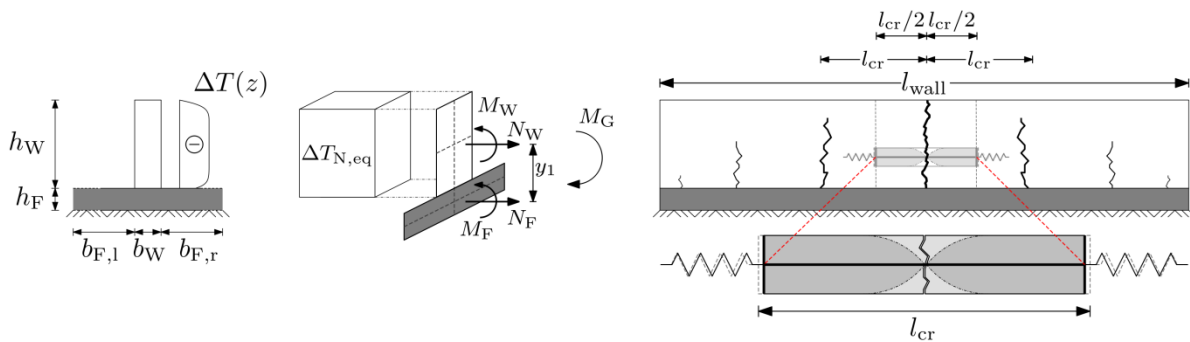


Figure 5 – Compatibility of deformations for design case of 'walls on foundations'.

Conceptual models for the determination of the geometrically set pattern of primary cracks for the two typical cases *ground slab* and *wall on foundation* can be found in [1], the background of these models is given in [2].

### 4. CRACK WIDTH AND REQUIRED MINIMUM REINFORCEMENT

The crack width of the primary crack without reinforcement can be determined directly from the restrained deformation and the distance between primary cracks. If this crack width exceeds the

crack width criteria an active crack width control with reinforcement is needed. In case of thicker members this can be provided with the creation of secondary cracks next to the primary cracks, as shown in Fig. 6. The required reinforcement can be determined with Eq. (3) and Eq. (4) according to the required number of secondary cracks as well as the decrease of restraint stressing after cracking. Further details are given in [6] and [7].

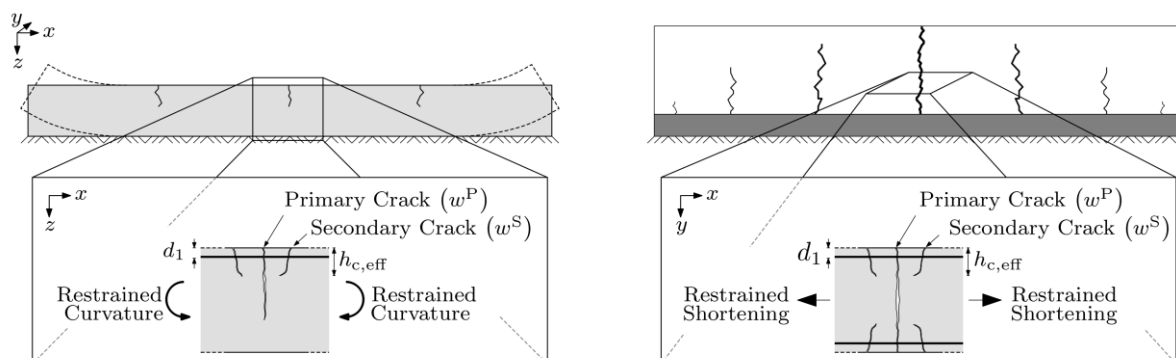


Figure 6 – Secondary cracking due to reinforcement in the vicinity of the primary crack. Left: bending cracks in ground slabs. Right: separating cracks in walls on foundations.

$$n = 1.1 \cdot \left( \frac{\varepsilon_{\text{rest}} \cdot l_{\text{cr}}}{w_k} \cdot \frac{k_{\text{mod}}}{a^{0.6}} - 1 \right) \quad (3)$$

$$n > 0: A_{s,\text{min}} = \sqrt{\frac{d_s \cdot b^2 \cdot d_1^2 \cdot f_{\text{ct,eff}} \cdot (0.5 + 0.34 \cdot n)}{w_k \cdot E_s}} \quad (4)$$

with:  $\varepsilon_{\text{rest}} \cdot l_{\text{cr}}$  ... restrained deformation to be absorbed by one crack system

$w_k$  ..... crack width criteria

$k_{\text{mod}}$  ..... factor for effect of crack formation, 0.6...0.85 depending on requirements and stressing

$a$  ..... degree of restraint in the uncracked state

$d_s$  ..... reinforcement diameter

$b$  ..... width in view direction (usually 1 m)

$d_1$  ..... edge-distance of the reinforcement

$f_{\text{ct,eff}}$  ..... decisive tensile strength of concrete

$E_s$  ..... elastic modulus of reinforcement

## REFERENCES

- [1] Schlicke, D., Tue, N.V.: "Minimum reinforcement for crack width control in restrained concrete members considering the deformation compatibility", Structural concrete 16, pp. 221-232 (2015) [doi: 10.1002/suco.201400058](https://doi.org/10.1002/suco.201400058)
- [2] Schlicke, D.: Mindestbewehrung zwangbeanspruchter Betonbauteile unter Berücksichtigung der erhärtungsbedingten Spannungsgeschichte und der Bauteilgeometrie (2. updated edition). PhD thesis, Graz University of Technology, Austria (2014) [doi:10.3217/978-3-85125-473-0](https://doi.org/10.3217/978-3-85125-473-0)
- [3] EN 1992-1-1:2004 + AC:2008: EUROCODE 2: Design of concrete structures - Part 1-1: General rules and rules for buildings.
- [4] Bjøntegaard, Ø.: Basis for practical approaches to stress calculations and crack risk estimation in hardening concrete structures, state-of-the-art report. COIN project report 31 (2011) [ISBN 978-82-536-1236](https://doi.org/10.1002/suco.201400058), 90p
- [5] Schlicke, D., Muja, G.: "Discrete modelling of hardening-induced cracking", In: 2<sup>nd</sup> Int. RILEM/COST Conference on Early Age Cracking (EAC02), Brussels, September 2017.

- [6] Bödefeld, J.: Rissmechanik in dicken Stahlbetonbauteilen bei abfließender Hydratationswärme, PhD thesis, University of Leipzig, Germany (2010)
- [7] Turner, K.: "Ganzheitliche Betrachtung zur Ermittlung der Mindestbewehrung für fugenlose Wasserbauwerke", PhD thesis, Graz University of Technology, Austria (2017)



## An improvement to Eurocode 2 and *fib* Model Code 2010 methods for calculating crack width in RC structures: mathematical model and simplified method



Maurizio Taliano  
M.Sc., PhD, Assistant Professor  
Politecnico di Torino, Department of Structural, Geotechnical and  
Building Engineering, Turin, Italy  
e-mail: [maurizio.taliano@polito.it](mailto:maurizio.taliano@polito.it)

### ABSTRACT

A mathematical model for the analysis of the mechanical behaviour of a reinforced concrete tie subjected to a monotonic loading, that considers the effect of the so-called Goto cracks (secondary cracks), is described here. It is shown that the average bond stress along the transmission length depends not only on the concrete strength as assumed by the *fib* Model Code 2010, but also on reinforcement ratio and bar diameter. The secondary cracks influence also the tension-stiffening effect, reducing it. On the basis of the main results obtained with the general model, an improvement to Eurocode 2 and *fib* Model Code 2010 methods for calculating crack width in RC structures is proposed. Finally, the theoretical results of crack spacing and crack width are compared with experimental data obtained from extensive research on RC ties.

**Key words:** cracking of an RC tie, average bond stress, crack spacing, crack width.

### 1. INTRODUCTION

In European standards (*fib* Model Code for Concrete Structures 2010 [1], Eurocode 2 [2]), cracking control can be performed through a direct calculation of the crack width. Two fundamental assumptions are considered, that means: bond stresses are evenly distributed along the length where stresses are transmitted from steel to concrete, with an average bond stress that only depends on the tensile strength of concrete [1]; in the stabilized cracking stage, where a fixed crack pattern is deemed to occur, the cracking analysis refers to the maximum crack width associated to the maximum crack spacing that is equal to twice the transmission length.

In order to achieve a better understanding of cracking, a mathematical model for the analysis of the mechanical behaviour of a reinforced concrete tie subjected to a monotonic loading in the stabilized cracking stage, has been set up [3], [4]. This refined model, here referred to as the general model, considers the effect of the so-called Goto cracks [5] or secondary cracks. The basic idea is to introduce a decreasing linear distribution of the bond stresses around a primary crack. This basically allows compliance with the equilibrium and compatibility conditions, which otherwise would not be the case.

### 2 GENERAL MODEL FOR ANALYSING CRACKING BEHAVIOUR

The cracking behaviour of an RC tie subjected to a monotonic axial force has been studied recently by Debernardi and Taliano [3], [4] through a general model based on the following second-order differential equation of the slipping contact between steel and concrete:

$$\ddot{s}_s(x) = \frac{4 \cdot \tau_{bs}}{E_s \cdot \phi_s} \cdot (1 + \alpha_e \cdot \rho_s) \quad (1)$$

The bond law proposed by *fib* Model Code 2010 is considered, assuming the exponent  $\alpha = 0.25$ .

Two stages are distinguished, that means crack formation stage and stabilized cracking stage.

For the crack formation stage Balázs [6] has already developed a mathematical model which allows the problem concerning a single crack to be solved in a closed form, leading to the formulation of the distribution of slips  $s_s$  and bond stresses  $\tau_{bs}$  from the zero slip section as well as the calculation of transmission length  $L_s$  and crack width  $w$ .

When the crack stabilizes, it is assumed a crack spacing equal to the maximum value, i.e. twice the transmission length, in order to obtain the maximum crack width (Fig. 1a). When the axial load increases it is possible to observe, from a kinematic point of view, that the slips increase along the transmission length. In effects, variations of steel and concrete strains correspond to this increase of slips (Fig. 1b). Correspondingly, from a statics point of view, to an increase of slips an increase of the bond stresses should correspond. And, variations of the concrete and steel normal stresses occur, apart from in the zero slip section, where the concrete stress  $\sigma_{cE}$  cannot change but has to remain equal to  $f_{ct}$ . However, for the equilibrium of forces acting on a concrete block included between the crack and the zero slip section, the resultant of bond stresses cannot increase, but has to remain equal to  $f_{ct} \cdot A_c$ . Likewise the average bond stress  $\tau_{bs,m}$ , which is developed along the transmission length, cannot change. This inconsistency cannot be accepted. The basic idea for overcoming this inconsistency is to consider a linear branch of bond stresses around the crack (Fig. 1c), followed by a non-linear distribution of bond stresses whose values depend on the slips according to the bond law. The extension  $l_{sc}$ , where the linear distribution of bond stresses occurs, increases while the axial load increases. It can be determined through an iterative procedure in such a way to satisfy the equilibrium condition.

Finally, considering that the resultant of bond stresses remains unchanged and equal to the cracking force during both the crack formation stage and the stabilized cracking stage, a formula in closed form can be obtained from the Balázs' solution [19] for calculating the average bond stress  $\tau_{bs,m}$  (Fig. 1c):

$$\tau_{bs,m} = \frac{\text{bond stresses resultant, equal to } f_{ct} A_c}{\text{surface of the concrete - steel interface}} = \frac{f_{ct} \cdot A_c}{n_s \cdot \pi \cdot \phi_s \cdot L_s} = \frac{\left( f_{ct}^2 \cdot \frac{\phi_s}{\rho_s} \right)^{\frac{\alpha}{1+\alpha}}}{4 \cdot \left( \frac{s_1^\alpha}{K^{1-\alpha}} \right)^{\frac{1}{1+\alpha}}} \quad (2)$$

It results that correlating the average bond stress to the concrete tensile strength only, as done by *fib* Model Code 2010, is misleading. Moreover, it is possible to obtain an improved formula of the transmission length, that does not present the corrective term associated with the concrete cover:

$$L_s = \frac{1}{4} \cdot \frac{f_{ct}}{\tau_{bs,m}} \cdot \frac{\phi_s}{\rho_s} \quad (3)$$

The formulation of the transmission length according to *fib* Model Code 2010 with a corrective term depending on the concrete cover leads to the equilibrium of forces no longer being fulfilled.

## 2.1 Parametric analysis

A parametric analysis is performed on the basis of the proposed general model, focusing attention on the stabilized cracking stage in order to compare the theoretical results with those obtained with the international standards (*fib* Model Code 2010, Eurocode 2). An RC tie reinforced with four high-bond bars under good bond conditions, embedded in confined concrete with cover of 30 mm and subjected to an axial force equal to half the design yield value, is considered, i.e.  $F_s = 0.5 \cdot f_{yd} \cdot A_s$  ( $f_{yd} = f_{yk}/\gamma_s$  with  $\gamma_s = 1.15$ ). The parameters that vary in the analysis are the bar diameter  $\phi_s$  (ranging from 8 to 20 mm) and the reinforcement ratio  $\rho_s$  (1.5% and 2.0–5.0%, step 1%). The mean tensile strength of concrete is  $f_{ct} = 2.90 \text{ N/mm}^2$ , the mean secant modulus of elasticity is  $E_{cm} = 31\,000 \text{ N/mm}^2$ . For the steel reinforcement a characteristic yield strength  $f_{yk} = 500 \text{ N/mm}^2$  and a modulus of elasticity  $E_s = 200\,000 \text{ N/mm}^2$  are assumed.

According to the parametric analysis, when compared to *fib* Model Code 2010 and Eurocode 2, the general model always gives higher values for the relative mean strain. This difference can be ascribed to the influence of the secondary cracks on the tension stiffening effect. Moreover, the theoretical values of the maximum crack width obtained with the general model are closer to those obtained with Eurocode 2 than those obtained with *fib* Model Code 2010.

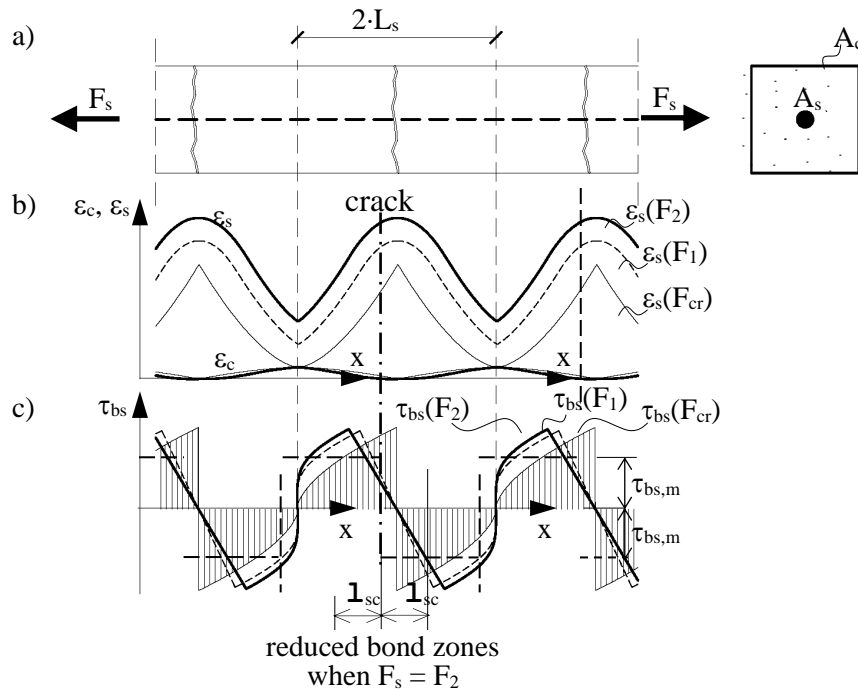


Figure 1 – Stabilized cracking stage: a) r.c. tie subjected to an increasing force  $F_s$  ( $F_{cr} < F_1 < F_2$  where  $F_{cr}$  is the tensile force at the beginning of the stabilized cracking stage); b) distribution of longitudinal strains of concrete and steel; c) distribution of bond stresses according to the proposed model and length of the reduced bond,  $l_{sc}$ , when  $F_s = F_2$ .

## 3 IMPROVED CALCULATION METHOD

The formulae proposed by European standards for calculating crack widths are improved here as follows. The maximum crack spacing  $s_{r,max}$  can be obtained as twice the transmission length given in Eq. (3). Therefore, the maximum crack width is calculated as follows, in which  $k_t = 0.45$  is assumed for short-term loading:

$$w_{\max} = s_{r,\max} \cdot (\varepsilon_{sm} - \varepsilon_{cm}) = 2 \cdot \left( \frac{1}{4} \cdot \frac{f_{ct}}{\tau_{bs,m}} \cdot \frac{\phi_s}{\rho_s} \right) \cdot \frac{\sigma_{s2} - 0.45 \cdot \frac{f_{ct}}{\rho_s} \cdot (1 + \alpha_e \cdot \rho_s)}{E_s} \quad (4)$$

#### 4 COMPARISON BETWEEN THEORETICAL AND EXPERIMENTAL DATA

The 135 short-term tests carried out by Farra [7] on RC ties with an initial length of 1000 mm and squared transversal section of side 100 mm, reinforced with a single central bar 10, 14 or 20 mm in diameter, made with concrete strengths over wide range from 29.9 to 87.1 MPa, are considered. The theoretical values are almost higher than the experimental results (Fig. 2).

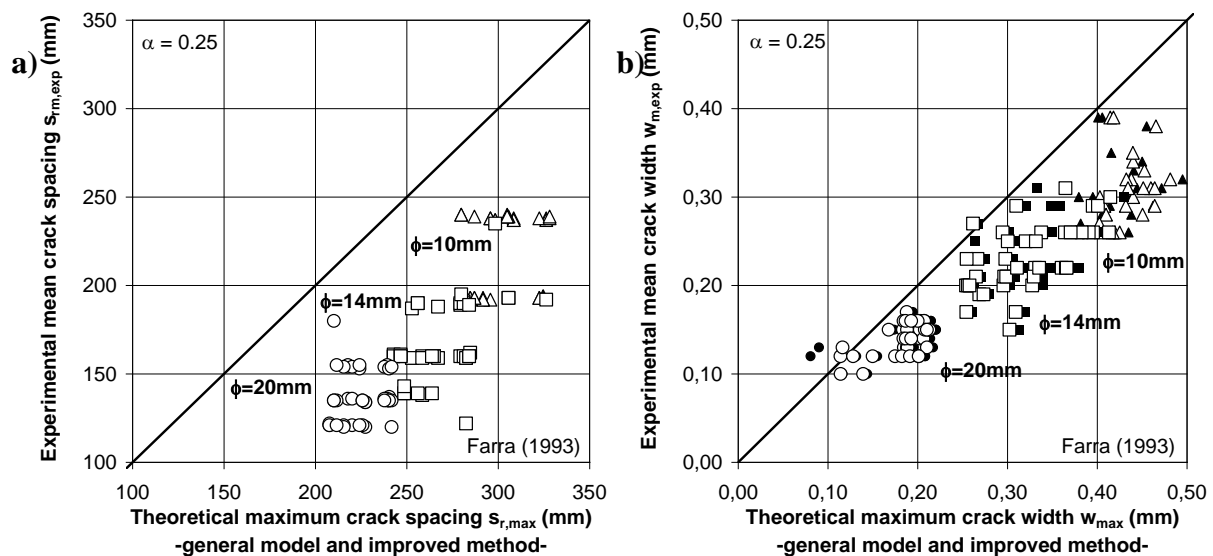


Figure 2 – Comparison between experimental results obtained from Farra’s tests in the stabilized cracking stage and corresponding theoretical values based on the general model (black boxes) and the improved method (white boxes): a) crack spacing; b) crack width.

#### 5. CONCLUSIONS

The general model considers the effect of the secondary cracks in the analysis of the cracking behaviour in the stabilized cracking stage. One of the main results is that during both the crack formation stage and the stabilized cracking stage the average bond stress along the transmission length  $\tau_{bs,m}$  remains unchanged and depends not only on the concrete strength, as assumed in *fib* Model Code 2010, but also on the reinforcement ratio  $\rho_s$  and bar diameter  $\phi_s$ . This result is at the base of the improved calculation method for calculating crack width in RC structures.

From a comparison with experimental data, the theoretical results obtained with the general model and the improved calculation method are almost on the safe side, without the need to introduce, for the crack spacing, a term depending on the concrete cover, as is the case in international standards (*fib* Model Code 2010, Eurocode 2).

#### REFERENCES

- [1] *fib*: “*fib* Model Code for Concrete Structures 2010”, International Federation for Structural Concrete, Ernst & Sohn, Berlin (2013).
- [2] CEN: EN 1992-1-1: “Eurocode 2: Design of Concrete Structures – Part 1-1: General Rules and Rules for Buildings”, European Committee for Standardization, Brussels (2004).
- [3] Debernardi, P.G., Guiglia, M., and Taliano, M.: “Effect of Secondary Cracks for Cracking Analysis of Reinforced Concrete Tie”, *ACI Materials Journal*, vol. 110, No. 2, 2013, pp. 209–216 (2013).

- [4] Debernardi, P.G., Taliano, M.: “An improvement to Eurocode 2 and fib Model Code 2010 methods for calculating crack width in RC structures”, *Structural Concrete*, Ernst & Sohn, Berlin, pp. 365-376 (2016).
- [5] Goto, Y.: Cracks Formed in Concrete around Deformed Tension Bars. *ACI Journal*, vol. 68, No. 4, 1971, pp. 244–251.
- [6] Balázs, G. L.: Cracking Analysis Based on Slip and Bond Stresses. *ACI Materials Journal*, vol. 90, No. 4, 1993, pp. 340–348.



**SEMINAR LECTURES**



## **Evaluation of crack width calculation methods used in design of offshore concrete structures**



Dan-Evert Brekke  
Senior Structural Engineer, M.Sc.  
Multiconsult ASA, Oslo, *Industri, Oil and Gas, Marine Structures*  
e-mail: Dan.Evert.Brekke@multiconsult.no  
+47 99101090

### **ABSTRACT**

Through the development of a post-processor and design software for concrete shell structures, first-hand experience with the complete and complex detail design process for large concrete structures has been obtained. The challenges related to interpretation of crack width calculation methods will be discussed in detail, and recommendations for further development will be suggested.

**Key words:** Crack width calculation methods, large concrete structures, interpretation of design codes, computer assisted design checks.

### **1. INTRODUCTION**

Through the development of a post-processor and design software for concrete shell structures called MultiCon, first-hand experience with the complete and complex detail design process for large concrete structures has been obtained [1]. This experience ranges from the ability to utilize results from large finite element analyzes, to keep track of and process these data in accordance with current regulations and finally document the capacity and need for sufficient reinforcement. This design tool has been the leading program system within the Norwegian offshore concrete business for more than 25 years, from the construction of the Troll A concrete platform for the North Sea in the early 1990s and up to today, with the Hebron concrete platform just completed and installed outside Newfoundland, Canada.

### **2. EVALUATION OF CRACK WIDTH CALCULATION METHODS**

Offshore concrete structures consist mostly of plates and shell structural parts. Most design codes for concrete structures, however, have their origin in beams and columns and one-way plates. Therefore, the interpretation of theoretical formulas in the design codes into practical use for complex plates- and shell structures, has been a challenge. In particular, the ultimate challenge has been the calculation of crack widths and the corresponding code checks related to such strains and cracks.

This presentation, therefore deals with the evaluation of crack width formulas and methods used in the design of offshore concrete structures, all based on experience through direct work within the projects in general, but mostly through the work with the interpretation and use of the design codes within MultiCon. The following topics will be discussed:

- The complexity of the formulas due to the influence of a large number of parameters.

- The challenge when adapting the one directional beam formulas to the two directional plates and shells with orthogonal reinforcement.
- Example of interpretations and misinterpretations in the program code.
- Specific challenges with many layers of reinforcement.

Most commercially available design computer programs perform design code checks for crack widths. However, compared to other types of design code checks, the results seem to vary to a greater extent. The reason for this seems to be a complicated regulatory framework, which is not well defined for a uniform interpretation in the various computer programs. Based on this, it is recommended that any design code should have gone through a data customization verification before deciding the final formula. It is almost impossible to think of all possible contingencies before one has been through an accurate programming phase.

### **3. CONCLUDING REMARKS**

The following concluding remarks are emphasized:

- The knowledge of how cracks really form and develop, and the uncertainty related to which effect the crack widths really have on sustainability, is not well reflected in the crack width formulas available in present design codes.
- Simplified calculation methods **MUST** always give conservative results, compared to formulas that are more complex and meant for overall usage.
- More research, testing and verification is required with the aim to define a more realistic and relevant design check for crack width control.

### **REFERENCES**

- [1] *Brekke, D.-E., Åldstedt, E. & Grosch, H.:* Design of Offshore Concrete Structures Based on Postprocessing of Results from Finite Element Analysis (FEA): Methods, Limitations and Accuracy. Proceedings of the Fourth (1994) International Offshore and Polar Engineering Conference, 1994.

## **Uncertainties of Crack Width Models for Macro and Meso Levels of RC Structural Elements**

Vladimir Cervenka<sup>1</sup>, Jana Markova<sup>2</sup>, Jan Mlcoch<sup>2</sup>, Alejandro Perez Caldentey<sup>3</sup>, Tereza Sajdlova<sup>1</sup> and Miroslav Sykora<sup>2</sup>

<sup>1</sup>Cervenka Consulting, Na Hrebekach 55, 15000 Prague 5, Czech Republic; email: vladimir.cervenka@cervenka.cz

<sup>2</sup>Klokner Institute, Czech Technical University in Prague, Solinova 7, 166 08 Prague, Czech Republic; email: miroslav.sykora@cvut.cz

<sup>3</sup>Polytechnic University of Madrid, Madrid 28040, Spain; email: apc@fhcor.es

### **ABSTRACT**

Crack widths for verification of serviceability limit states can be calculated by simplified formulas provided by codes of practice. Such models are used in design practice. They can be also used for large structural elements such beams and shells in finite element-based structural analysis, referred also as a “macro level” of modelling. Alternatively, a rational crack model can be based on fracture mechanics implemented in a nonlinear finite element method. Authors performed a pilot study with the aim to develop a methodology for assessment of model uncertainty involved in the crack width analysis. Experimental data of four beams were used as a reference of real physical evidence for model validation. Two crack models were investigated, namely a model proposed by the *fib* Model Code 2010 and a numerical model based on the smeared crack with fracture mechanics approach. The results indicate that both models tend to underestimate the real maximal crack width. The mean crack widths are well simulated by the numerical model.

**Key words:** model uncertainty; crack width; numerical simulation; reinforced concrete; fracture mechanics.

### **1. INTRODUCTION**

Adequate description of the uncertainties in resistance models was recognised as one of the key issues in reliability investigations of new and existing reinforced concrete structures. This is namely due to the simplifications in resistance models describing a complex nature of reinforced concrete behaviour. So far the attention has been focussed mainly to the uncertainty of ultimate limit states, see Cervenka (2013). The uncertainties involved in models for serviceability states, namely in the crack width predictions, are not yet sufficiently investigated. An overview of engineering models of cracking in serviceability states is offered by Balázs et al. (2013). It included 23 analytical models for the calculation of crack spacing and 33 different formulae for the crack width estimate.

The present pilot study provides an insight into quantification of model uncertainty in crack width predictions. The experimental data provided by Pérez A. et al. (2013) are used as a reference for the model uncertainty assessment. Two types of models are investigated, namely, the engineering model according to MC2010 *fib* model code and the numerical simulations based on the nonlinear finite element analysis.

### **2. MODEL UNCERTAINTY CONCEPT**

According to the Probabilistic Model Code of the Joint Committee on Structural Safety - JCSS (2001), the model uncertainty covers the simplifications in mathematical formulation of a real

behaviour as observed in tests. It covers the lack of knowledge of the theoretical modelling of structural behaviour and is referred as the epistemic uncertainty. The model uncertainty of crack width is defined as the ratio

$$\theta = w_{exp} / w_{mod} \quad (1)$$

where  $w_{exp}$  is the experimental crack width value and  $w_{mod}$  the crack width calculated by a model. Considering  $\theta$  as a random variable, it can be evaluated for a test series and described by statistical parameters and probability density function.

### 3 EXPERIMENTS

Four specimens from the test series of Pérez et al. (2013) are considered in this study. Beams have identical cross section dimension (35x450mm) but variable reinforcement and cover, see Figure 2 and 2. No stirrups are used. Loading was by four-point bending with a central constant moment region of 3.42m and the end overhanging cantilevers.

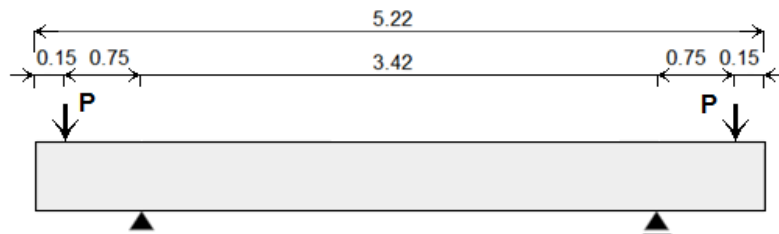


Figure 1. Test setup.

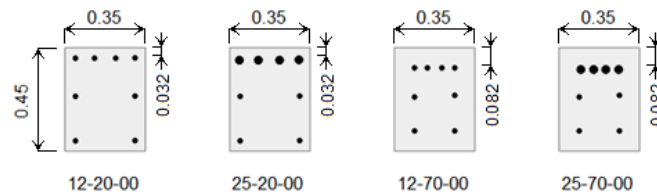


Figure 2. Beam cross-sections.

The reinforcement arrangement is marked by the code under each cross section indicating bar diameter, concrete cover and stirrup spacing (no stirrups in this case), respectively. The series include two bar diameters, 12mm and 25mm, and two cover sizes, 20 and 70mm. Concrete strength was  $f_c = 26.9$  MPa, reinforcement  $f_{yk} = 500$  MPa, reinforcing ratios 0.3 and 1.5%. The test was designed for the investigation of a crack development in a sufficiently long undisturbed constant moment region.

### 3. CRACK WIDTH ACCORDING TO MC2010

#### 3.1 Model for maximum crack width from MC2010

The *fib* model code MC2010 is based on an equilibrium condition for the transfer of the steel stress in crack to the concrete by means of bond stress. The maximum crack width is obtained from the following formula:

$$w_{model} = 2 [k c + 0.25(f_{ct} / \tau_b)(\phi_l / \rho_{s,ef})] [(\sigma_s - \beta \sigma_{sr}) / E_s] \quad (2)$$

where  $k = 1$  - Coefficient of concrete cover effect.  
 $c$  - Concrete cover size.

$f_{ct} / \tau_b \approx 1/1.8$  - Ratio on tensile and bond strengths.

$\sigma_s$  - Steel stress in crack for the applied load.

$\beta = 0.6$  - Tension stiffening factor for short term loading.

$E_s = 200$  GPa - Elastic modulus of reinforcement.

$\sigma_{sr} = (f_{ct} A_{c,ef} / A_{sl}) (1 + \alpha_e A_{sl} / A_{c,ef})$  - Steel stress at crack formation stage.

$A_{c,ef} = b \times \min[2.5(h - d), (h - x)/3, h/2]$  - Effective area of concrete in tension,  $x$  is the distance from neutral axis to compression edge.

### **3.2 Model uncertainties of crack widths by MC2010**

For each specimen the crack width is obtained from Equation (2) and is considered as a maximal crack width. Model uncertainty is obtained from Equation (1). For the sake of this investigation the MC2010-cracks were also compared with the experimental mean cracks.

The statistical parameters of model uncertainties, denoted as  $\mu$  for mean and  $V$  for coefficient of variation, are shown for both crack models in Table 3. The table columns show the loading level corresponding approximately to the target crack width 0.2, 0.4 and 1 mm.

It can be observed that the maximal crack widths predicted by MC2010 are significantly underestimated. The MC2010 maximal cracks are also smaller than experimental mean cracks. There is a strong effect of the reinforcement diameter and somehow smaller effect of the cover. However, the pilot verification is based on a limited database and further investigations are needed to justify these preliminary findings.

## **4. CRACK WIDTHS BY NUMERICAL SIMULATIONS**

### **4.1 Model for numerical simulations**

The numerical simulation is performed by a non-linear finite element analysis with constitutive models for concrete, reinforcement and their interaction. The concrete constitutive model is based on a decomposition of total strain into elastic, plastic and fracture parts in order to describe different failure modes. Real discrete cracks are not modelled. Instead the cracks are represented by a strain localization within continuum. Principles of the model can be characterized by the following features:

- Smearred cracks within finite elements;
- Crack band control of strain localization including effects of crack orientation and element shape function;
- Fixed crack model;
- Two modes of failure are considered on the crack face, Mode I due to normal stress action (crack opening controlled by fracture) and Mode II due to shear stress (shear deformation controlled by a shear factor and shear strength depending on aggregate interlock);
- Reduction of compressive strength due to damage by cracks.

The constitutive model is described in more detail in paper by Cervenka et al. (2008). The calculations are performed by the commercial program ATENA. Bond slip between bars and concrete was modelled by a bond stress-slip relation according to MC2010. The following parameters for concrete were used in simulations: compressive strength  $f_c = 27$  MPa, tensile strength  $f_{ct} = 2.14$  MPa and fracture energy  $G_f = 50$  N/m. The shear factor 20 was used for the Mode II behaviour, which reflects a shear retention stiffness in the cracked state.

#### 4.2 Model uncertainties of crack widths from numerical simulations

A comparison of crack patterns at ultimate loads between experiment and simulations is shown in Figure 3 for the beam specimen 12-70-00 (bar 12mm, cover 70mm) and illustrates a good match of simulations with reality. The prediction of mean cracks by numerical simulation, see Table 1, is almost exact in average, indicating a good model validation.

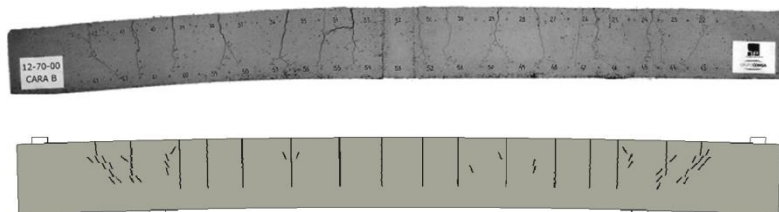


Figure 3. Comparison of crack patterns from experiment and simulation for beam 12-20-00 at  $P=70kN$ .

Table 1. Uncertainties of crack widths models.

		Loading for crack width targets [mm]			Model uncertainty parameters	
		0.2	0.4	1.0	$\mu_{\theta}$	$V_{\theta}$
<b>MC2010</b>	$\theta_{w\ mean}$	1.542	1.295	1.179	<b>1.34</b>	<b>0.40</b>
	$\theta_{w\ max}$	2.427	2.015	2.004	<b>2.15</b>	<b>0.37</b>
<b>NLFEM</b>	$\theta_{w\ mean}$	1.218	1.071	0.978	<b>1.09</b>	<b>0.35</b>
	$\theta_{w\ max}$	1.831	1.496	1.264	<b>1.53</b>	<b>0.36</b>

The results indicate a greater scatter of experimental crack widths, which can be attributed to a random material distribution within specimen, but not considered in simulation. It is a motivation for the future research and development of the numerical model.

#### 5. APPLICATIONS

The above cracks models have been extensively applied by users of the commercially available code ATENA.

The macro-level model based on a simplified equilibrium assumptions according to MC2010, is used in the most industrial applications, where elements of large size are a practical solution. In such cases high order layered shell elements and beams with fibre integration scheme are typically used. An example of such an application is the nuclear containment structure tested in BARC project in India shown in Figure 4.

Figure 5 shows an assessment of crack width for existing tunnel in Rotterdam. This analysis is based on fracture mechanics and smeared crack approach. The aim was to evaluate the reliability of the tunnel damaged by corrosion after 70 years in service.

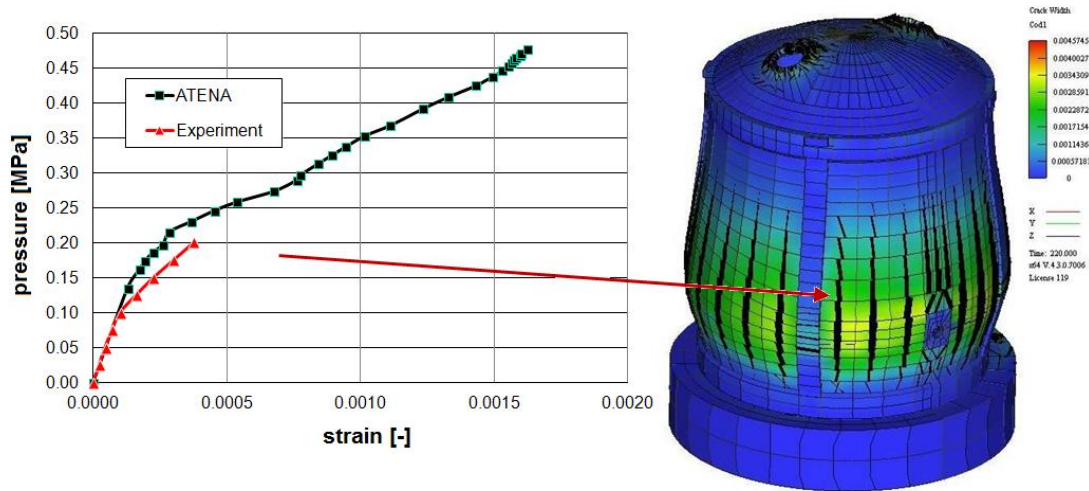


Figure 4. Simulation of nuclear containment test, BARC, India.

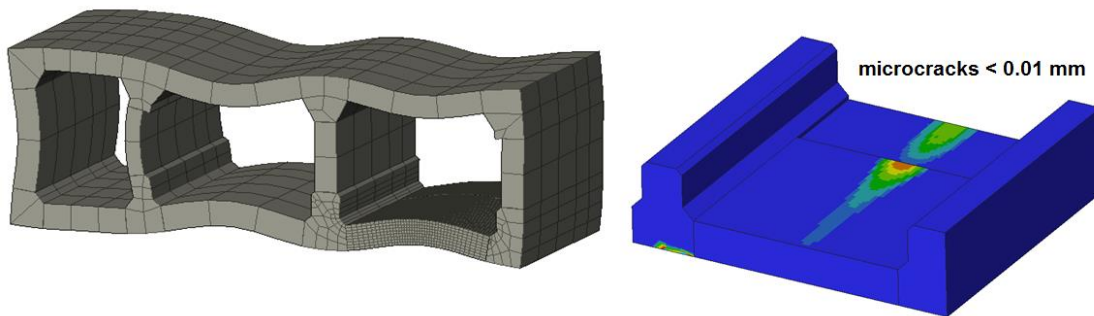


Figure 5. Crack width analysis of Maastunnel in Rotterdam.

## 6. CONCLUSIONS

The uncertainty of crack width models was investigated in this pilot study based on the experiments of four beams. The engineering model from the *fib* Model Code 2010 seems to underestimate both mean crack widths ( $\mu_\theta = 1.34$ ,  $V_\theta = 0.42$ ) and maximal crack widths ( $\mu_\theta = 2.15$ ,  $V_\theta = 0.38$ ), meaning that the maximal crack is underestimated by about 55%. Moreover the scatter is very large.

The numerical model reflects well the mean experimental crack widths ( $\mu_\theta = 1.09$ ,  $V_\theta = 0.35$ ). The maximal crack widths ( $\mu_\theta = 1.53$ ,  $V_\theta = 0.36$ ) are underestimated by about 35%. This is attributable to the fact that the maximal crack width from numerical simulations was not based on a probabilistic model and the effect of spatial variability of material properties could not be fully captured. This issue shall be addressed in future investigations. For generally valid conclusions more extensive investigation based on a larger experimental database base should be made.

## ACKNOWLEDGEMENTS

This work has been supported by the Czech Science Foundation within the project 16-04132S. The contribution of Jan Mlcoch has been supported by Grant SGS16/195/OHK1/2T/31 supported by the Czech Technical University in Prague.

## REFERENCES

Balázs, G. et al. (2013). "Design for SLS According to *Fib* Model Code 2010." *Structural Concrete* 14 (2): 99-123.

Cervenka, J., Papanikolaou, V.K. (2008). Three Dimensional Combined Fracture-Plastic Material Model. *Int. Jour. Plasticity*, Vol 24(12), 2008, pp. 2192-2220.

Cervenka, V. (2013). Reliability-based non-linear analysis according to *fib* Model Code 2010, *Structural Concrete*, Vol. 14, March 2013, pp. 19-28.

*fib* (2013). *fib Model Code for Concrete Structures 2010*. Lausanne: *fib*.

Holicky, M. et al. (2016). "Assessment of Model Uncertainties for Structural Resistance." *Probabilistic Engineering Mechanics* 45: 188-197.

JCSS (2001). *JCSS Probabilistic Model Code (Periodically Updated, Online Publication)*, Joint Committee on Structural Safety.

Pérez, A. et al. (2013). "Cracking of RC Members Revisited: Influence of Cover,  $\phi/\rho_{s,ef}$  and Stirrup Spacing - an Experimental and Theoretical Study." *Structural Concrete* 14 (1): 69-78.

Sykora, M. et al. (2015). "Uncertainties in Resistance Models for Sound and Corrosion-Damaged RC Structures According to EN 1992-1-1." *Materials and Structures* 48 (10): 3415-3430.

## **The modelling uncertainty of non-linear finite element analyses of concrete structures**



Morten Engen  
M.Sc. PhD-candidate  
Multiconsult ASA, Oslo, Norway & NTNU, Norwegian University of Science and Technology, Department of Structural Engineering, Trondheim, Norway  
morten.engen@multiconsult.no



Max A. N. Hendriks  
PhD, Professor  
NTNU, Norwegian University of Science and Technology, Department of Structural Engineering, Trondheim, Norway & Delft University of Technology, Faculty of Civil Engineering and Geosciences, Delft, The Netherlands  
max.hendriks@ntnu.no

### **ABSTRACT**

The modelling uncertainty of non-linear finite element analyses of reinforced concrete structures is discussed along with different measures of the modelling uncertainty often encountered in the literature. It is emphasized that a pure modelling uncertainty without additional contributions from measuring uncertainties and physical uncertainties is not trivial to obtain.

**Key words:** Large concrete structures, non-linear finite element analyses, modelling uncertainty.

### **1. INTRODUCTION**

Non-linear finite element analyses (NLFEA) have received increased attention in the engineering community during the last decade, particularly after the introduction of the semi-probabilistic safety formats for NLFEA in *fib* Model Code 2010 [1]. In order to perform a NLFEA, the analyst must select a suitable solution strategy, which consists of all the choices related to equilibrium, kinematic compatibility and material models [2]. Since the mechanical models that are used in the NLFEA are only simplifications of the reality, the outcome of the analysis will only be an approximation to the real observable outcome. This deviation is normally called the modelling uncertainty. Usually, the modelling uncertainty is discussed for models simulating the ultimate limit state of a structure, however, the concept applies equally well to serviceability state predictions. In this contribution, the modelling uncertainty is defined and common measures often encountered in the literature are presented and discussed [3].

### **2. THE MODELLING UNCERTAINTY**

Our mechanical models consist of mathematical expressions describing complex physical phenomena [4,5]. The mathematical expressions can be of variable degree of complexity and can depend on a limited number of basic variables, and the model can be selected from a range of different models describing the same physical phenomenon. The degree of complexity and the number of variables is usually limited either by lack of knowledge or for practical reasons.

The modelling uncertainty thus arises due to the limited number of variables that are included in the model, the complexity of the mathematical model and the likelihood of the selected model being correct. In addition, if the model is empirically based, the parameters of the model are also uncertain since they are estimated from experiments. The accuracy of the estimated values of the parameters depends on the number of observations that the estimate is based on, and can generally

be improved if the number of observations is increased [5]. It is emphasized that the fact that the models are uncertain does not mean that the outcomes of our models are random. In fact, if a NLFEA prediction of the load-carrying capacity of a structure is repeated, the outcome will always be the same, however, the outcome is uncertain, since the model is only a simplification of the reality.

A model can have a set of variables that need to be treated as basic variables. If some of the variables are not directly available or directly observable in standard material tests, and there exist models expressing any of the variables as function of other variables, these models can be used as sub-models. This is common in NLFEA of concrete structures, where material models for concrete usually take many basic variables. It is important to note that as soon as a sub-model is used for estimating the value of one of the variables, the sub-model becomes a part of the model, and the modelling uncertainty of the sub-model contributes to the modelling uncertainty of the whole model. The variable that is estimated changes from a variable that is explicitly modelled as a basic variable to a variable that is implicitly taken care of by the model. In other words, what is not explicitly considered in the model, implicitly contributes to the modelling uncertainty [4,6].

In the context of NLFEA, the modelling uncertainty,  $\theta$ , is usually defined as

$$\theta = \frac{R_{\text{exp}}}{R_{\text{NLFEA}}} \quad , \quad (1)$$

where  $R_{\text{exp}}$  is the measured outcome from an experiment, and  $R_{\text{NLFEA}}$  is the predicted outcome of the experiment using NLFEA [1,7]. Due to the relation in Eq. (1), the *estimated* modelling uncertainty depends on the uncertainty in the outcome and measurement of  $R_{\text{exp}}$  [6,8].

### **3. MEASURES OF THE MODELLING UNCERTAINTY**

The models used in engineering analyses are only approximations of the reality. The question that must be asked is whether the model is suitable for the particular application where it is to be used. This can be assessed by quantifying the modelling uncertainty. The modelling uncertainty of a solution strategy for NLFEA,  $\theta$  as defined in Eq. (1), is usually assumed represented by a log-normally distributed variable. The probability distribution for the modelling uncertainty can be given in terms of the mean,  $\mu_\theta$ , and the coefficient of variation,  $V_\theta$ , that are generally unknown parameters and should be estimated by performing benchmark analyses, i.e. comparing NLFEA predictions to known experimental outcomes.

The mean can be denoted the *bias* and indicates the average fit to experimental results. Note that if a model with free parameters is calibrated to experimental outcomes, the bias will be  $\mu_\theta = 1.0$  for the set of experiments it was calibrated to. However, using a model without free parameters that are calibrated,  $\mu_\theta \neq 1.0$ . The coefficient of variation is a measure of the *spread* of the NLFEA predictions. For example, if no NLFEA prediction is found to be equal to the experimental outcome, the predictions can still on average be close to the experimental outcomes, however having a coefficient of variation that depends on the respective deviations from the average.

In the literature, one can encounter one of the following three limiting cases when NLFEA predictions are compared to experimental outcomes: i) one experimental outcome is compared to NLFEA predictions using different solution strategies, ii) the outcomes of a number of nominally equal experiments are compared to one NLFEA prediction of the experiment using one solution

strategy and iii) one experimental outcome from each of a range of different experiments are compared to corresponding NLFEA predictions using one solution strategy.

If the modelling uncertainty is estimated in each of the cases, the estimate will describe three different effects. In the first case, the estimator for the modelling uncertainty,  $\theta_1$ , becomes

$$\theta_{1,i} = \frac{R_{\text{exp}}}{R_{\text{NLFEA},i}} \quad , \quad (2)$$

where  $R_{\text{NLFEA},i}$  is NLFEA prediction  $i$ . By taking the expected value of Eq. (2) it can be shown that the bias will be the ratio between the experimental outcome and the average NLFEA prediction. By finding the coefficient of variation of Eq. (2), it can be shown that this only depends on the variation of the NLFEA predictions.  $\theta_1$  is thus a measure of the inherent randomness in the population of models, or *between-model* uncertainty, and describes the obtained uncertainty in the prediction if a model was selected randomly to predict the experimental outcome. Interesting to note is that if  $R_{\text{exp}}$  was an average of the outcomes from a number of nominally equal experiments instead of only the outcome from one of the experiments, this would only influence the bias and not the coefficient of variation of  $\theta_1$ . Case 1 is the typical outcome from blind prediction competitions.

In the second case, the estimator for the modelling uncertainty,  $\theta_2$ , becomes

$$\theta_{2,i} = \frac{R_{\text{exp},i}}{R_{\text{NLFEA}}} \quad , \quad (3)$$

where  $R_{\text{exp},i}$  is the outcome of experiment  $i$ . Since  $R_{\text{NLFEA}}$  is a constant,  $\theta_2$  only describes the average and the variation of the experimental outcomes, scaled by the constant NLFEA prediction. Eq. (3) thus describes the physical variation of the experiment.

In the third case, the estimator becomes

$$\theta_{3,i} = \left( \frac{R_{\text{exp}}}{R_{\text{NLFEA}}}_i \right) \quad , \quad (4)$$

and  $\theta_3$  describes the uncertainty in the prediction obtained with the selected solution strategy. Opposed to  $\theta_1$  which describes between-model uncertainty,  $\theta_3$  describes *within-model* uncertainty. It is emphasized that if Eq. (4) is to give reasonable results, the engineer must have available the experimental outcome  $R_{\text{exp}}$  and the corresponding values of the basic variables that are needed for input to the NLFEA prediction [4,5]. In addition, if values of some of the basic variables need to be estimated using available sub-models, the sub-models must be applied consistently from case to case. Otherwise,  $\theta_3$  will not describe the modelling uncertainty of the specific solution strategy. Interesting to note here is that if  $R_{\text{exp}}$  in Eq. (4) was replaced by the average of the outcomes from a number of nominally equal experiments instead of only one outcome, both the estimated bias and the coefficient of variation of the modelling uncertainty would be influenced. This indicates that the estimated modelling uncertainty also gets contributions from the uncertainty of the measurement of the experimental outcome, and from the physical uncertainties related to the experimental outcome. A pure modelling uncertainty without

additional contributions from measuring uncertainties and physical uncertainties is thus not trivial to obtain [6].

Often, the modelling uncertainty for a defined range of values of the basic variables, or for specific failure modes, is sought. In that case, only a sample of experimental outcomes could be selected, reflecting the defined range. If however, the relevant subset of values for the basic variables and the failure mode is unknown, the sample of benchmark experiments should cover a larger range. This would be relevant in a design situation, where the failure mode is not known on beforehand, it can be different for different values of the basic variables and the failure mode might be due to interaction between different sectional forces. Several studies where the modelling uncertainty has been quantified using Eq. (4), can be found in the literature [2,6,8].

### **3. DISCUSSIONS AND CONCLUSIONS**

With the present methods for quantifying the modelling uncertainty, the estimate will always have contributions from physical uncertainties. The phenomena that are not explicitly considered in the benchmark analyses from which the modelling uncertainty is estimated, are implicitly included in the modelling uncertainty. This can be unfortunate, since the modelling uncertainty will carry most of the uncertainties, and the engineer is left with few possibilities for reducing the epistemic uncertainties of the problem. However, it can also be useful, since all the uncertainties that could not be isolated in the benchmark analyses, are included in the modelling uncertainty, and should thus not be included in later analyses. Future design codes could include brief guidance for how NLFEA should be used in the design process. The codes should be open to let the designers develop their own solution strategies, but should also provide values for the modelling uncertainty that could be used by the designer. A suggestion is to study within- and between-model uncertainty, represented by  $\theta_3$  and  $\theta_1$  in order to estimate a suitable upper bound value. The modelling uncertainty could be given either as a bias and a coefficient of variation, or as a global resistance factor.

### **ACKNOWLEDGEMENTS**

The funding from Multiconsult ASA and the Research Council of Norway is highly appreciated.

### **REFERENCES**

- [1] *fib: fib* Model Code for Concrete Structures 2010. Ernst & Sohn, 2013.
- [2] Engen, M., Hendriks, M. A. N., Øverli, J. A. & Åldstedt, E.: Solution strategy for non-linear Finite Element Analyses of large reinforced concrete structures. *Structural Concrete*, 2015, 16(3), 389-397.
- [3] Engen, M.: Aspects of design of reinforced concrete structures using non-linear finite element analyses: Solution strategy, modelling uncertainty and material uncertainty. PhD Thesis, NTNU, Trondheim, Norway.
- [4] Ditlevsen, O.: Model uncertainty in structural reliability. *Structural Safety*, 1982, 1(1), 73-86.
- [5] Der Kiureghian, A. & Ditlevsen, O.: Aleatory or epistemic? Does it matter? *Structural Safety*, 2009, 31(2), 105-112.
- [6] Engen, M., Hendriks, M. A. N., Köhler, J., Øverli, J. A. & Åldstedt, E.: A Quantification of the Modelling Uncertainty of Non-linear Finite Element Analyses of Large Concrete Structures. *Structural Safety*, 2017, 64(1), 1-8.
- [7] JCSS: Probabilistic Model Code, 12th draft. Joint Committee on Structural Safety, 2001.
- [8] Holický, M., Retief, J. & Sýkora, M.: Assessment of model uncertainties for structural resistance. *Probabilistic Engineering Mechanics*, 2016, 45, 188-197.

## **Influence of cracking on reinforcement corrosion**



Karla Hornbostel  
M.Sc., Ph.D., Senior engineer  
Norwegian Public Roads Administration, Trondheim, Norway  
e-mail: [karla.hornbostel@vegvesen.no](mailto:karla.hornbostel@vegvesen.no)



Mette Geiker  
M.Sc. Ph.D., Professor  
Norwegian University of Science and Technology, Department of  
Structural Engineering, N-7491 Trondheim  
e-mail: [mette.geiker@ntnu.no](mailto:mette.geiker@ntnu.no)

### **ABSTRACT**

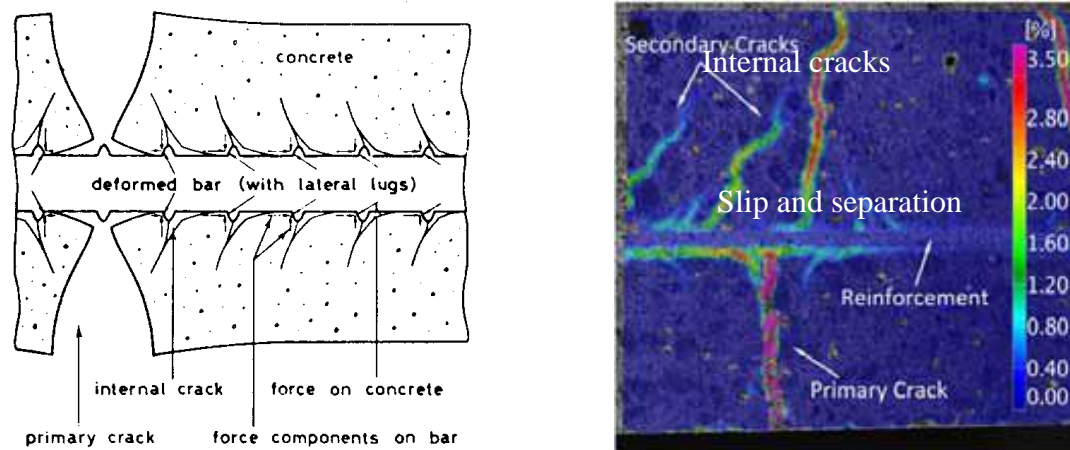
This extended abstract gives a brief overview of the state-of-the-art on the impact of concrete cracking on the corrosion of embedded reinforcement. There is consensus that cracks promote the ingress of among others carbon dioxide and chloride, and thus facilitate initiation of corrosion of possible exposed reinforcement. However, contradicting conclusions regarding propagation of corrosion are reached based on short- and long-term observations. Whereas short-term studies suggest that corrosion is enhanced by cracks, the few reported long-term studies indicate limited impact of small cracks. Consequently, there is need for detailed long-term data and improved understanding of the mechanisms of corrosion propagation of steel reinforcement embedded in cracked concrete.

**Key words:** Cracking, durability, corrosion, consequences of cracking.

### **1 INTRODUCTION**

This extended abstract briefly summarises the state-of-the-art regarding the impact of cracking on the corrosion initiation and propagation of reinforcement embedded in concrete. The text is to a large extent based on recent State-of-the-Art reports, especially [1-3].

Reinforcing steel is protected by the surrounding concrete. The high alkalinity of sound concrete causes a passive layer to form on the steel, and the concrete cover protects the steel from aggressive substances. Cracking of concrete may occur due to several reasons. Causes and characteristics of cracking as well as the impact of cracking on transport of matter are outside the scope of this extended abstract; the interested reader is referred to e.g. [2, 4-8]. Most of the cracks considered and described in the literature are cracks perpendicular to the reinforcement. After a primary crack has formed, a further increase in stress in the reinforcement bar will lead to the formation of internal cracks due to loss of adhesion (debonding) (Figure 1). Debonding is observed as slip (parallel relative displacement of concrete from steel) and separation (series of local perpendicular displacements in the vicinity of the ribs, see Figure 1a). Further stress increase can cause the internal cracks to penetrate to the surface and become secondary cracks [6].



a) Schematic illustration of damage and cracking (primary and internal cracks) at the steel-concrete interface [6].  
b) Photogrammetric assessment of cracking in reinforcement concrete beams subjected to bending. Tensile stresses at bottom. After [2].

Figure 1 – Crack morphology of cracks perpendicular to the reinforcement.

There is consensus that cracks promote the ingress of among others carbon dioxide and chloride, and thus facilitate initiation of corrosion of possible exposed reinforcement. Depending on the moisture content, cracking also facilitate transport of water and/or oxygen into the concrete. However, the extent to which cracking influences corrosion propagation is unclear.

The potential impact of cracks on durability is commonly controlled through crack width requirements (cf. Eurocode 2, MC2010 etc.). One of the central documents for the present crack width regulations is a report by Beeby [9] containing the following statement concerning the influence of cracks on corrosion: “...It should also be noted that, from the point of view of corrosion control, the permissible crack width of 0.3 mm specified in CP110 (or indeed any other width) cannot be justified in any logical way from test evidence: it is simply a guess.”

In the following, the initiation and propagation of corrosion in cracked concrete are treated separately.

## 2 IMPACT OF CRACKING ON CORROSION INITIATION

As mentioned in the introduction, there is consensus that cracks promote the ingress of among others carbon dioxide and chloride, and thus facilitate initiation of corrosion of possible exposed reinforcement. However, there is no consensus regarding possible critical crack width with regard to corrosion initiation as illustrated in Figure 2.

The possible impact of internal cracking (cf. Figure 1) on corrosion initiation was studied by Michel et al. [10] using an instrumented rebar with isolated carbon steel sensors placed in 17 holes with 10 mm spacing. Cracked beams with instrumented rebars were exposed to a sodium chloride solution in the cracked area and the location dependent electrochemical potentials and corrosion rates were monitored up to 25 days after exposure ((a) and (b) Figure 3. The bottom (c) figure (Figure 3) illustrates the extent of debonding (slip and separation). Potential drop and corrosion initiation were observed along the rebar in the debonded area shortly after exposure. [10]

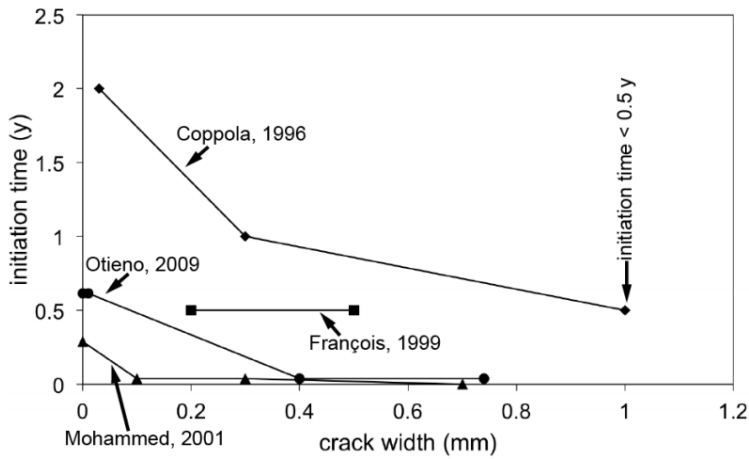


Figure 2 - Literature review on corrosion initiation, figure from [3]. References can be found in the reference list to this extended abstract [11-14].

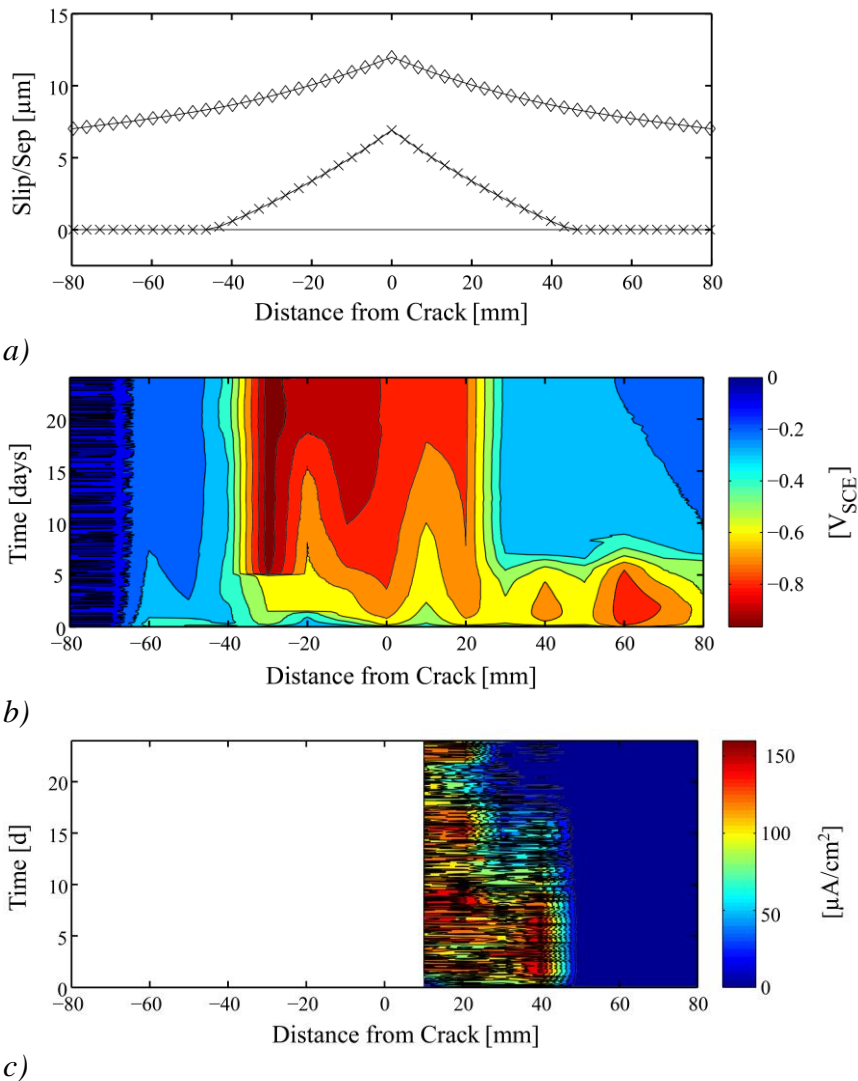


Figure 3 – Short-term impact of cracking on corrosion initiation monitored using an instrumented rebar. a): Slip and separation, b) and c): location dependent electrochemical potentials and corrosion rates. “0” corresponds to location of primary crack at reinforcement. After [10].

### 3 CORROSION MECHANISMS IN CRACKED CONCRETE

Two potential corrosion mechanisms are described for reinforcement intersecting a crack: cf. Figure 4 [15]:

- Micro-cell corrosion, where both anodic and cathodic reactions occur in the cracked area (Figure 4 a)). This corrosion mechanism is comparable to that of atmospherically exposed steel.
- Macro-cell between the more noble (i.e., passive) reinforcement in the undamaged concrete and the exposed (and active) reinforcement in the crack (Figure 4 b)).

The macro-cell mechanism (Figure 4 b)) is proposed to dominate corrosion propagation for cracked concrete and high corrosion rates are to be expected due to the high cathode/anode ratio [15].

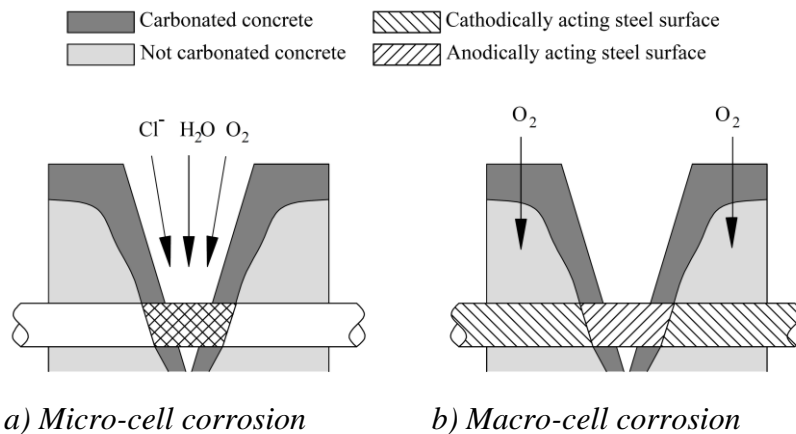


Figure 4 – Corrosion mechanism in cracked concrete. After [15].

### 4 IMPACT OF CRACKING ON CORROSION PROPAGATION

Whereas it is commonly agreed that cracks facilitate corrosion initiation (cf. earlier section), no consensus on the influence of cracking on corrosion propagation has been reached.

Schiessl and Raupach [16] observed time-dependent differences for the impact of crack width on the corrosion rate. Using cyclic chloride exposure, the mass loss of reinforcement due to corrosion was determined 24 and 88 weeks after corrosion initiation. Increasing corrosion rate was found with increasing crack width (0.1 – 0.5 mm crack width tested) after 24 weeks, whereas no pronounced difference was observed after 88 weeks. The results indicate that the influence of crack width on corrosion rate is decreasing with time [16]. The apparent decreasing long-term influence of crack width on corrosion propagation was confirmed in other experimental and in-situ investigations for comparable crack widths (0.5 mm and less), [17-21].

Different types of self-healing are the general hypotheses for reduced corrosion propagation or even re-passivation: precipitation in cracks [19, 22], (in seawater exposure typically magnesium hydroxide and calcium carbonate), deposition of corrosion products in cracks [17, 23] and blocking of the cracks by other means e.g. debris and dust [17, 23].

The assumed positive effect of self-healing of the cracks has not been reported for cracks reopened due to cyclic loading (dynamic cracks). Cyclic loading can lead to further damage development,

reduced crack tortuosity, and removal of deposits in the crack [24]. In line with this, are observations by Otieno, Alexander [12] who reported higher corrosion rates under cyclic loading compared to dormant cracks. Re-passivation is neither expected for cracks with larger crack widths, low cover thickness or high porosity, water flowing through cracks and combined presence of chlorides and carbonation [25].

Dependent on the crack morphology, concrete cover thickness (and quality) appears more decisive for corrosion propagation than the surface crack width [16, 17, 26-28]. A possible explanation is the lack of correlation between crack width at the surface and near the rebar. In addition, the effect of debonding between the steel-concrete interface was suggested to have an influence on the corrosion extent, supposedly be more important than surface crack width [2, 10, 29].

In addition to crack morphology and cover quality the orientation of the crack compared to the reinforcement must be considered. Cracks longitudinal to the reinforcement showed a higher mass loss compared to cracks transverse to the reinforcement (crack width < 0.4 mm) [15]. However, for transverse cracks the cathode-to-anode-area-ratio is higher than for longitudinal cracks, which may lead to a higher local cross section reduction [5, 30-32].

Considering the cathode-to-anode-area-ratio, it may be expected that increased crack frequency (smaller crack distances) causes reduced local corrosion rate due to the limited available cathode area [16, 33]. However, using smaller bar diameters and a denser reinforcement network to distribute cracks and reduce the crack width, can result in overall increased corrosion damage. The effect is explained by the relative cross section loss being higher for small bar diameters compared to large diameters [16, 19, 26, 34].

## **5 SUMMARY**

In the literature, there is consensus on the promoting influence of concrete cracking on the initiation of reinforcement corrosion.

Corrosion propagation in cracked concrete is not yet fully understood. Contradicting conclusions are reached based on short- and long-term observations. Short-term investigations (up to a few years) indicate that corrosion rates are enhanced by cracks and mainly depend on cover depth and concrete quality rather than on crack width. The few undertaken long-term studies indicate that small cracks have limited influence on corrosion propagation. However, we do at present not have sufficient background for such a general statement. Thus, there is a need for detailed long-term data and understanding of mechanism of corrosion propagation of steel reinforcement embedded in cracked concrete.

## **ACKNOWLEDGEMENTS**

This extended abstract is partly based on unpublished material prepared in collaboration with Brad Pease. The contribution from Brad Pease is greatly acknowledged. We should also like to thank Reignard Tan and Alexander Michel for discussions on crack formation.

The extended abstract is prepared as part of the “Ferry free E39”, project WP 7.1.1. The funding from the Norwegian Public Road Authority is very much appreciated.

## **REFERENCES**

1. The Concrete Society, *Relevance of cracking in concrete to reinforcement corrosion*, in *Technical Report 44*. 2015.

2. Pease, B., *Influence of concrete cracking on ingress and reinforcement corrosion*, in *Department of Civil Engineering*. 2010, Technical University of Denmark.
3. Angst, U.M., *Påvirker riss i betongen korrosjon på armeringen?*, in *Fagdag Varige Konstruksjoner*. 2016: Oslo, Norway.
4. Berrocal, C.G., et al., *Characterisation of bending cracks in R/FRC using image analysis*. Cement and Concrete Research, 2016. **90**: p. 104-116.
5. CEB, *Non-structural cracks in concrete*, in *Concrete Society Report no.22*. 1992: London.
6. Goto, Y., *Cracks formed in concrete around deformed tension bars*. Journal of the American Concrete Institute, 1971. **68**(4): p. 244-251.
7. Michel, A., *Reinforcement Corrosion: Numerical Simulation and Service Life Prediction*, *Doctoral Thesis*. 2013, Technical University of Denmark.
8. Klausen, A.B.E., *Consequences of cracking related to tightness*, in *Nordic mini-seminar: Crack width calculation methods for large concrete structures*. 2017: Oslo, Norway.
9. Beeby, A.W., *Concrete in the oceans; cracking and corrosion*. CIRIA/UEG & Cement and Concrete Association & Department of Energ. 1978, Wexham Springs. 77 p.
10. Michel, A., et al., *Experimental investigation of the relation between damage at the concrete-steel interface and initiation of reinforcement corrosion in plain and fibre reinforced concrete*. Corrosion Science, 2013. **77**: p. 308-321.
11. Coppola, L., et al., *Corrosion of Reinforcing Steel in Concrete Structures Submerged in Seawater*. American Concrete Institute, 1996. **163**: p. 127-150.
12. Otieno, M.B., M.G. Alexander, and H.D. Beushausen, *Corrosion in cracked and uncracked concrete - influence of crack width, concrete quality and crack reopening*. Magazine of Concrete Research, 2010. **62**(6): p. 393-404.
13. Francois, R. and G. Arliguie, *Effect of microcracking and cracking on the development of corrosion in reinforced concrete members*. Magazine of Concrete Research, 1999. **51**(2): p. 143-150.
14. Mohammed, T.U., et al., *Effect of crack width and bar types on corrosion of steel in concrete*. Journal of Materials in Civil Engineering, 2001. **13**(3): p. 194-201.
15. Schiessl, P., *Einfluss von Rissen auf die Dauerhaftigkeit von Stahlbeton- und Spannbetonbauteilen*. Deutscher Ausschuss fuer Stahlbeton. 1986, Berlin: Ernst. 129 S.
16. Schiessl, P. and M. Raupach, *Laboratory studies and calculations on the influence of crack width on chloride-induced corrosion of steel in concrete*. Aci Materials Journal, 1997. **94**(1): p. 56-62.
17. Schiessl, P., *Zur Frage der zulaessigen Rissbreite und der erforderlichen Betondeckung im Stahlbetonbau unter besonderer Beruecksichtigung der Karbonatisierung des Betons*. Deutscher Ausschuss fuer Stahlbeton Heft 255. 1976, Berlin: Ernst.
18. Yachida, M., *Cracking and reinforcement corrosion in reinforced concrete bridges*. Journal of Materails - Concrete Structures and Pavements, 1987. **6**(378): p. 195-202.
19. Arya, C. and F.K. Ofori-Darko, *Influence of crack frequency on reinforcement corrosion in concrete*. Cement and Concrete Research, 1996. **26**(3): p. 345-353.
20. Beeby, A.W., *Cracking - What Are Crack Width Limits For*. Concrete, 1978. **12**(7): p. 31-33.
21. Schiessl, P. and E. Woelfel, *Konstruktionsregeln zur Beschränkung der Rissbreite - Grundlage zur Neufassung DIN 1045, Abschnitt 17.6 Beton- und Stahlbetonbau*, 1986. **81**(1): p. 8-15.
22. Ramm, W. and M. Biscopig, *Autogenous Healing and Reinforcement Corrosion of Water-Penetrated Separation Cracks in Reinforced Concrete*. Nuclear Engineering and Design 1998. **179**(2): p. 191-200.

23. Tuutti, K., *The corrosion of steel in concrete - the effect of cracks in the concrete cover* in *CBI Forsk.* 1978, Swedish Cement and concrete Research Institute at the Institute of Technology, Stockholm.
24. Edvardsen, C., *Water permeability and autogenous healing of cracks in concrete.* *Aci Materials Journal*, 1999. **96**(4): p. 448-454.
25. Bertolini, L., et al., *Corrosion of steel in concrete prevention, diagnosis, repair.* 2nd, completely rev. and enlarged ed. 2013, Weinheim: Wiley-VCH. 414 S.
26. Houston, J., A. E., and P. Ferguson, *Corrosion of reinforcing steel embedded in structural concrete* in *Research Report 112-1F.* 1972, Center for Highway Research, University of Texas at Austin.
27. Kamiyama, H., *Rust of steel bars in concrete (in Japanese).* *Cement and Concrete*, 1972. **308**: p. 50-57.
28. Nishiyama, H. *Experiments of Steel Corrosion due to Cracking.* in *Proceedings of the 30th Annual Conference of the Japan Society of Civil Engineers.* 1975.
29. Pease, B., et al., *The design of an instrumented rebar for assessment of corrosion in cracked reinforced concrete.* *Materials and Structures*, 2011. **44**(7): p. 1259-1271.
30. Jaffer, S.J. and C.M. Hansson, *The influence of cracks on chloride-induced corrosion of steel in ordinary Portland cement and high performance concretes subjected to different loading conditions.* *Corrosion Science*, 2008. **50**(12): p. 3343-3355.
31. Poursaei, A. and C.M. Hansson, *The influence of longitudinal cracks on the corrosion protection afforded reinforcing steel in high performance concrete.* *Cement and Concrete Research*, 2008. **38**(8-9): p. 1098-1105.
32. Nuernberger, U., *Chloridkorrosion von Stahl in gerissenem Beton.* Deutscher Ausschuss fuer Stahlbeton. 1988, Berlin: Beuth. 144 S.
33. Raupach, M., *Zur chloridinduzierten Makroelementkorrosion von Stahl in Beton (in German).* Deutscher Ausschuss für Stahlbeton. Vol. Heft 433. 1992, Berlin: Beuth Verlag GmbH.
34. Schiessl, P. and M. Raupach, *Laboruntersuchungen und Berechnungen zum Einfluss der Rissbreite des Betons auf die chloridinduzierte Korrosion von Stahl in Beton.* *Bauingenieur*, 1997. **69**(11): p. 439.



## **Control of cracking due to restrained deformations imposed at early ages or later (Related to a new Annex proposed for Eurocode 2)**



Terje Kanstad  
Professor, Dr.ing.  
NTNU, Department of structural engineering  
N-7491 Trondheim  
E-mail: [terje.kanstad@ntnu.no](mailto:terje.kanstad@ntnu.no)

### **ABSTRACT**

The paper is related to the ongoing revision work of EN 1992 (Eurocode 2), and deals with the proposed new Annex for handling of cracking due to imposed deformations. The paper refers ongoing work, and the presented approach is therefore not final. Assessment of temperature history, calculation of stresses and crackwidths is considered, and the most important material properties are described.

**Key words:** Cracking, Restrained deformations, Calculations, Standard

### **1. INTRODUCTION**

This paper is due to the ongoing revision of EN 1992-1-1 (Eurocode 2), and its new Annex D, which has working title: “Control of cracking due to restrained deformations imposed at early ages or later.” Formally, the work on the Annex is under the umbrella of CENTC250/SC2/WG1, (which is the main committee for Eurocode 2), but it is handled by its technical committee on time-dependent effects (TG2), and the undersigned in particular. Presently, Annex D is under elaboration by the project team (PT), who actually writes the 1<sup>st</sup> version of the standard text. Therefore, the current extended abstract, and the miniseminar-presentation must be considered as a step on the road.

It is now estimated that the 1<sup>st</sup> full draft of the modified Eurocode 2 will be finished within two years from now, but still the final publishing date might come as late as in 2025. It is also important to be aware of that the new Eurocode 2 in addition shall replace EN 1992-2 Reinforced and prestressed concrete bridges, and EN 1992-3 Liquid retaining and containing structures.

### **2. SCOPE**

The major focus is on through-cracks, which may span over the whole thickness of the concrete member, and occur in the cooling phase of the hardening process, typically between 2 and 30 days after casting, but also develop at later ages. Possible measures to reduce the amount of through-cracking are to use concretes with low heat production during hydration, concretes with low coefficient of thermal expansion, cooling pipes in the hardening concrete, heating cables in the restraining structural elements, reduced fresh concrete temperature, or to reduce the degree of restraint for structural members prone to cracking.

The following three states might be considered:

- (1) At temperature-equilibrium between the recently cast and the restraining member.
- (2) During the design service life

If particular demands are related to tightness, durability or appearance, cumulative impact of early age effects, load effects and later imposed deformations must be considered in the crack control verification. Otherwise, the crack control corresponding to these states can be verified separately. To avoid cracking, requirements can be related to stresses through the crack risk expressed by stresses, while to restrict cracking, limiting calculated crack widths or minimum reinforcement may be used.

### 3. CALCULATION METHODS FOR STRESSES AND CRACKWIDTHS

A reliable temperature calculation or estimate is an important prerequisite to achieve accurate stress/strain or crack width calculation. Computer programs, hand calculations and diagrams from handbooks and guidelines may be used. The most decisive parameters, referred to Figure D1 below, are: the fresh concrete temperature ( $T_{ci}$ ), ambient temperature history, insulation conditions, climatic conditions as wind velocity and solar radiation, temperature of the restraining structure ( $T_o$ ), and finally the additional maximum temperature difference due to daily and/or seasonal variations ( $\Delta T_{min}$ ). The parameter  $t_{crit}$  is the time when the hardening member is assumed to be in temperature equilibrium with the restraining structure (within a limit of 2°C).

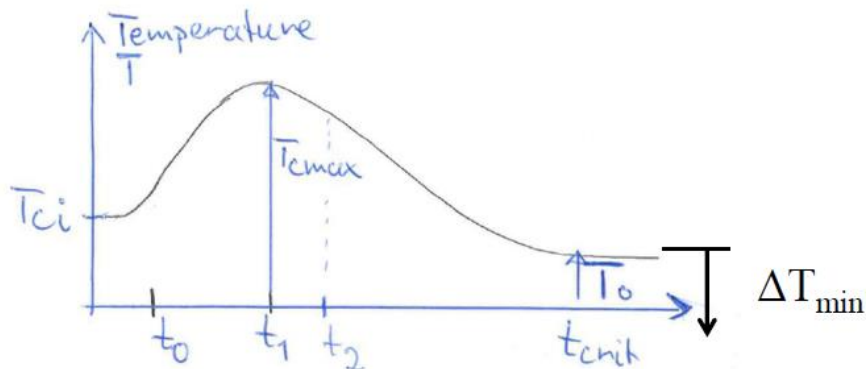


Figure 1. Typical temperature history for a structural concrete member during hardening.

For stress calculations, a method based on the age-adjusted effective E-modulus method is included.

The degree of restraint,  $0 < R < 1.0$ , is the main parameter describing the structural properties of a member restrained by an adjoining structural system. In the uniaxial case it may be defined as the stiffness of the restraining structure divided by the total stiffness.

The equations for crackwidth calculations are based on the same equations as for load dependent cracking, and referring to situations with edge or end restraint situations, similarly as Eurocode 2 part 3 presently does. In the first case the equations for stabilized cracking shall be used, while in the latter case, the crack-formation stage is considered

### 4. RELEVANT MATERIAL PROPERTIES

The preferred state parameter is the equivalent time ( $t_{eq}$ ), also denoted maturity as already defined in Eurocode 2. It is dependent on the material property commonly denoted Activation Energy which is a parameter that should be handled in more general terms than as the constant it is in the

present Eurocode 2. Currently, there is no European standard for experimental determination of this parameter.

The total amount of hydration heat ( $Q_{\infty}$  (kJ/kg binder) released during hydration and its time-function strongly depend on binder fineness and composition and w/b-ratio. Furthermore the strength class strongly influences the binder content, and therefore also the amount of hydration heat. The property may be determined in accordance with the standards: prEN 12390-14 «Testing hardened concrete - Part 14: Semi-adiabatic method for the determination of heat released by concrete during its hardening process», or prEN 12390-15 «Testing hardened concrete - Part 15: Adiabatic method for the determination of heat released by concrete during its hardening process». Table values and diagrams are available from cement suppliers, in text-books and in guidelines. The development versus equivalent time can be described as:  $Q(t_{eq}) = Q_{\infty} \exp(-(\tau/t_{eq})^{\alpha})$  or with piecewise linear curves based directly on experimental data.

The values for the heat conductivity may vary within the range 1,2-3,0 J/(s m°K), and a recommended default value is 2.5 J/(s m°K). The thermal diffusivity is the conductivity divided by the heat times the capacity and specific heat (m<sup>2</sup>/s).

The surface convectivity may vary in the range from about 3.3J/(s m<sup>2</sup>°K) for 18mm plywood formwork and no wind to 15J/(s m<sup>2</sup>°K) for a free concrete surface with 5m/s wind.

The heat capacity corresponds to the specific heat concrete density. The specific heat varies typically in the range 0,85-1,15 kJ/(kg °K), and the default value is 1,0 kJ/(kg °K).

The start time for stress development ( $t_o$ ) is decisive for the stress calculation, and may also be termed “end of the dormant phase”. Typically, it varies between 8 and 13 maturity hours, and the default value is 10 hours. The parameter may be strongly influenced by admixtures, and it is important that the choice of parameter is coordinated with basic shrinkage, and the temperature development curves. The parameter may be determined from the compressive strength development, from ultrasonic stiffness or heat release measurements, or from restrained shrinkage-tests.

The thermal dilation coefficient ( $\alpha_T$ ) may vary with the concrete age, the humidity conditions and the aggregate type within the range 7-14E-6. The recommended default value is 10E-6.

The basic (autogenous) shrinkage,  $\epsilon_{cb}(t)$ , may be calculated from Eq 3.11. It should, however, be noted that the uncertainty is large, which yields both the final value and the time function. Furthermore, the temperature influence on this parameter is not yet fully understood especially for modern concrete with blended cements.

The time-development of the mechanical properties, for  $t < 28$  days, may be described as:

$$f_c(t_{eq}) = \beta f_{c28} \quad \beta = \exp \left[ s \left( 1 - \sqrt{\frac{28-t_o}{t_{eq}-t_{dor}}} \right) \right] \quad f_t(t_{eq}) = \beta^{0,5} f_{t28}, \quad E_c(t_{eq}) = \beta^{0,3} E_{c28}$$

Default values for  $s$  and  $t_{dor}$  are given in Table D1 below. In the PT's present version of the Annex, this approach is slightly modified by including an opening for another reference age than 28 days without changing the model parameters.

*Table 1*

Cement type	High early strength R		Ordinary early strength N		Low early strength S	
	s	t <sub>dor</sub> (d)	s	t <sub>dor</sub> (d)	s	t <sub>dor</sub> (d)
<C35	0,3	0,35	0.35	0,45	0.4	0,5
C40-C55	0.2	0,3	0.25	0,4	0.35	0,45
>C60	0.1	0,3	0.17	0,35	0,3	0,4

Creep properties should be described with respect to the equivalent age at loading, and the time period under load. Models based on linear viscoelasticity for aging materials have proven to be accurate, and should be preferred. The same creep parameters may be used for both tensile and compressive creep. Temperature effects other than those included in the equivalent age concept are of minor importance and may be neglected. Accurate approaches to creep modelling should include the time variable “start time for stress development -  $t_o$ ”, and account for the large creep occurring at very early ages.

#### **ACKNOWLEDGEMENTS**

The present extended abstract is partly based on work performed in the User-driven Research-based Innovation project DaCS (Durable advanced Concrete Solutions, 2015 - 2019).

Furthermore, the current text is based on draft-versions of correspondence and presentations inside the CEN-committee CENTC250/SC2/WG1, and it’s technical committees.

## **Consequences of cracking related to tightness**



Anja B. E. Klausen  
M.Sc., Ph.D., Researcher  
SINTEF Byggeforsk and NTNU, Department of structural engineering  
Post: Pb 4760 Sluppen, NO-7465 Trondheim  
E-mail: anja.klausen@sintef.no

### **ABSTRACT**

Tightness towards gaseous and liquid substances may be an important parameter when it comes to structural design of concrete. The permeability and hence the tightness of sound (uncracked) concrete is closely related to the porosity of the concrete. When cracking occurs, the governing crack mechanism in connection with gas and liquid tightness of concrete is through-cracking; under such conditions the permeability is no longer porosity-dependent but rather crack-dependent. Requirements and specifications regarding concrete tightness can be found in prevailing codes and handbooks, however, the background and reasons for such requirements may appear vague and not always self-evident.

**Key words:** Cracking, consequences of cracking, tightness.

### **1. CONSEQUENCES OF CRACKING RELATED TO TIGHTNESS**

The present extended abstract constitutes a summary of the memo "The impact of cracks on gas and liquid tightness of concrete" [1], which was prepared within the User-driven Research-based Innovation project DaCS (Durable advanced Concrete Solutions, 2015 – 2019). The memo is available upon request.

Concrete is frequently used in structures where tightness towards gaseous and liquid substances is important. For all such structures, concrete tightness is an essential part of the design. When it comes to the permeability of sound (uncracked) concrete, porosity is the decisive material parameter. Adequate porosity, and hence low permeability, can be obtained by carefully considered mix design, and more specific by keeping the water to binder ratio below 0.4.

Naturally, cracks have a major impact on the gas and liquid tightness of concrete. Micro-, surface- and flexural cracks, i.e. cracks that do not go through the whole section, will increase the concrete permeability. However, for such cracks, the gas or liquid still has to be transported through sound concrete and the permeability is thus still porosity-dependent. Through-cracking is the governing crack mechanism when it comes to gas and liquid tightness of concrete; under such conditions the permeability is no longer porosity-dependent but rather crack-dependent. The flow rate through a concrete through-crack is proportional to the width cubed, and hence the permeability increases considerably with increasing crack width. Concrete leakage rates can be estimated by calculation approaches, but such estimations are connected with great uncertainties due to variations in 1) the crack width throughout the section thickness (caused by e.g. reinforcement design and ratio, concrete inhomogeneity and possible self-healing), 2) crack surface roughness and 3) the actual cracking pattern in the given concrete structure.

Self-healing (also denoted autogenous healing) is the ability of a concrete to repair itself due to formation of calcite in the cracks: the water flow gradually decrease over time, and in some cases, the cracks seal completely. A critical upper crack width for complete self-healing is found to be

approximately 0.2 mm for ordinary concrete, which most likely constitutes the background for some of the given crack width tightness requirements.

Requirements and specifications regarding concrete gas and liquid tightness can be found in prevailing codes and handbooks. Such requirements involve e.g. crack width limits, minimum compressive zones, minimum sectional thicknesses, maximum membrane stresses and maximum axial stress resultants. The background and reasons for the given requirements are not always self-evident, which is probably related to the fact that the research topic "the impact of cracks on gas and liquid tightness of concrete" is far from "solved" and still connected to uncertainties.

#### **ACKNOWLEDGEMENTS**

The present extended abstract is based on work performed in the User-driven Research-based Innovation project DaCS (Durable advanced Concrete Solutions, 2015 - 2019).

#### **REFERENCES**

- [1] Klausen, A.: "The impact of cracks on gas and liquid tightness of concrete", Memo prepared within the project DaCS WP1.2, Trondheim, (2017).

## Crack Width Verification of Large Disturbed Regions in Practice



Kenneth C. Kleissl  
M.Sc., PhD  
Specialist,  
COWI, Department of International Bridges,  
Parallelvej 2, Kgs. Lyngby, Denmark  
e-mail: [kekl@cowi.com](mailto:kekl@cowi.com)



Uffe Graaskov Ravn  
M.Sc., PhD  
Chief Specialist,  
COWI, Department of International Bridges,  
Parallelvej 2, Kgs. Lyngby, Denmark  
e-mail: [ugj@cowi.com](mailto:ugj@cowi.com)

### ABSTRACT

Large reinforced concrete bridges involve a series of massive structural elements with non-linear strain distribution that has to be dealt with as disturbed regions designed by plastic design methods, of which the Strut and Tie Method is the most internationally acknowledge approach. In practice and under the assumption that a reasonable strut-and-tie model is considered, the crack width calculation is performed based on the steel stress in the reinforcement ties. This extended abstract discusses the challenges associated with this approach and the various minimum reinforcement demands for control of cracking and how they are dealt with in practice.

**Key words:** disturbed regions, plasticity methods, large concrete bridges, complementary energy, crack width verification.

### 1. INTRODUCTION

Large reinforced concrete bridges involve a series of massive structural elements such as pile caps, pier heads, anchor blocks etc., which due to their geometry and/or loading cannot be analysed as flexural members by classical beam theory.

The typical way to design these structural members are by plasticity methods such as the strut and tie method. However, one of the biggest drawbacks with the plasticity methods are that they are in principle only applicable for limit state analysis. When such methods are used for service analysis, such as crack width verification, it is essential that the engineer considers a statically admissible stress field reasonable close to that actually expected during the given load state.

The only ways to evaluate the chosen stress field is by comparison with the corresponding uncracked linear elastic stress trajectories from Finite Element Analysis or by minimization of the complementary elastic energy. In practice, only the former is realistic even though it is an approximation, as it does not include the stress redistribution after the crack formation state.

### 2 'REASONABLE' PLASTICITY MODEL

A principal assumption in the applied *Lower-bound theorem of plasticity* is that the material is rigid- or elastic-perfectly plastic, i.e. have unlimited ductility or sustain load over infinite deformation. Concrete, even with applied minimum reinforcement, can only sustain loading over

a limited deformation and can therefore not fulfil the basic ductility assumption for applying the lower-bound theorem.

When designers, despite of this, still applies the very useful lower-bound method they are obligated to ensure that the design model considered do not demand more ductility than what can be expected. In practice, this is dealt with by relying on a series of rules of thumbs, based on observations of elastic stress trajectories, such as:

- Spread angle 1:2
- Saint Venant principle
- 40/60 compression/tension depths

These are also illustrated in Figure 1 for a simple concentrated load.

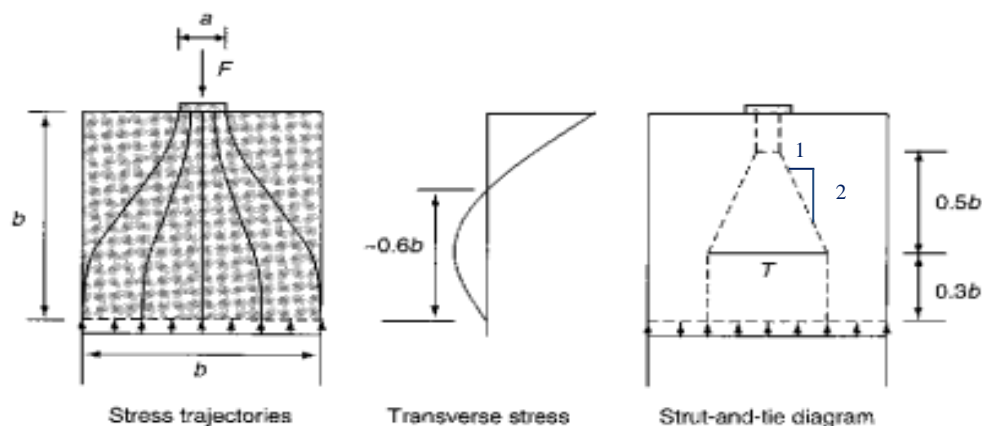


*Figure 1 – Typical rules of thumbs applied in practice.*

So usually, when designers discuss if a plasticity model is good or reasonable they refer to if the stress field is close enough to the actual expected and thus only demands a limited ductility.

However, the above principles and the lower-bound theorem itself are in theory only applicable for the ultimate limit state (ULS) and cannot be applied for any service limit state (SLS) analysis, such as crack width verification, as compatibility is not fulfilled.

The Eurocode does though give recommendation for how designers may deal with SLS, e.g. EN 1992-1-1 5.6.4 (2) states that "*Verifications in SLS may also be carried out ... if approximate compatibility for strut-and-tie models is ensured ...*". By approximate compatibility is here referred to that the position and direction of important struts shall be oriented according to compressive stress trajectories in the uncracked state based on linear elastic theory.

The definition of a reasonable model depends therefore on if it is for ULS or SLS. For SLS a reasonable model has to fulfil at least approximate compatibility while for ULS a reasonable model means that only a limited plastic redistribution, within the expected ductility capacity, is needed. Despite that, the requirements for a SLS model is stricter, the more free approach from ULS are in practice used for both.

An example could be the design of a deep beam, where the designer usually would apply a model with compression and tension stringers located as extreme as possible even though compatibility sometimes would have the compression strut positioned closer to the centre as illustrated in Figure 2c. A fair ULS approach that results in an unsafe SLS design.

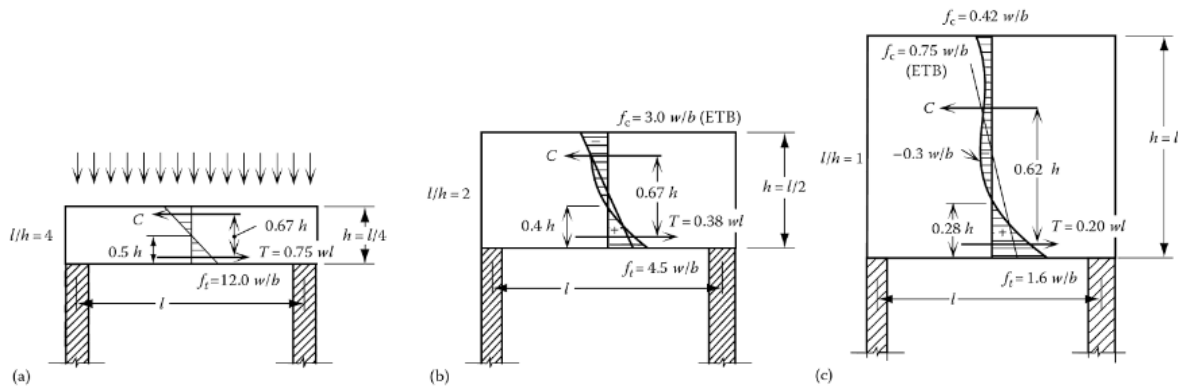


Figure 2 – Strain distribution for different depth to span ratios (reproduced from "Reinforced Concrete Design of Tall Buildings" by B. S. Taranath, 2009).

Attempting to fit once model with stress trajectories from linear elastic uncracked state can be somewhat inaccurate as nonlinearities due to crack formations occurs during SLS. The ideal approach is therefore to fit the model to the stress trajectories from the cracked state, which is most easily done by minimizing the complementary elastic energy ( $W^* = \frac{1}{2} \sigma_{xx} \epsilon_{xx} = \frac{1}{2E} \sigma_{xx}^2$ ) of the statically admissible stress field.

By doing this numerical exercise for the simple concentrated load example shown in Figure 3, one would for 1% reinforcement ratio find that the optimal strut slope is approx. 1:3. Following the ULS principles of a 1:2 slope would therefore in this case yield a conservative SLS design.

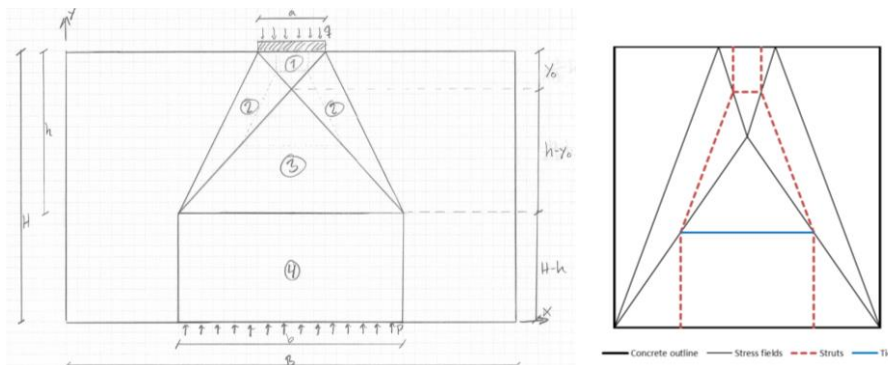


Figure 3 – Simple concentrated load example and the corresponding homogeneous stress field model with minimum complementary elastic energy.

### 3 CRACK WIDTH VERIFICATION

Once a model with approximate compatibility have been obtained for the disturbed region, the crack width verification is in practice solely based on a stress limit criteria for the reinforcement ties, usually in the order of 200-250 MPa. An approach in line with Eurocode that in EN 1992-1-1 7.3.1 (8) states that "... it is possible to use the forces in the ties to obtain the corresponding steel stresses to estimate the crack width".

Crack width in tension ties due to concentrated forces are usually verified based on a fixed service stress limit of 250 MPa, in accordance with EN 1992-2 clause 8.10.3 and VSL PT guide [1].

For the remaining ties, the indirect method in Eurocode is often applied even though the tables' assumptions not always fit very well, especially the small cover and pure bending assumption.

If one instead applies the direct calculation method for e.g. a deep member designed by Strut-and-Tie, the tie would have to be considered as (near) pure tension, significantly affecting the stress limit. On the other hand, as several layers of reinforcement are typically applied it should be fair to reduce the effective concrete area accordingly.

Table 1 summarizes the resulting reinforcement stress limits for a typical 0.3mm design crack width and 50mm cover.

Table 1 – Reinforcement stress requirement to limit crack width to 0.3mm assuming  $c=50\text{mm}$ ,  $h_{c,eff}=c+1.5d_b$ ,  $f_{ck}=40\text{MPa}$ ,  $k_1=0.8$ ,  $k_3=3.4$ ,  $k_4=0.425$ ,  $k_t=0.4$  and  $k_2=1.0$  (pure tension).

Bar spacing [mm]	Bar size			
	20	25	32	40
75	235	238	243	249
125	208	206	208	212
150	201	197	196	199
200	194	185	180	180
250	166	180	170	167
300	145	160	165	159

For typical surface bar spacings of 125-150 mm the stress limit is around 200 MPa.

#### 4 CRACK CONTROL AND DUCTILITY REINFORCEMENT

To ensure that the concrete can sustain loading over limited deformation a minimum amount of reinforcement has to be present to control crack widths and provide a reasonable level of ductility.

While some codes provide a direct requirement for this minimum amount of reinforcement, others are more vague. Eurocode (EN 1992-1-1 5.6.1 (2)P) e.g. only states that "*The ductility of the critical sections shall be sufficient for the envisaged mechanism to be formed*". This is certainly correct but is in practice effectively ignored due to the lack of a concise requirement.

AASHTO [2] on the other hand is much clearer with a fixed minimum requirement of 0.3% reinforcement for the portion effectively utilized by compressive struts (not just the idealised prismatic strut area). Furthermore is the spacing of this crack control reinforcement, both vertical and horizontal, limited to a maximum of 300mm, which are impractical and non-economical for large massive structures. If not provided, the concrete efficiency factor would have to be reduced further, perfectly in line with theory [3] where  $\nu = 2/\sqrt{f_c}$  is recommended for severely cracked concrete.

However, in practice the tradition is that massive structures designed by plastic principles do often not have any reinforcement in the central volume. E.g. major bridge pile caps are only constructed with surface and bottom reinforcement, leaving the critical diagonal bottle-shaped struts without crack control reinforcement.

#### REFERENCES

- [1] Rogowsky, D.M. and Marti, P.: "Detailing for Post-Tensioning", Published by VSL International LTD. (1996).
- [2] AASHTO LRFD Bridge Design Specifications, 7th Edition incl. Interim Revisions 2015 and 2016.

- [3] M.P. Nielsen, L.C. Hoang: "Limit Analysis and Concrete Plasticity", 3rd Edition, CRC Press (2010).



## Finite element analysis with the Cracked Membrane Model



Mário Pimentel  
Assistant Professor  
CONSTRUCT-Labest, Faculty of Engineering (FEUP), University of  
Porto.  
R. Dr. Roberto Frias s/n 4200-465 Porto, Portugal  
e-mail: [mjsp@fe.up.pt](mailto:mjsp@fe.up.pt)

### ABSTRACT

The implementation in a finite element code of the Cracked Membrane Model is briefly presented. The model aims for the efficient nonlinear analysis of large scale structural elements that can be considered an assembly of membrane elements, such as bridge girders, shear walls, transfer beams or containment structures. As the equilibrium equations are established directly at the cracks, the crack widths play a key role in the constitutive laws. Some application examples are presented illustrating the model capabilities in the analysis of plane stress problems, with a special focus on the determination of the crack widths and crack spacing.

**Key words:** Tension chord model, cracked membrane model, structural concrete, crack width.

### 1. INTRODUCTION

The practical application of nonlinear finite element models to the analysis of large scale RC structures is computationally more efficient if each finite element is capable of reproducing the behaviour of an array of cracks. In this context, most of the available models treat reinforced concrete material as a new material with its own stress-strain characteristics, which are valid only in spatially averaged terms. A distinctive feature of the Cracked Membrane Model (CMM) developed by Kauffman and Marti [1] is that the equilibrium equations of the cracked membrane element are established directly at the cracks. This enables using well established theoretical models for the individual mechanical phenomena governing structural concrete behaviour, such as nonlinear compressive behaviour, aggregate interlock (including crack dilatancy effects), tensile bridging stresses and bond stress transfer between the reinforcement and concrete, in a transparent manner. The spatially averaged stress and strain fields are obtained as a by-product of the local behaviour at the cracks and of the bond stress transfer mechanisms, allowing the crack spacing and crack widths to be obtained directly from first principles. This is very appealing for structural engineers and allows bridging the gap between nonlinear numerical analyses of concrete structures and current structural engineering methods.

### 2 MODEL ESSENTIALS

The material model described in this paper is a fixed-crack version of the CMM, here designated as F-CMM [2]. The model is implemented in the software DIANA as a user supplied subroutine as described in [3]. A total strain concept is followed and set of state variables is used to monitor damage evolution and to establish suitable loading/unloading conditions. The updated stress tensor  $\sigma$  is explicitly determined from the current total strains  $\epsilon$  and from the updated values of state variables collected in the vector  $k$ . For uncracked concrete, an isotropic damage like formulation is adopted, requiring only one state variable [3]. After cracking, concrete is treated as an orthotropic material and a local coordinate system is introduced ( $n-t$  coordinates) where the constitutive laws are established. These constitutive laws are described in [2]. Two uniaxial stress

fields are assumed along the two orthogonal  $n$ - $t$  directions and the Poisson effect in the cracked concrete is neglected ( $\nu=0$ ). The crack direction is determined by the principal tensile direction of the concrete stress tensor at impending cracking,  $\theta$ . This angle remains fixed and is kept in memory as a state variable. If the original CMM is selected, here designated as R-CMM, the local coordinate axes coincide with the directions of the current principal average strains.

The Tension Chord Model (TCM) developed by Marti *et al.* [4] is a crucial component of the CMM for modelling the bond stress transfer between the reinforcement and concrete. A stepped rigid-plastic bond shear stress-slip law is adopted allowing the explicit determination of the steel stresses at the cracks ( $\sigma_{srx}$  and  $\sigma_{srx}$ ) from the spatially averaged total strains  $[\varepsilon_n \ \varepsilon_t \ \gamma_{nt}]^T$ . The average crack spacing  $s_{rm}$  is calculated imposing that the tensile stress in the concrete in-between the cracks cannot exceed  $\lambda f_{ct}$ , with  $f_{ct}$  being the concrete tensile strength and  $0.0 \leq \lambda \leq 1.0$ . For  $\lambda = 0$  the crack spacing becomes null, which is equivalent to neglect the tension stiffening effects. The average crack width is obtained from equation (1):

$$w_m = s_{rm} \left( \varepsilon_n + \nu \varepsilon_t - \frac{\sigma_{cm}}{E_c} \right) \quad (1)$$

where  $\sigma_{cm}$  is the average concrete stress in the direction normal to the cracks determined using the TCM and  $E_c$  is the concrete E-modulus. For details refer to [2, 3, 5].

### 3 VALIDATION

#### 3.1 Shear panel PP1

An extensive element level validation of the R- and F-CMM can be found in [2]. This validation was performed using 54 tests on structural concrete panels subjected to in-plane shear and axial stresses. Validation with the results of panels subjected additionally to out-of-plane bending is given in [5]. Here the panel PP1 tested by Marti and Meyboom [6] is analysed. A slow sliding failure occurred along a crack that had formed in the early load stages. The y- reinforcement yielded, whereas the x-direction reinforcement remained elastic. Localized cover spalling was observed. The failure mode is correctly predicted by the model, see Figure 1a. The predicted and measured maximum crack openings are presented Figure 1b. with a good match being obtained. Near failure, with the increasing shear slip, the accompanying opening movement due to crack dilatancy leads the crack width to increase more rapidly.

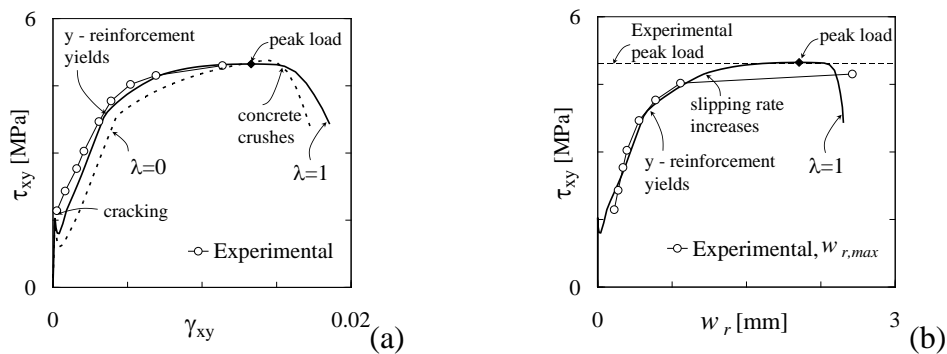


Figure 1 – Panel PP1: (a) applied shear stress vs. average shear strain; (b) applied shear stress vs. maximum crack width.

### 3.2 Beam segments failing in shear

The beams VN2 and VN4 tested by Kaufmann and Marti [7] under combined axial force, shear and bending are used for validation at the structural level, see Figure 2. The axial force in beam VN2 is null while in beam VN4 a constant axial force inducing a compressive stress of 3.2MPa was applied. Beam VN2 failed due to rupture of the stirrups, while beam VN4 failed due to web concrete crushing. These failure modes are correctly predicted by the F-CMM. A good match is also obtained in the force-deformation curves of Figure 2b. The crack pattern representation at failure provided by the model is shown in Figure 2c and compared to the experimental evidence. The crack widths along the web of the beam VN2 are shown for two load steps in Figure 2(c). It can be seen that the crack widths can be estimated with reasonable accuracy.

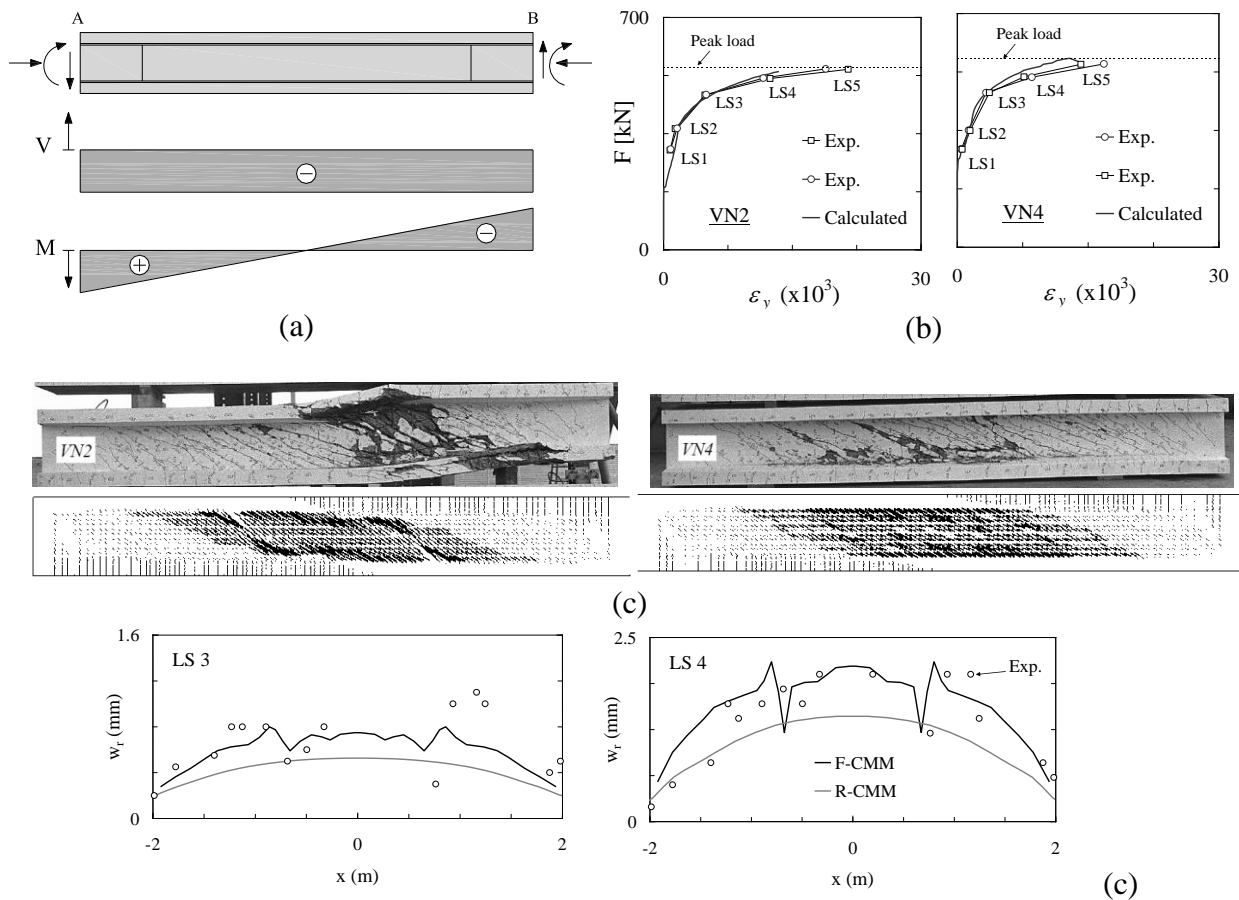


Figure 2 –VN series: (a) Geometry; (b) Force vs. average vertical deformation at the 1/2 span; (c) experimental and numerical crack patterns; (c) crack width distribution along the beam VN2 for load steps LS3 and LS4. The photographs are taken from the test report [7].

### 3.3 Blind prediction: shear wall of Concrack benchmark

Within the scope of the French research project CEOS.fr four squat shear walls were tested. Two of them were included in an international benchmark in which the participants were invited to deliver blind predictions of the behaviour. Here the blind predictions one of these shear walls are presented. The shear wall is made of C40 concrete, is 4200mm long, 1070mm high, 150mm thick and reinforced with a square mesh of  $\text{Ø}10/0.15$ . The wall is confined by two stiff parts with 400m thickness and 700m of height where the horizontal forces are applied. For details refer to [8]. The wall failed due to concrete crushing in the top edge of the wall, starting in the vicinity of the force application area. This failure mode is correctly reproduced by the model as well as the force-displacement curve (Figure 3a). The crack width distribution when the horizontal applied force

$F=4\text{MN}$  is shown in Figure 4b. The maximum crack widths occur near the force application area, which corroborates the experimental findings. The evolution of the crack widths at the central part of the wall (element 481) is shown in Figure 4c and compared to the measurements performed in two cracks close to this area. In the re-analysis after the results were known, a more realistic tensile strength value was adopted and a better fit to the experimental values could be obtained. The maps with the crack spacing are shown in Figure 4d, showing a notorious agreement with the reported experimental average crack spacing of 98mm.

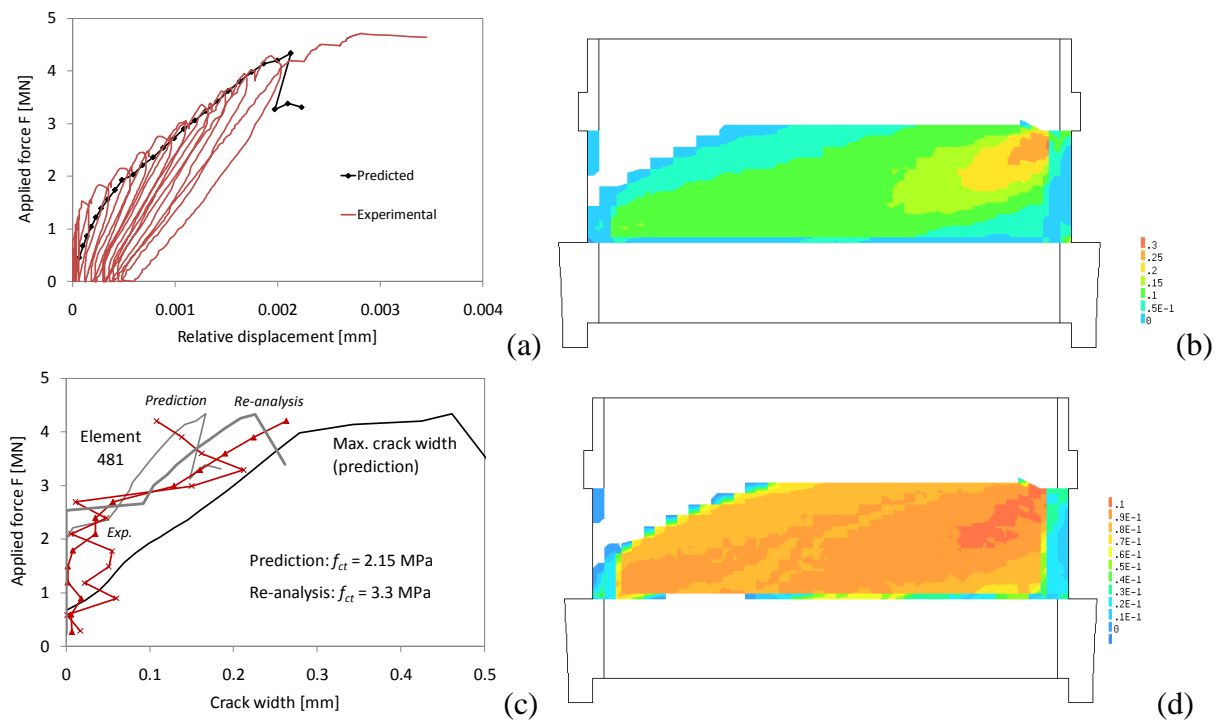


Figure 3 – Shear wall blind-results: (a) Force vs. relative horizontal displacement between the top and bottom beams; (b) colour maps with the crack widths at  $F=4.0\text{MN}$ ; (c) crack widths (in mm) at the centre of the wall and maximum crack width occurring near the loading plate in the upper right corner; (d) colour maps with the average crack spacing (in meters).

## REFERENCES

- [1] Kaufmann, W., Marti, P.: "Structural Concrete: Cracked Membrane Model." Journal of Structural Engineering, Vol. 124(12), pp. 1467-1475, (1998).
- [2] Pimentel, M., Brühwiler, E., and Figueiras, J.: "Extended cracked membrane model for the analysis of RC panels.", Engineering Structures, Vol. 32(8), pp. 1964-1975, (2010).
- [3] Pimentel, M., Figueiras, J.: "Efficient finite element analysis of large scale structures based on a phenomenological approach to RC membrane behaviour", Engineering Computations, Vol. 30, pp. 30774-791, (2013).
- [4] Marti, P., Alvarez, M., Kaufmann, W., and Sigrist, V.: "Tension Chord Model for Structural Concrete.", Structural Engineering International, Vol. 98, pp.287-298, (1998).
- [5] Pimentel, M.: "Numerical modelling for the safety examination of existing concrete bridges", Doctoral thesis, Faculty of Engineering of the University of Porto, (2011).
- [6] Marti, P., and Meyboom, J.: "Response of Prestressed Concrete Elements to In-Plane Shear Forces." ACI Structural Journal, Vol. 89(5), pp. 503-514, (1992).
- [7] Kaufmann, W. and Marti, P.: "Versuche an Stahlbetonträgern unter Normal- und Querkraft." Swiss Federal Institute of Technology Zürich, Zürich, (1996).

- [8] Buffo Lacarriere, L., Rospars, C., Delaplace, A.; Duong, A., Jason, L.: “International Benchmark Concrack – Synthesis of the results”, 2nd Workshop on Control of cracking in RC structures ConCrack 2, Paris – France, June 20-22, (2011).



## **Crack width verification challenges for large RC structures in practice**



Uffe Graaskov Ravn  
Chief Specialist, M.Sc. PhD

Bridge International, COWI A/S  
Parallevej 2 2800 Lyngby, Denmark  
e-mail: [ugj@cowi.com](mailto:ugj@cowi.com)



Kenneth C. Kleissl  
Specialist, M.Sc. PhD

Bridge International, COWI A/S  
Parallevej 2 2800 Lyngby, Denmark  
e-mail: [kekl@cowi.com](mailto:kekl@cowi.com)

### **ABSTRACT**

Cracks in reinforced concrete structures may be characterised as either cracks caused by externally applied loads or cracks caused by imposed deformation. Most codes do not consider the two types of cracks separately and it is often a topic of discussion whether the crack width from externally applied loads and imposed deformations should be combined. In addition, it is frequently discussed whether the sectional forces for crack width calculations should be determined assuming uncracked, linear elastic section properties.

**Key words:** Cracked stiffness, imposed deformation, minimum reinforcement

### **1. INTRODUCTION**

Reinforced concrete (RC) is a nonlinear material where the stiffness change as function of crack development. Initially the cross-section will be uncracked and behaves in a linear elastic manner. For an increasing load the tensile capacity of the concrete will be reached, which will result in the first cracks appearing. With increasing load new cracks will be formed (crack formation stage) until a stabilized cracking stage has been reached. In the stabilized cracking stage no new cracks will form but the existing cracks will become wider. At a certain point the reinforcement will start to yield, see e.g. [1, 2].

When designing large, complex structures with many different load case scenarios the use of FE software is required to determine the sectional forces. As crack development is quite challenging to model, linear elastic section properties are very often chose in practice when calculating the sectional forces to determine the crack widths.

It is very often a topic of discussion (e.g. between designer and checker) whether a reduced stiffness should be applied in the FE calculations to simulate that the cracked stiffness is lower than the uncracked stiffness, thus reducing the required amount of reinforcement. In this respect, the challenge is what that reduction in stiffness should be, as it dependent on the type of loading. For example, for imposed deformation (e.g. shrinkage) it is the axial stiffness that is in question, whereas for an externally applied load (e.g. uniform distributed load) it is the bending stiffness.

Furthermore, an additional topic of consideration is opened, as to whether the crack width due to imposed deformation should be combined with the crack width caused by externally applied loads, and what minimum reinforcement is needed to control those cracks. In recognized codes, e.g. Eurocode [3], there is not much guidance.

In this extended abstract, the two topics outlined above will be further explained. It is only the intention here to address the problems and not to give specific solutions, as these will vary from case to case.

## 2 Cracks in reinforced concrete structures

### 2.1 General

Cracks in reinforced concrete structures are caused by externally applied loads and/or imposed deformations. It is import to distinguish between these two types of cracks as:

- The crack width caused by externally applied loads will, if sufficient minimum reinforcement is provided, be a function of the size of the load. The strain level will typically correspond to the stabilized crack stage where the final number of cracks have been formed (number of cracks is constant).
- The crack width due to imposed deformations (creep, temperature and shrinkage) is caused by restrained movements. Typically, the strain level is limited which means that the cracking stage is between the formation of the first crack and the stabilized cracking stage.

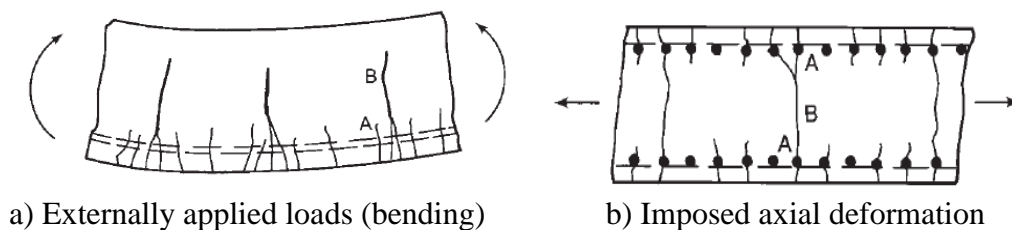


*Figure 1 – Cracking induced by bending and by imposed deformation [4]*

Eurcode [3] does not consider the two types of cracks in combination. In practice, the consequence is that the crack width is found as the sum of the crack width caused by externally applied loads and the imposed deformation. That is supported by *fib* Model Code [2]. However, is that approach right?

According to Arslan [5] the crack width due to externally applied loads and imposed deformation should only be combined when the strain due to imposed deformation exceeds 0.08%. In many design situations, that requirement means that the crack widths should not be combined.

### 2.2 Minimum reinforcement to control cracks

In Eurocode [3] the minimum amount of reinforcement required to control cracks is given by Eq. (1):

$$A_{s,min} \sigma_s = k_c k f_{ct,eff} A_{ct} \quad (1)$$

For definition of  $A_{s,min}$ ,  $\sigma_s$ ,  $k_c$ ,  $k$ ,  $f_{ct,eff}$  and  $A_{ct}$  see [3].

Eq. (1) is based on the strain distribution of the stabilized cracking stage (i.e. all cracks are formed). The minimum reinforcement area  $A_{s,min}$  is a function of the actual reinforcement stress  $\sigma_s$  and, thus, the strain. If the crack width  $w_k$  is plotted against  $\sigma_s$  a linear relationship is shown, see Figure 2.

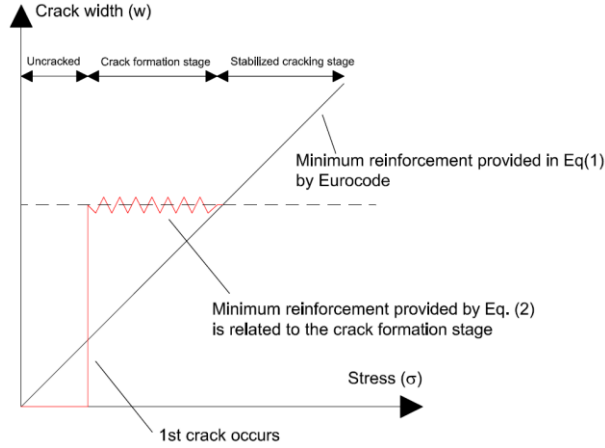


Figure 2 – Crack width as function of stress.

As mentioned previously, shrinkage and temperature cracks occur typically at the lower strain levels corresponding to the crack formation stage. This has been treated in [1] where it has been proposed to use Eq. (2) to determine the required minimum reinforcement in the crack formation stage to control cracks.

$$\rho = \sqrt{\frac{\phi f_{ct,eff}}{4E_{sk}kw_k}} \quad (2)$$

Here  $\phi$  is the reinforcement diameter,  $f_{ct,eff}$  where the first crack occurs is suggested to be  $0.5\sqrt{0.1f_{ck}}$ ,  $E_{sk}$  is the modulus of elasticity of the steel reinforcement,  $k$  is a factor (either 1 or 2) depending on the cracking system considered as explained in [6], and  $w_k$  is the design crack width. It is noted that in the crack formation stage the crack width is independent of  $\sigma_s$ . In contrast it is the number of cracks that increases with increasing reinforcement stress.

Eq. (2) has been adopted in the Danish National Annex to Eurocode [6]. Given that minimum reinforcement is provided according to Eq. (2) it is Danish practice not to combine shrinkage and temperature loads with externally applied loads when calculating the crack width according to clause 7.3.4 in Eurocode [3].

In the crack formation stage, the minimum reinforcement requirement provided by Eq. (2) to control cracks will often results in a larger amount of reinforcement compared to Eq. (1), as illustrated in Figure 2. On the other hand, if the minimum reinforcement to control cracks is provided according to Eq. (1), and assuming the stabilized cracking stage (e.g.  $\sigma_s = 200\text{MPa}$ ), Eq. (2) yields a lower amount of minimum reinforcement compared to Eq. (1). For a slab subjected to pure tension as shown in Figure 3, the minimum reinforcement provided by Eq. (1) can be found to be  $A_{s,min} = 7525\text{mm}^2$  and by Eq. (2) to be  $A_{s,min} = 3608\text{mm}^2$  corresponding to  $\phi 25/130\text{mm}$  and  $\phi 25/270\text{mm}$  respectively in both faces. Eq. (2) provides in this case a significantly saving in reinforcement to control crack development.

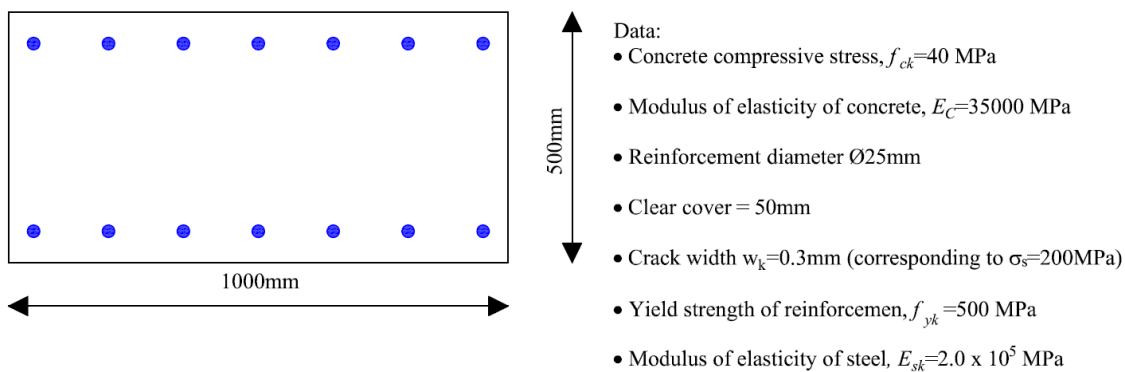


Figure 3 – Cross-section and data

### 3 Uncracked versus cracked stiffness

As mentioned in the introduction uncracked, linear elastic properties are often assumed in practice when calculating the sectional forces to determine the crack widths. Advanced FE analysis that takes the gradual evolution of cracking into account, and hence redistribute the forces due to change in stiffness, can be performed. However, this is time consuming as the nonlinearity prevents the use of superposition of forces.

In contrast to such advanced FE analysis, fully cracked stiffness is in practice often obtained by adjusting the uncracked, linear elastic stiffness by a factor lower than 1.0. For the cross-section in Figure 3, assuming pure bending and  $\varnothing 25/150$ mm in both faces, the stiffness ratio cracked/uncracked can be found to be approximately 0.25. The question is then, if a fully cracked section can be assumed for the entire structure when calculating the crack width? Furthermore, what about the axial stiffness and the torsional stiffness?

For the service limit state it is debatable whether the cross-section for the entire structure can be assumed to be fully cracked as it depends on the actual strain level. Some codes mention specifically that linear elastic analysis with uncracked cross-section properties shall be used, while others state that gradual evolution of cracking may be considered for obtaining the stiffness.

### REFERENCES

- [1] Christiansen, M. B.: "Service limit state analysis of reinforced concrete structures", Department of Structural Engineering and Material, Technical University of Denmark, Series R No. 69, (2000)
- [2] *fib* Model Code 2010: "*fib* Model Code for Concrete Structures 2010 ", Ernst & Sohn, (2013).
- [3] EN1992-1-1:2004: "Eurocode 2: Design of concrete structures – Part 1-1: General rules and rules for buildings", European Committee for Standardization, (2004).
- [4] Wight, J.K and MacGregor, J.G.: "Reinforced concrete – Mechanics and Design", Pearson, 6. Edition, (2012)
- [5] Arslan, A.: "Zur Begrenzung der Reissbreiten bei dicken wänden, u.a. am Fernbahntunnel Berlin", Ernst & Sohn, Bautechnik Vol. 86, Heft 6, DOI: 10.1002/bate.200910029, pp. 329-338 (2009)
- [6] DS/EN 1992-1-1 DK NA:2011: "National Annex to Eurocode 2; Design of concrete structures – part 1-1: General rules and rules for buildings , Energistyrelsen, Denmark, (2011)

## **Evaluation of crack width calculation methods according to Eurocode 2 and fib Model Code 2010 and suggestions to improvements**



Reignard Tan  
M.Sc. PhD Student.  
Norwegian University of Science and Technology  
Richard Birkelands vei 1A, N-7491 Trondheim  
e-mail: [reignard.tan@multiconsult.no](mailto:reignard.tan@multiconsult.no)

Max A.N. Hendriks, Professor  
Delft University of Technology, Faculty of Civil Engineering &  
Geosciences, Stevinweg 1, 2628CN Delft, the Netherlands  
Norwegian University of Science and Technology  
Richard Birkelands vei 1A, N-7491 Trondheim  
e-mail: [max.hendriks@ntnu.no](mailto:max.hendriks@ntnu.no)  
Terje Kanstad, Professor  
Norwegian University of Science and Technology  
Richard Birkelands vei 1A, N-7491 Trondheim  
e-mail: [terje.kanstad@ntnu.no](mailto:terje.kanstad@ntnu.no)

### **ABSTRACT**

The current crack width calculation methods according to Eurocode 2 and *fib* Model Code 2010 have been evaluated. The physical nature of the equations is found to be inconsistent, which limits the generalization of the formulas. An improvement of the formulas is suggested by looking to more physical realistic assumptions in a reinforced concrete tie model.

**Key words:** Crack widths, calculation, reinforced concrete tie, Eurocode 2, *fib* Model Code 2010, concrete structures.

### **1. INTRODUCTION**

The main purpose of this study has been to investigate the range of applicability for the current crack width formulas according to Eurocode 2 (EC2) [2] and *fib* Model Code 2010 (MC2010) [4]. The formulas tend to work relatively well in design of one-way bearing beams and slabs with relatively small cross-sections. However, in lack of more general crack width calculation methods, the formulas are also used in design for relatively large complex concrete structures such as two-way bearing slabs and shell structures. In this paper, the experimental observed behaviour of reinforced concrete ties (RC) has been compared to the theoretical background of the formulas.

### **2. OBSERVED EXPERIMENTAL BEHAVIOR OF RC TIES**

The experimental behaviour of RC ties in the literature can be conveniently elucidated by considering a plane in an axisymmetric model, see figure 1. It is observed that the behaviour of plain bars is quite different from deformed bars. In plain bars, a physical *slip* in the interface between concrete and steel occurs, implying that the steel actually experiences larger deformations than the concrete [3]. In deformed bars, however, the concrete at the steel bar level is observed to follow the same displacement field as the steel due to the rib interaction, which in turn causes the concrete to crack internally. In this case, slip becomes analogous with the

formation of internal cracks. Goto [5] was the first to describe the phenomenon, before being acknowledged by other authors later [6,7]. Furthermore, slip can be defined as the relative displacement between steel and the *undisturbed* concrete and consists of two parts [3]; the relative displacement in the interface between concrete and steel, and the shear deformation of the concrete, which have been denoted as  $S_s$  and  $S_i$  respectively in figure 2.

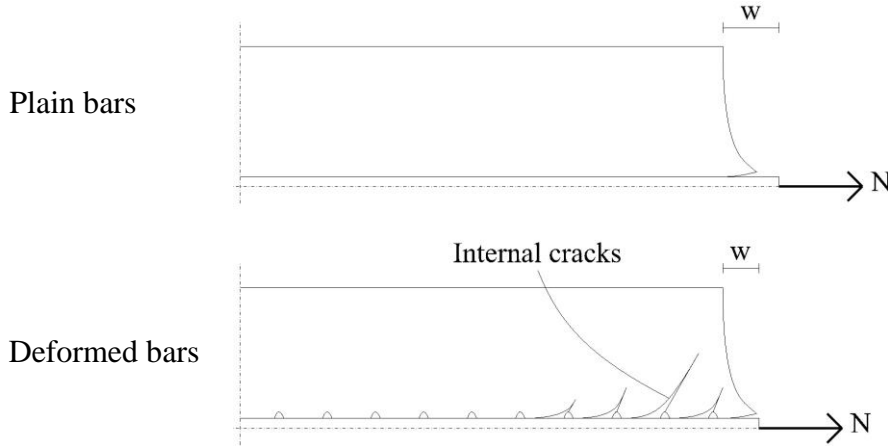


Figure 1 – Cracking behaviour of reinforced concrete ties [11]

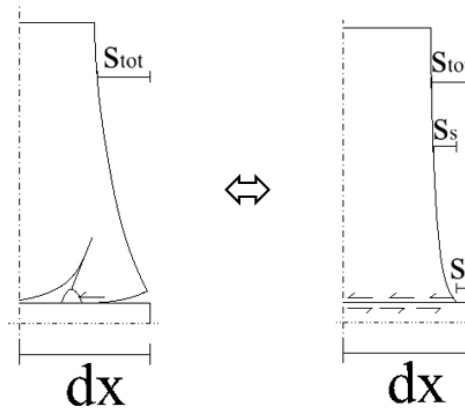


Figure 2 – Simplified and equivalent model to account for internal cracking.

### 3. SIMPLIFIED MODEL

Attempting to explicitly account for the internal cracking in an analytical calculation model will most likely be too complicated. However, an equivalent yet simplified model can be formulated by treating both steel and concrete as elastic materials and lumping all non-linearity related to frictional stress, internal- and splitting cracks as a bond-slip relationship in the interface between concrete and steel, see figure 2. Considering the equilibrium and the compatibility of such an infinitesimal element, the following relations may be derived

$$\int_{A_c} d\sigma_c dA_c = \tau(s_i)\pi\phi dx \quad (1)$$

$$d\sigma_s A_s = -\tau(s_i)\pi\phi dx \quad (2)$$

$$\frac{ds_i}{dx} = \varepsilon_{sx} - \varepsilon_{cx} \quad (3)$$

where  $\tau(s_i)$  are bond stresses as a function of the slip at the interface,  $\sigma_c$  and  $\sigma_s$  are concrete and steel stresses respectively,  $\varepsilon_{sx} - \varepsilon_{cx}$  is the difference between steel and concrete strains. By using the derived relations and assuming that Hooke's law applies, the shape of the concrete strain distribution only is a function of the cover and the Poisson's ratio can be neglected, the following expression for the slip can be derived

$$\frac{d^2 s_i}{dx^2} - \chi \tau(s_i) = 0 \quad (4)$$

The complexity of the solution of equation (4) is dependent of the chosen bond-slip relationship. Moreover, the solution of equation (4), (1) and (2) yields the stress and strain distribution for concrete and steel, which in turn finally yields the crack distance and the crack width.

#### 4. CRACK WIDTH CALCULATION METHODS ACCORDING TO EC2 AND MC2010

Instead of explicitly solving the derived relations above, the formulas in EC2 [3] and MC2010 [5] are derived by considering a relatively simplified model. By considering the deformation compatibility of a segment between two consecutive cracks in a *fully* cracked RC tie, the following relationship may be easily derived

$$w_k = S_{r,max}(\varepsilon_{sm} - \varepsilon_{cm}) \quad (5)$$

where  $\varepsilon_{sm}$  and  $\varepsilon_{cm}$  are mean steel and concrete strains respectively and  $S_{r,max}$  is twice the transfer length  $L_t$  to each side of a crack. The composed transfer length  $L_t$  is based on two theories, which in the literature may be referred to as the "slip-theory" and the "no-slip-theory" [1]. The slip-theory takes basis in solving equation (1) for a constant bond-slip relationship and assuming a constant strain distribution over the cover, i.e. acknowledging that a physical slip occurs in the interface between concrete and steel, however, without accounting for any shear deformations over the cover. The no-slip-theory acknowledges the presence of shear deformations, but not that a physical slip in the interface occurs. In contrary to the slip-theory, no mathematical equations are explicitly solved, but a "traditional engineering rule" claiming that the transfer length is proportional to the cover is utilized. Hence, the crack distance (or rather twice the transfer length) may be expressed as

$$S_{r,max} = 2L_t = 2k_{0,95} \left( k_c c + \frac{1}{4} \frac{f_{ctm}}{\tau_{bm}} \frac{\varphi}{\rho_{s,ef}} \right) \quad (6)$$

Furthermore, the difference in mean strains in equation (5) is derived in a relatively simplified manner by considering an assumed strain distribution over the transfer length. Claiming that an integration constant  $\beta$  is representative for both the steel and concrete strain distribution, an expression for the difference in mean strains can be conveniently derived. From a physical point of view, the integration constant  $\beta$  determines the amount of tension stiffening and is determined experimentally. The expressions in front of the  $c$  and  $\frac{\varphi}{\rho_{s,ef}}$  in equation (6) are also determined experimentally when claiming that the bond stress  $\tau_{bm}$  is proportional to  $f_{ctm}$ , thus highlighting the semi-empirical nature of the formulas.

The ground principles of the formulas can be justified, at least from a simplistic and practical point of view, and are relatively easy and transparent in daily use. However, the formulation for

the composed transfer length appears to be inconsistent and unphysical. The conceptual interpretation of equation (6) is that incompatibility and compatibility in strains occurs for the similar section within the transfer length. In addition, compatibility in strains actually occurs twice within the same transfer length according to the concept in the slip and no-slip-theory. The sudden merging of two theories using completely opposite assumptions is ambivalent, and opposes the basic principles in solid mechanics. The notion that the adjusting empirical constants most likely are based on tests from relatively simple static systems and small specimens limits the general application for the formulas, and care should be taken when applied to more general RC structures. A suggestion to improvement would be to calculate the tension stiffening, the transfer length and the crack width directly by explicitly solving equation (4), which can be considered a more consistent approach, at least judging from a statics point of view.

## **5. CONCLUSION**

The observed experimental behaviour of cracking has been discussed and compared to the physical nature of the formulas in EC2 and MC2010. The merging of the two theories using completely opposite assumptions leads to an inconsistent and unphysical formulation. Also, the notion that the formulas have been adjusted empirically based on relatively small test specimens and simple static systems, limits the general application of the formulas. A suggestion to improvement would be to consider a more consistent and physical approach, e.g. by solving equation (4) explicitly.

## **ACKNOWLEDGEMENT**

The work presented in this paper is part of an ongoing PhD study funded by the Norwegian Public Roads Administration as a part of the Ferry-free coastal route E39 project.

## **REFERENCES**

- [1] Beeby, A. W.: "The prediction of crack widths in hardened concrete", *The Structural Engineer*, Vol. 57 A, No. 1, pp. 9-17, (1979).
- [2] CEN. EN-1992-1-1.: "Eurocode 2, Design of concrete structures – Part 1-1: General rules and rules for buildings", Brussels, Belgium: CEN European Committee for Standardization, (2004).
- [3] *fib* International Federation du béton.: "*fib* bulletin 10 Bond of reinforcement in concrete", Sprint-Druck, Stuttgart, (2000).
- [4] *fib* International Federation for Structural Concrete.: "*fib* Model Code for concrete Structures 2010, Ernst & Sohn, Berlin", (2013).
- [5] Goto, Y.: "Cracks Formed in Concrete Around Deformed Tension Bars", *ACI Journal*, 244-251, (1971).
- [6] Pedziwiatr, J.: "Influence of internal cracks on bond in cracked concrete structures", *Archives of Civil and Mechanical Engineering*, Vol. 3, No. 3, pp. 91-105, (2008).
- [7] Tammo, K. and Thelandersson, S.: "Crack Behavior near Reinforcing Bars in Concrete Structures", *ACI Structural Journal*, Vol. 106, No. 3, pp. 259-267, (2009).

## Crack predictions using random fields



Ab van den Bos  
B.Sc.  
DIANA FEA b.v., Department of engineering  
e-mail: [a.vandenbos@dianafea.com](mailto:a.vandenbos@dianafea.com)



Angelo Garofano  
M.Sc. Phd  
DIANA FEA b.v., Department of engineering  
e-mail: [a.garofano@dianafea.com](mailto:a.garofano@dianafea.com)

### ABSTRACT

Real crack predictions for reinforced concrete (RC), and especially hybrid reinforced concrete (SFRC), are hard to make for real life engineering projects. In the case of plates (slabs and walls), the strain over a region length is often constant and crack localisation on element level cannot be found. In the new DIANA 10 release it is possible to automatically adapt the material properties on integration point level via a real variation contribution over the model using random fields. Based on the material covariance the material strength parameters are randomly distributed over the integration points with taking into account a correlation influence length.

This paper describes the background of implementation of random fields. In addition, shows the difference in crack predictions when using random fields in FEA models in comparison to the constant smeared crack approach. Moreover, proves that the results, having utilised the random fields, show a better localisation of cracks. Finally, a real live slab case is analysed via different material approaches.

**Key words:** DIANA FEA, random field, JCSS, concrete, shrinkage.

### 1. INTRODUCTION

In the field of engineering, plates, horizontal slabs, and/or vertical walls, the shrinkage and restrained boundary effects are often neglected in the calculations.

If the calculations are performed based on e.g. Noakowski (1985), and others based on a tension cord, the results for real engineering projects tend to lead to a high reinforcement ratio.

With the use of the finite element method, the geometry of a real project can be taken into account including the project specific boundary constraints.

Most nonlinear Finite Element Analyses (FEA) are done with a smeared crack approach. The disadvantage is that localisation of cracks is hard to model. More often in the model, cracked regions, over several integration points, and or multiple elements can be seen. This holds especially for less brittle concrete like steel fibre reinforced concrete (SFRC), which is acting more as a (soft) plastic material.

This paper will show the difference in crack predictions when using random fields in FEA models as compared to a constant smeared crack approach.

## 2. MATERIAL PROPERTY DIFFERENCES

When modelling concrete with a smeared crack approach, a typical method in DIANA is to use a total strain based material model and a tension curve crack model Hordijk according to DIANA (2016).

For plain concrete as a brittle material, one would expect one crack, but since there is not any imperfection in a finite element analysis (fea) model under tension this is not always happening. More common is an output of a cracked region without localisation of cracks.

When looking at fig. 1 it is obvious that the localization of cracking will become even more difficult with a steel fibre reinforced concrete (SFRC). During cracking up to more than 30 ‰, the concrete will remain its strength depending on the amount and type of fibres.

A typical amount of energy in plain concrete is about 0.1-0.15 Nmm and in SFRC this will be more like 4 Nmm (30-35 kg/m<sup>3</sup>-hooked end- high yield).

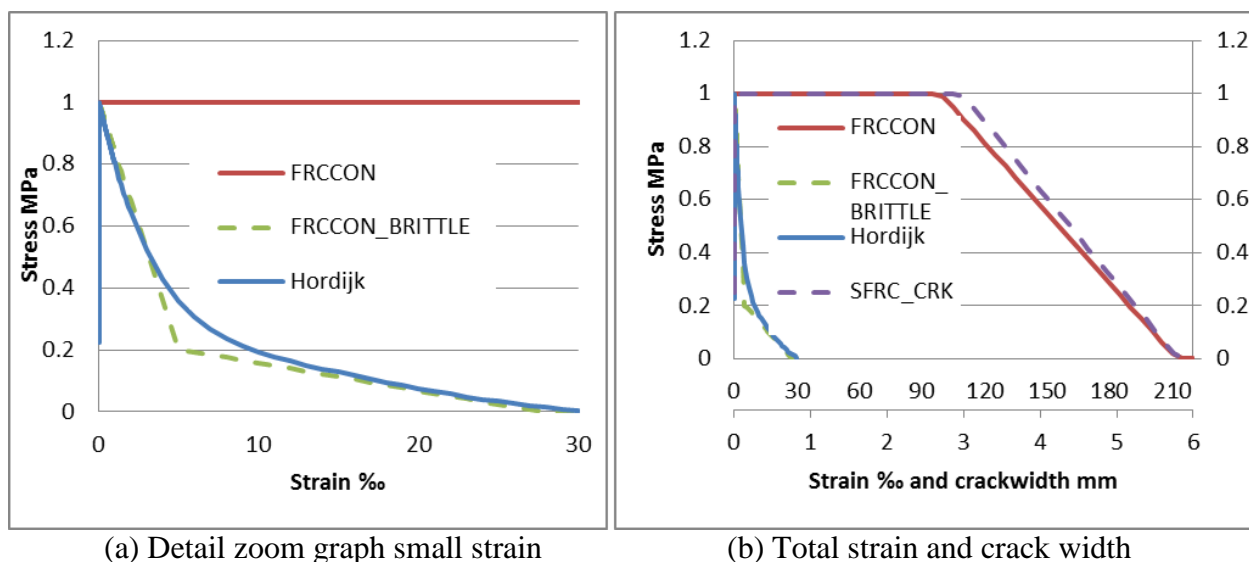


Fig. 1. Different tensile behaviour

The materials used are a MC2010 (2012) model for the SFRC (red line) indicating 1 Mpa still up to 30‰ of crack strain, the crack width at that stage is approximately 0.8 mm. The stress of 1 MPa holds til about 3 mm crack mouth opening when using 30-35 kg/m<sup>3</sup> of Hookend Fibre with a high yield stress > 1400Mpa.

A Hordijk material model is used with a Gf1= 0.135 Nmm for the plain concrete variant (RC). The blue line represents this. The stress is falling down to 0 MPa at 30 ‰.

With adapted MC2010 input parameters, a brittle behavior similar to the Hordijk behavior is modelled. The amount of Gf1 is calculated by DIANA as Gf1=0.132 Nmm. The characteristic length is important for the relation between the strain and the crack width. In this model, it is set to be 25 mm (being the element length).

$$\varepsilon = \frac{w}{lcs}$$

The two FRCCON model input parameters will be used for the study on crack width prediction in this paper.

For the Random field parameter input a co-variance method according to Van der Have (2015) is used. In 3D engineering projects, this method is used to make real 3D random fields in all 3 directions. Other methods can be used depending on the type of project model.

For the decomposition of the matrix, three different solvers can be chosen; the standard is the Cholesky solver according to DIANA (2016).

### 3. GEOMETRY TEST MODEL FOR COMPARISON

We chose the old, very well-known example of Rizkalla, S.H., Hwang (1984). A concrete reinforced tensile member with different reinforcement ratios.

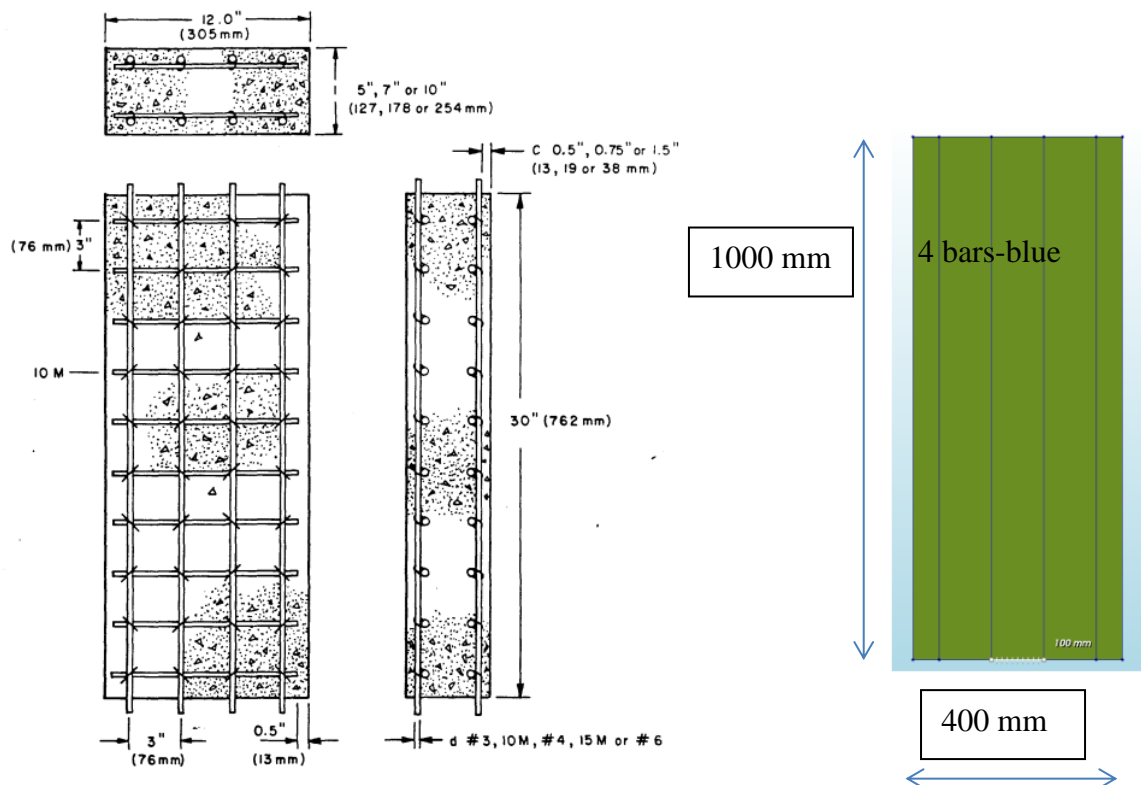


Fig. 2. Test set up for different ratios (a) test in laboratory (b) test in FEA model

The comparison is based on the model variant with a concrete depth of 250 mm, a width of 400 mm and a length of 1000 mm. The reinforcement ratios are varied with different steel bars. The variations undertaken are displayed in Tab. 1.

The fea model is made with a two dimensional plane stress element over the depth of 250 mm. The reinforcement is implemented as a bar with an automatic generated interface around the perimeter of the bar. The bond is taken as a nonlinear stress strain relation.

The model is loaded by means of pulling at the upper and bottom ends of the reinforcement bars. Geometry nonlinearity is taken into account because of non-symmetry of the random fields and the cracking.

*Table 1. Specimen details*

No	bars pieces	Diam mm	As mm <sup>2</sup>	Ab mm <sup>2</sup>	As/Ac (-)	As/Ac (%)
1	2*4	6	226.2	250*400	0.0023	0.23
2	2*4	8	402.1	250*400	0.0040	0.40
3	2*4	10	628.3	250*400	0.0063	0.63
4	2*4	12	904.8	250*400	0.0090	0.90
5	2*4	14	1231.5	250*400	0.0123	1.23
6	2*4	16	1608.5	250*400	0.0161	1.61

#### 4. OUTPUT RESULTS TENSILE SPECIMEN

When comparing the plain concrete behavior with or without reinforcement for a non-random field material distribution the crack strain is developing over a region of about 2/3 of the specimen, instead of localization to a few cracks.

This especially holds true for low reinforced specimens ( $\rho_s < 0.6\%$ )

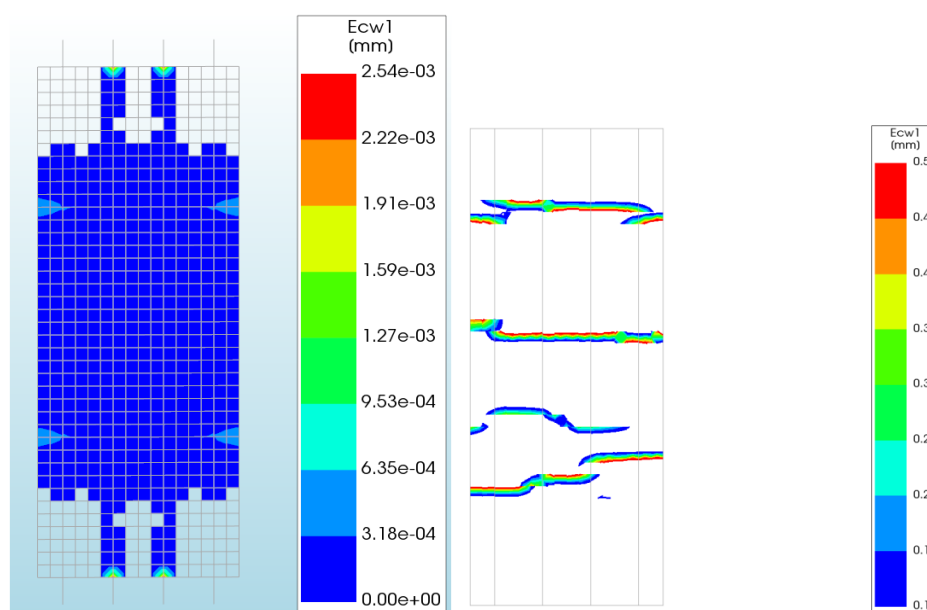


*Fig. 4. Crack region over tensile specimen nr 1 (6 mm bar) without (a) and with random (b)*

It can be observed that on pure tensile regions it can be very difficult for FEA analysis to come to a good crack agreement with laboratory test results.

When looking at the force strain diagrams, comparing the uniform material case and the random field material case, the graphs look similar. Only the belonging crack width and spacing looks completely different because of the localization of cracks in the random field model.

It becomes more interesting to look at the crack width propagation for reinforced concrete with a plain concrete matrix (RC) and reinforced concrete with a steel fibre matrix (SFRC). One would

expect steel fibres to reduce on crack width and that is just what can be seen when using random field material.

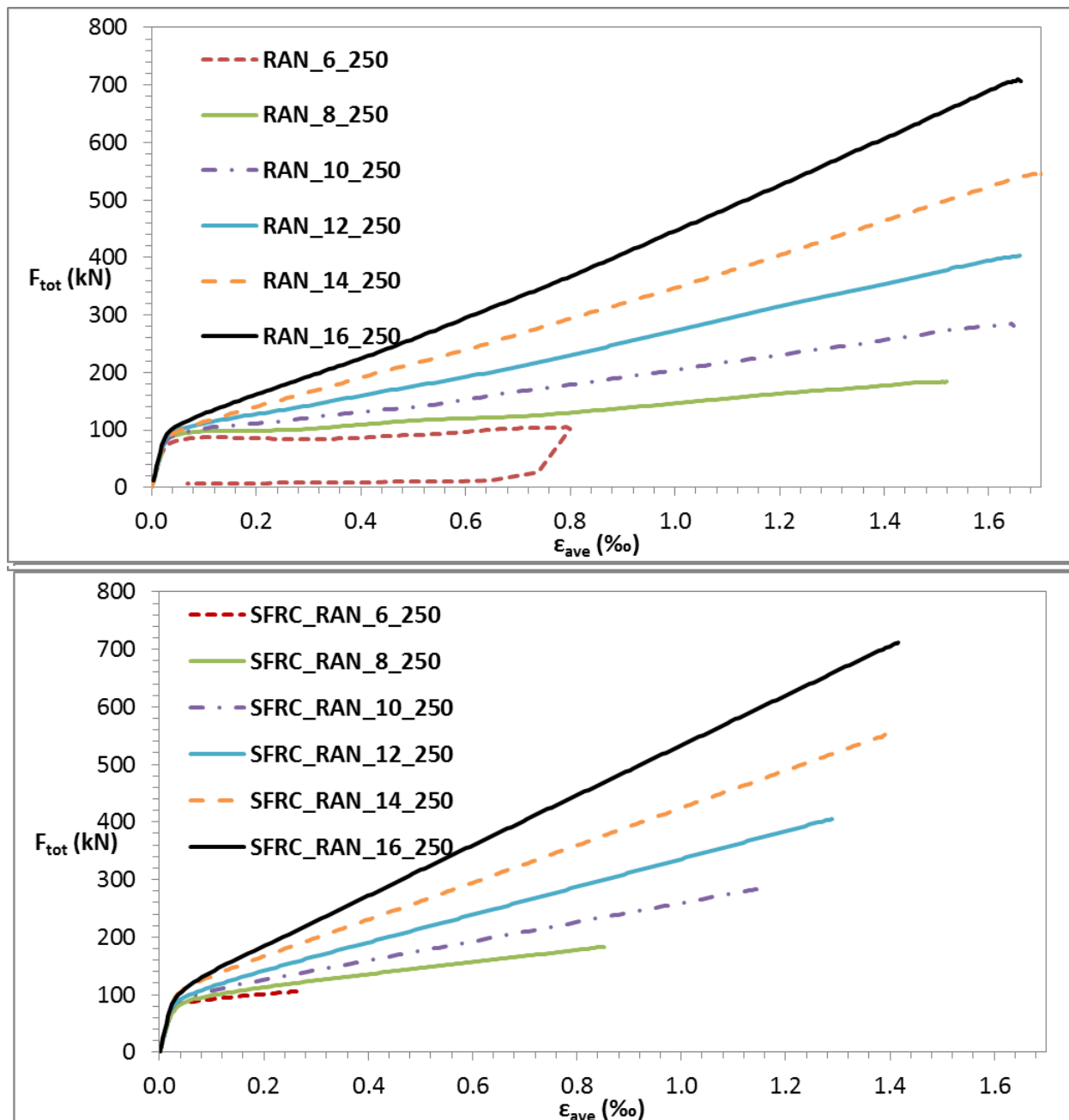


Fig. 5. Force strain diagrams tensile specimen RC (a) and SFRC (b)

It can be seen from fig 5 that the strain at a certain force/stress level is reduced when using Hybrid SFRC as compared with traditional RC. From tab 2 it can be observed that the strain (or crack width) is reduced between 18 to 60%. For a high reinforcement ratio the reduction will be less because the SF is not contributing as much as the traditional reinforcement, but especially in lower reinforced projects the contribution to the crack width will be considerably.

If we have a closer look at the crack spacing for the different specimen, we can observe the reduction.

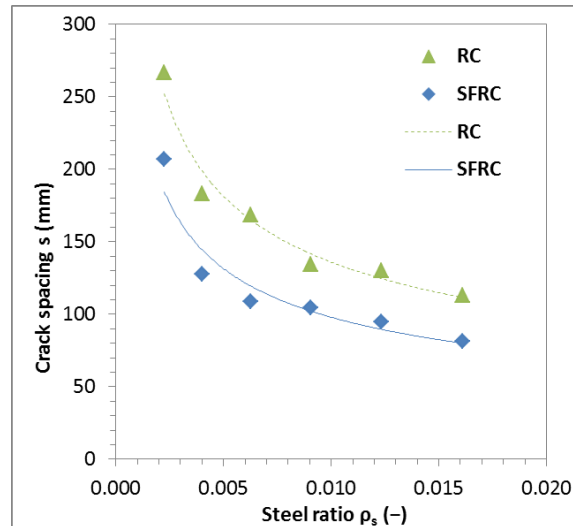


Fig. 6. Crack spacing with different RC ratio

When looking at the crack distribution pictures, the behavior becomes clearer. When adding SF to the RC and using random field material the amount of cracking increases and the crack width is reducing. The second thing that can be shown is that with hybrid SFRC it is hard to localize cracks even though random field for the material is used.

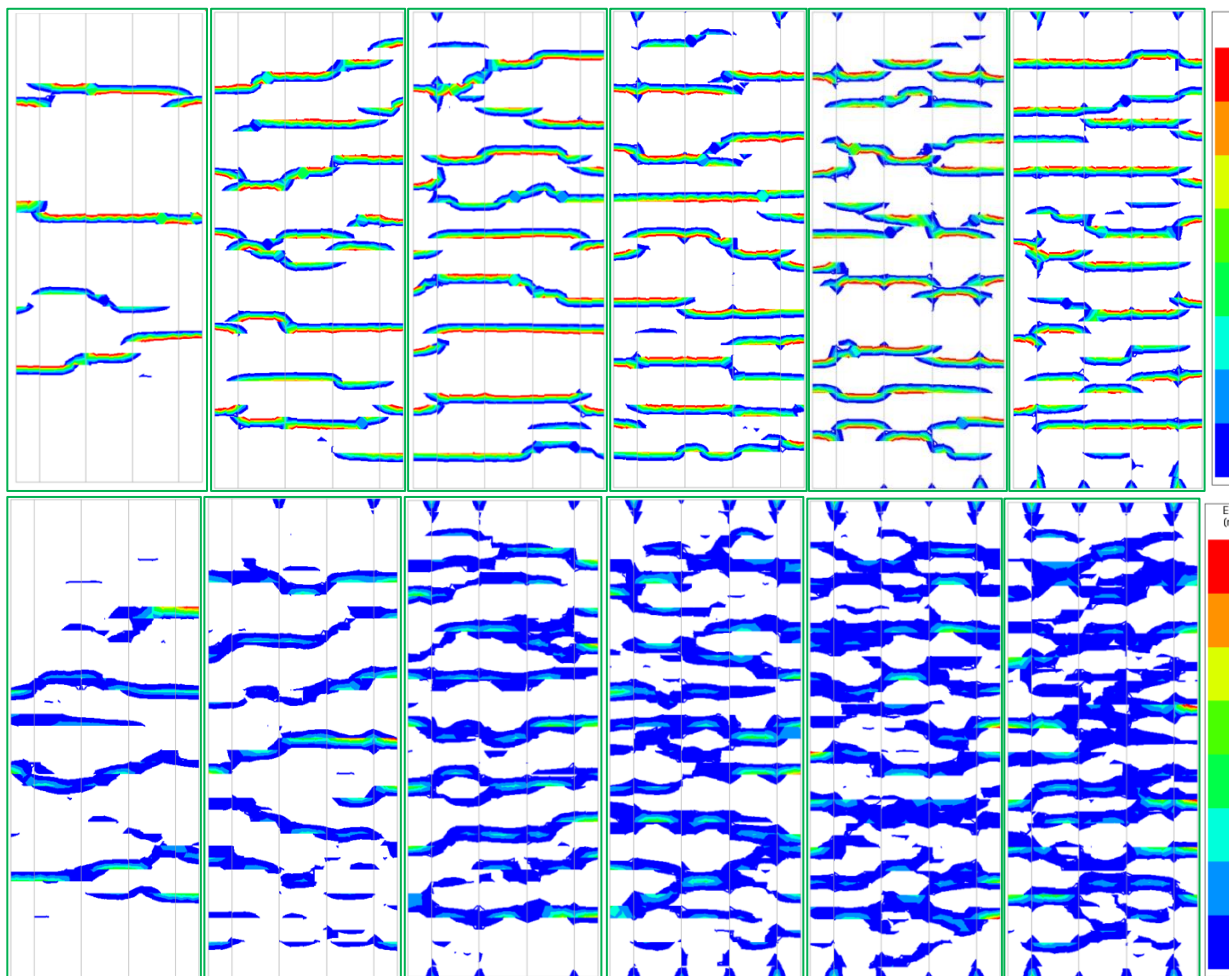


Fig. 7. Crack width with different ratio bars: 6/8/10/12/14/16 mm RC(a) SFRC(b)

## 5. RESULTS FOR PRACTICAL ENGINEERING PROJECT

When using this material option in a concrete project one can see the advantage for the SLS crack width and spacing predictions. According to the JCSS code (2016), it is possible to calculate a slab on grade that is shrinking because of normal drying shrinkage.

We assume a slab for a logistic center with a typical pouring length of 50 m (2500 m<sup>2</sup>) as a day production. In the model we use symmetry in global X direction modelling 25 m (fig 8). In the global Y direction, we assume used 1 m for simplicity's sake.

We model a no tension interface underneath the slab as a subsoil/grade. The compression modulus we assume at  $k=0.06\text{N/mm}^3$ . The friction we assume at 10% stiffness of the vertical one. As a reinforcement grid, a typically used upper grid of 8-100 mm is used.

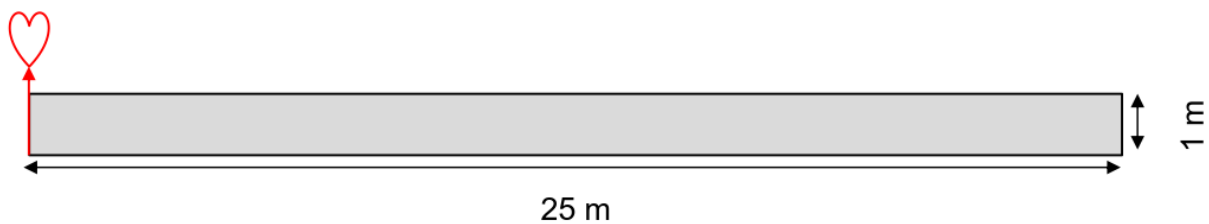


Fig. 8. Input for the slab model

As a load, we apply a shrinkage strain of about 0.3%. The shrinkage at the top is a slightly higher than the bottom because these slabs typically tend to dry at the top more.

When calculating this shrinkage strain with just an isotropic material without a random field the cracks will not be localized. The crack prediction is very low but on a very large region (fig. 9a).

In our model, we have analyzed three random field calculations to show the positive effects. The second calculation is with a random field specified in the JCSS code. The third and fourth calculations are random field according to the MC2010 material, just like in the tensile specimen displayed above, with and without the use of steel fibres.

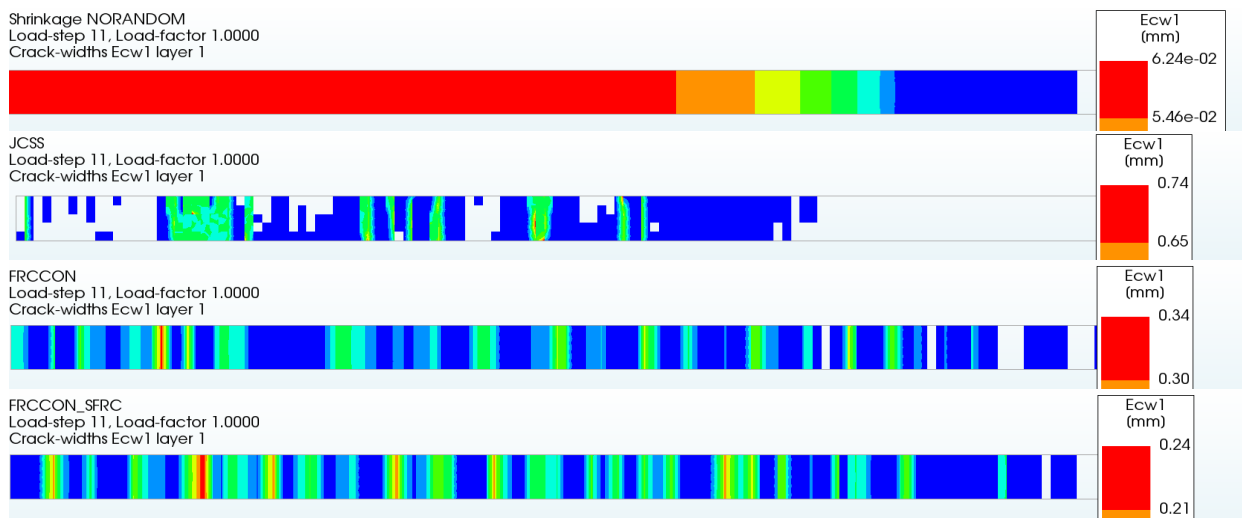


Fig. 9. Crack width with different material models no-rnd(a), JCSS(b), RC(c),SFRC(d)

It can be seen that the amount of cracks that will occur in the model will define the crack width. By using the JCSS crack variation random prescription the estimated crack width will be 0.7 as a maximum and a spacing of macro cracking of about 4 m.

With a MC2010 material model a maximum crack width of 0.34 mm is predicted with a spacing of 2.5 m. Adding SFRC will reduce the cracks to 0.24 with a spacing of about 2 m.

The cracking on the actual projects that are made with this material and length vary between 0.2 and 0.3 mm with a typical crack distance ranging between 0.5 and 3 m.

## **6. CONCLUSIONS**

In this paper, it is shown that localization of cracks in concrete members under tension in fea models become much better when adding random fields to the material strength of the concrete in the model.

Via a small test specimen, it is shown that adding steel fibres will reduce the concrete crack spacing and width.

As a practical example, a concrete slab on grade is modelled with a variation of material models. The shrinkage of the concrete will induce cracking and again the cracking will be reduced when adding SFRC.

## **REFERENCES**

- [1] Noakowski P.: "Continuous Theory for the Determination of Crack Width under the Consideration of Bond". Beton- und Stahlbetonbau, vol. 80, nos. 7/8, p. 185 -190 & 215 - 221, (1985).
- [2] DIANA FEA B.V.: "DIANAFEAS Manual 10.0, <http://dianafea.com>, 2016, Delft FIB, MC2010, (2012)
- [3] Van der Have, R.: "Random Fields for Non-Linear Finite Element Analysis of Reinforced Concrete", Master thesis, (2015)
- [4] Rizkalla, S.H., Hwang: "Crack prediction for members in uniaxial tension". ACIjournal 84, (1984).
- [5] JCSS, probabilistic model code : [http://www.jcss.byg.dtu.dk/Publications/Probabilistic\\_Model\\_Code.aspx](http://www.jcss.byg.dtu.dk/Publications/Probabilistic_Model_Code.aspx), (2000).
- [6] Vandenbos A., Garofano A.: "Crack predictions using random fields" (2016)

## **Strain level and cracking of the lightweight aggregate concrete beams**



Jelena Zivkovic  
M.Sc. PhD-candidate  
Department of Structural Engineering  
Faculty of Engineering Science  
Norwegian University of Science and Technology  
N-7491 Trondheim, Norway  
e-mail: [jelena.zivkovic@ntnu.no](mailto:jelena.zivkovic@ntnu.no)



Jan Arve Øverli  
PhD, Professor  
Department of Structural Engineering  
Faculty of Engineering Science  
Norwegian University of Science and Technology  
N-7491 Trondheim, Norway  
e-mail: [jan.overli@ntnu.no](mailto:jan.overli@ntnu.no)

### **ABSTRACT**

The main disadvantages of lightweight aggregate concrete (LWAC) compared with normal weight concrete (NDC) are its brittleness at the material level in compression and uncontrolled crack propagation. This experimental investigation consists of six beams with lightweight concrete with Stalite as aggregate. Main goal were to investigate cracking and strain level in compression of the beams subjected in four-point bending test. Compressive strain level was much higher than expected, and cracking was similar as for normal weight concrete beams.

**Key words:** Lightweight Aggregate Concrete, Testing, Bending, Strain level, Shear Reinforcement.

### **1. INTRODUCTION**

#### **1.2 General**

This investigation is part of the ongoing research program “Durable advanced concrete structures (DaCS)”. One part of this program is to investigate structural behaviour of lightweight aggregate concretes (LWAC), concretes with an oven dry density below 2000 kg/m<sup>3</sup>. General characteristic of LWAC is the very high degree of brittleness at the material level and especially in compression. The brittleness of concrete is characterized by sensitivity to stress concentrations and a rapid crack/fracture development. This influences the behaviour of concrete where the tensile strength is important, as for instance the shear and bond strength [1,2].

To investigate the cracking and strain level of LWAC in compression, six beams with different reinforcement layout were subjected in a four-point bending test. The test setup was designed to produce a constant moment zone of 1 m between the loading points. The size of the beams were (width x height x length) 210-330 x 550 x 4500 mm. The main test parameters were the stirrup spacing, amount of compressive reinforcement and size of concrete cover. All the beams failed in compression between the two loading points. Cracking of the compression area in the beams depending the most of the reinforcement detailing. Cracking of the beam without shear reinforcement in compression area was the largest, while beam that contain shear reinforcement at the dense spacing had the smallest cracking. Strain level in the concrete and reinforcement were recorded with strain gauges (SG) and Linear Variable Differential Transformers (LVDT) at one

side of the beam. On the other side Digital Image Correlation (DIC) method was used [3,4]. Average compressive strain level recorded in all the beams was in scope 3,4‰ and 3,8‰. In addition, for control of the material characteristics small specimens were tested. To produce the concrete, a lightweight aggregate Stalite was used to achieve an oven-dry density of about 1850 kg/m<sup>3</sup> and a compressive cylinder strength of about 65 MPa.

## 2. EXPERIMENTAL TEST PROGRAM AND RESULTS

The experimental program consist of six reinforced LWAC beams which were subjected to a four point bending test, with a constant moment zone of 1m between the loading points. Main test parameters that were varied in the testing zone were the stirrup spacing, amount of compressive reinforcement and size of concrete cover. All the beams were overreinforced in order to provide the bending failure. Outside of the testing zone, all the beams had the same stirrups distribution designed to avoid shear failure. The program and results are given in Table 1. The beams measured (width x height x length) 210-330 x 550 x 4500 mm. Detailed test setup of the beams and reinforcement layout of cross section are shown in Figure 1.

Table 1-Test parameters and results

Beam	s [mm]	c [mm]	A <sub>c</sub>	f <sub>lc,cube</sub> [MPa]	P <sub>fer</sub> [kN]	P <sub>cr</sub> [kN]	P <sub>u</sub> [kN]	P <sub>calc</sub> [kN]	P <sub>u</sub> / P <sub>calc</sub>	ε <sub>c</sub> [‰]	ε <sub>t</sub> [‰]
1	-	20	2ø12	74.2	53	318	724	729	0.99	3.70	-
2	200	20	2ø12	74.2	54	350	645	729	0.88	3.77	2.04
3	60	20	2ø12	74.2	78	319	707	729	0.97	3.74	2.41
4	100	20	2ø12	74.2	69	324	700	729	0.96	3.75	2.08
5	100	40	2ø12	74.2	64	339	663.4	726	0.91	3.61	2.17
6	200	40	2ø25	74.2	64	250	750	800	0.94	3.4	2.35

where *s* is stirrup spacing; *c* -size of concrete cover; A<sub>c</sub> –compressive reinforcement; f<sub>lc,cube</sub>-compressive cube strength; P<sub>fer</sub> – load level for first bending crack; P<sub>cr</sub> – load level for first shear crack; P<sub>u</sub> – load level of maximum load; P<sub>calc</sub> – calculated load according EC2[5]; ε<sub>c</sub> – average concrete compressive strain; ε<sub>t</sub> – average concrete tension strain;

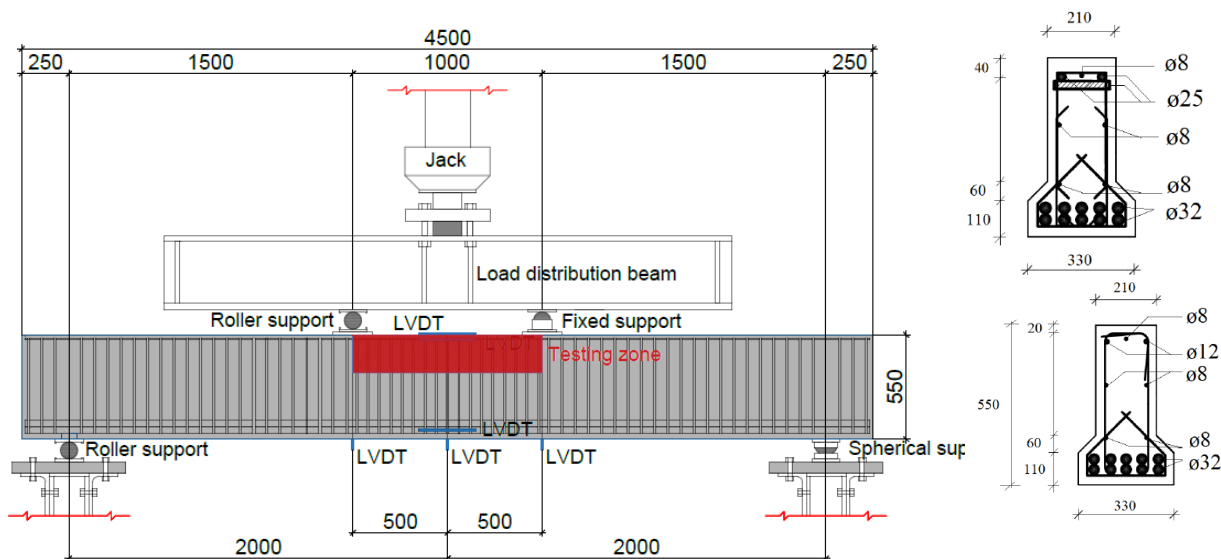


Figure 1 – Detailed test setup of beams and cross sections with the reinforcement layout

The moment and shear capacity of the beams has been calculated in accordance with Eurocode 2 [5], and these values are 729 kN, 726 kN and 800 kN respectively. The strain level which is used in calculation was 2,52‰.

### **3. DISCUSSION**

The first bending crack was observed in the constant moment region on the tension side between the loading points. As the load was increased, new bending cracks propagated symmetrically until they reached the top of the beam flange. Development of bending cracks slowed down when shear cracks appeared. The first shear cracks appeared in the middle of the shear zone, between the neutral axis and the beam flange. Additional loading lead to further crack propagation of both bending and shear side. In beam 6, shear cracks appeared from bending cracks, which was different from the other beams. Crack propagation for certain load steps are very similar for all the tested beams. Only difference was in cracking of the compression zone and that depend from tests parameters. Failure happened when compression zone between loading points cracks. This type of failure is defined as compressive failure in the bending moment zone, see Figure 2. In general, observed cracking in all the beams were very similar like for normal weight concrete beams, because all beams were able to stand almost doubled load after formation of diagonal shear cracks. Beams with reduced stirrup spacing and lower concrete cover showed the lowest spoiling and decrease in crack propagation. The beam containing the largest compressive reinforcement resisted the largest load but crack propagation and spoiling were the similar like for the beam with same stirrup spacing and concrete cover. The beam 1, which do not contain stirrups in testing area showed the largest brittle spoiling and uncontrolled crack propagation, typical for LWAC [1,2].



*Figure 2– Final failure state of beam 4*

By using DIC, detailed strain fields of the observed compressive zones have been recorded, see Figure 3. In general, measuring devices were in a good agreement but in a failure faze larger strains and localization were measured using DIC, compared to the strain values measured with the SGs and LVDTs. Localization of strains actually present nice picture of formed cracks and strains development between them. In addition, it is visible that reinforcement layout will influence the most the crack development and that cracks which will actually lead till failure were formed between stirrups. Average compressive strain level recorded in all the beams was in scope 3,4‰ and 3,8‰. Having in mind that EC2 [5] has special rules for LWAC, which are reduction factors applied to regular design criterion, the results in this study indicate that EC2 underestimates LWAC. Recorded maximum strains in the tested beams were for 30-50 % larger than the allowed maximum strain for this type of concrete.

### **4. CONCLUSIONS**

For all tested beams in this research, cracking of the beams were the similar except for the testing area. All beams showed the ductile behaviour since they were able to stand more loading after formation of shear cracks.

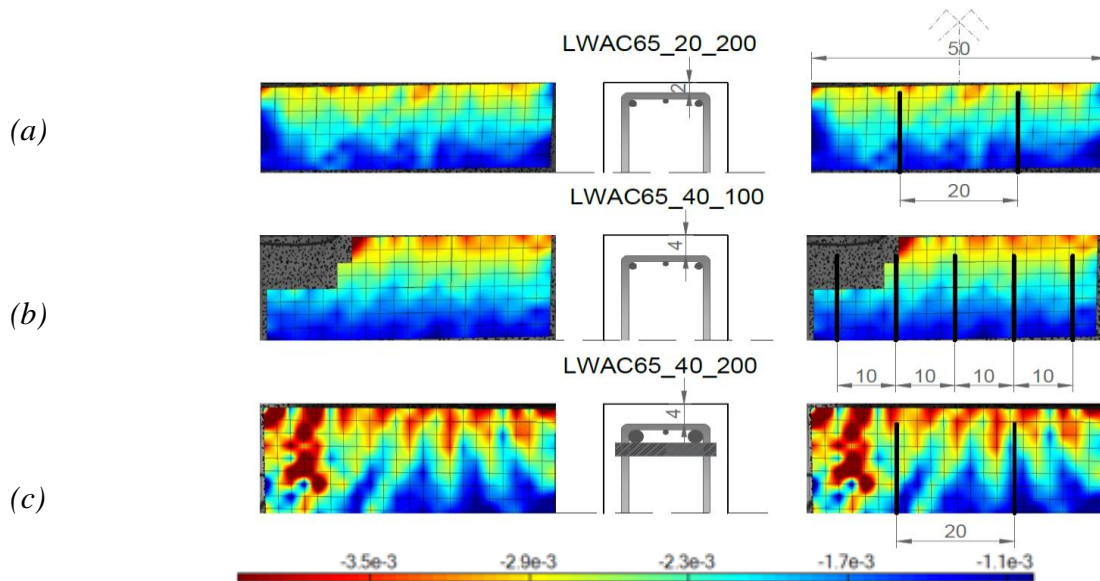


Figure 3– Detailed strain field from 3D-DIC (element size 23mm, colorbar scaling from 1‰-4‰); (a) beam 2; (b) beam 5; (c) beam 6;

Cracking of the testing area depend from the test parameters varied in this experiment. Beams with the dense stirrup spacing showed small, shallow cracks and spoiling were the smallest. In beams where cover was deeper spoiling and cracking were larger. The beam containing the largest compressive reinforcement resisted the largest load.

In general, characteristics of LWAC mostly depend on the type of used lightweight aggregate (LWA). EC2 do not differentiate between types of LWAs used in LWAC. From the experimental results in this experiment, it is indicated that EC2 underestimates strain level 30-50% from one proposed for designing. Since in this study LWAC showed behaviour similar to NDC, further investigation of LWAC as a structural material should be continued. In addition, the way how EC2 treats different types of LWAC should especially be investigated.

### Acknowledgment

The work presented in this paper is part of ongoing PhD study in scope of the DACS project (Durable Advanced Concrete Solutions). The DACS partners are Kværner AS (project owner), Norwegian Research Council, Axion AS (Stalite), AF Gruppen Norge AS, Concrete Structures AS, Mapei AS, Multiconsult AS, NorBetong AS, Norcem AS, NPRA (Statens vegvesen), Norwegian University of Science and Technology (NTNU), SINTEF Byggforsk, Skanska Norge AS, Unicon AS and Veidekke Entreprenør AS. Jelena Zivkovic would like to express his outmost gratitude to the supervisors and all the project partners for contributions and making this PhD study possible.

### REFERENCES

- [1] EuroLightCon. Lwac Material Properties. Document BE96-3942/R2, December 1998.
- [2] ACI Committee 213. Guide for Structural Lightweight Aggregate Concrete (ACI 213R-03). American Concrete Institute. Farmington Hills, MI, United States: American Concrete Institute; 2003.
- [3] T.M. Fayyada and J.M Leesb. Application of Digital Image Correlation to Reinforced Concrete Fracture. Procedia Materials Science 3 (2014) 1585 1590, 20th European Conference on Fracture (ECF20), 2014.

- [4] N. McCormick and J. Lord. Digital Image Correlation for Structural Measurements. ICE institution. Civil Engineering, 165 (CE4), pages 185–190, 2012.
- [5] EN 1992-1-1 (2004), “Eurocode 2: Design of concrete structures – Part 1-1: General rules and rules for buildings”.

**A list of previous and upcoming Nordic Workshops and Miniseminars is available on**

[www.nordicconcrete.net](http://www.nordicconcrete.net)



Nordic  
Concrete  
Federation

ISBN: 978-82-8208-057-6